SORPTION OF VX TO CLAY MINERALS AND SOILS: THERMODYNAMIC AND KINETIC STUDIES

Kevin M. Morrissey
Amanda M. Schenning
Richard L. Cheicante

SCIENCE APPLICATIONS INTERNATIONAL CORPORATION
Gunpowder, MD 21010-0068

Kenneth B. Sumpter

RESEARCH AND TECHNOLOGY DIRECTORATE

December 2012

U.S. ARMY RDECOM

Disclaimer

REPORT DOCUMENTATION PAGE

Form Approved
OMB No. 0704-0188

1. REPORT DATE *(DD-MM-YYYY)* XX-12-2012	2. REPORT TYPE Final	3. DATES COVERED *(From - To)* Oct 2009 - Sep 2010
4. TITLE AND SUBTITLE Sorption of VX to Clay Minerals and Soils: Thermodynamic and Kinetic Studies		5a. CONTRACT NUMBER DAAD13-03-D-0017
		5b. GRANT NUMBER
		5c. PROGRAM ELEMENT NUMBER
6. AUTHOR(S) Morrissey, Kevin M.; Schenning, Amanda M.; Cheicante, Richard L. (SAIC); and Sumpter, Kenneth B. (ECBC)		5d. PROJECT NUMBER
		5e. TASK NUMBER
		5f. WORK UNIT NUMBER
7. PERFORMING ORGANIZATION NAME(S) AND ADDRESS(ES) Science Applications International Corporation, P.O. Box 68, Gunpowder, MD 21010-0068 Director, ECBC, ATTN: RDCB-DRC-C, APG, MD 21010-5424		8. PERFORMING ORGANIZATION REPORT NUMBER ECBC-TR-1016
z.9. SPONSORING / MONITORING AGENCY NAME(S) AND ADDRESS(ES)		10. SPONSOR/MONITOR'S ACRONYM(S)
		11. SPONSOR/MONITOR'S REPORT NUMBER(S)

12. DISTRIBUTION / AVAILABILITY STATEMENT
Approved for public release; distribution is unlimited.

13. SUPPLEMENTARY NOTES

14. ABSTRACT

Organophosphorus-based chemical warfare agents are unique military chemicals that are extremely toxic and could be found in the soils of military installations and former production facilities. Little data exists on the fate and transport of these chemicals in soil environments, particularly when the agent is present in low concentrations. This report summarizes data from a study in which isothermal titration calorimetry was used to examine the sorption of VX to clay minerals and soils. Thermodynamic characteristics such as observed enthalpy of binding, entropy, free energy, binding and dissociation constants, and saturation capacity were obtained. Complementary sorption/desorption profiles and batch equilibrium sorption isotherms were also generated during the study. Kinetic time-point samples were analyzed using a variety of analytical techniques to provide insights into the sorption pathways, and to distinguish sorption from degradation occurring in the bulk solutions. In a montmorillonite clay, there was a sharp break in the thermodynamic profile that corresponded to the lower critical temperature (LCT) of VX. The predominant mechanism above the LCT was an exothermic physisorption process, consistent with an ion-exchange mechanism. Below the LCT, bimodal behavior was observed, with a second type of endothermic interaction occurring after the initial ion exchange.

15. SUBJECT TERMS				
Clay	Soil	Lower critical temperature	Sorption	Gibbs free energy
Thermodynamics	Kinetic	Isothermal titration calorimetry	ITC	VX
Enthalpy	Entropy	Binding constant	Dissociation constant	Settling rate

16. SECURITY CLASSIFICATION OF:			17. LIMITATION OF ABSTRACT	18. NUMBER OF PAGES	19a. NAME OF RESPONSIBLE PERSON Renu B. Rastogi
a. REPORT U	b. ABSTRACT U	c. THIS PAGE U	UU	106	19b. TELEPHONE NUMBER *(include area code)* (410) 436-7545

Standard Form 298 (Rev. 8-98)
Prescribed by ANSI Std. Z39.18

Blank

PREFACE

The work described in this report was authorized under contract no. DAAD13-03-0017. The experimental work began in October 2009 and was completed in September 2010.

The use of either trade or manufacturers' names in this report does not constitute an official endorsement of any commercial products. This report may not be cited for purposes of advertisement.

This report has been approved for public release.

Blank

EXECUTIVE SUMMARY

Accurately predicting the fate and transport of chemical warfare agents in environmental scenarios requires a mechanistic understanding of the interaction with environmental surfaces. While sorption of contaminants to soil components, such as clays, is a major factor influencing fate and transport of commercial pesticides in soil environments, little data exists regarding the sorption of chemical warfare agents in these environments. In the current study, isothermal titration calorimetry was determined to be a useful technique for elucidating the sorption of VX to environmental substrates. This calorimetric technique is particularly useful when coupled with both kinetic profiling and equilibrium sorption isotherms. The current study is the first known study to examine the sorption of VX from dilute aqueous solution onto environmental sample matrices, in which thermodynamic and sorption parameters were measured and reported.

The sorption of VX to a natural clay at temperatures *above* the lower critical temperature of VX (~10 °C) was determined to occur rapidly (<15 min) as a physisorption type of process, consistent with an ion-exchange mechanism. The reaction of VX with clay is exothermic, as indicated by the negative enthalpy values. The enthalpy values measured at 25 °C in the current study (−12.6 to −8.44 kJ/mol) are consistent with literature values for cation exchange on clays.

The sorption of VX to a natural clay at temperatures *below* the lower critical temperature of VX (~10 °C) was bimodal, with both exothermic and endothermic heat flows. The initial interaction (Site 1) was determined to occur rapidly (<15 min) and to be a physisorption type of process consistent with an ion-exchange mechanism. The interaction of VX with Site 1 was exothermic, as indicated by the negative enthalpy values. The second interaction (Site 2) occurred once the Site 1 interaction was complete, and was endothermic, as indicated by the positive enthalpy values. The interaction of VX with Site 2 is thought to be a ligand-exchange mechanism via the phosphorus, but this has not been confirmed. The binding of VX to clay was found to be 3.5 times stronger when the sorption occurred below the lower critical temperature of VX.

The process of sorption of VX onto a natural montmorillonite clay was determined to preserve the VX, as demonstrated by quantitative recovery of VX from the clay after 8 days of storage at room temperature. In a reported study, an amine was found to be stable for at least 5 months when sorbed to a natural montmorillonite clay. In both the current study and the reported study, the reported stabilities should be considered lower limits because the experiments were terminated after 8 days or 5 months, respectively.

Blank

CONTENTS

FIGURES

TABLES

Blank

SORPTION OF VX TO CLAY MINERALS AND SOILS:
THERMODYNAMIC AND KINETIC STUDIES

1.   INTRODUCTION

1.1   Background

          Accurately predicting the fate and transport of the persistent chemical warfare
agent (CWA) *O*-ethyl-S-[2-*N*,*N*-(diisopropylamino)ethyl] methylphosphonothioate (VX,
Chemical Abstracts Service [CAS] no. 50782-69-9) in environmental scenarios requires a
mechanistic understanding of the interaction of VX with environmental surfaces. Although
sorption to soil components such as clays and organics is a major factor influencing fate and
transport of pesticides in soil environments,[1–3] little data exists regarding the sorption of VX in
these environments. In a literature review, multiple studies were found that examined the fate of
VX on concrete, asphalt, sand, and sorbents,[4–13] but none of these studies were focused on
sorptive behavior in an aqueous environment, as would be found in natural soil systems. The
majority of these studies utilized nuclear magnetic resonance (NMR) techniques and were
focused on VX degradation and reaction pathways. Two recent NMR studies did examine the
interaction of VX with soil and soil components, but again, the emphasis was on VX degradation
and reaction pathways,[14,15] not on sorption processes. Two other studies examined the
degradation of VX on various soils but used gas chromatographic (GC) and enzymatic protocols
to determine the presence of VX and select degradation products.[16,17] Again, the emphasis of
these two GC-based studies was on VX degradation and reaction pathways and not on sorption
processes. Only one study was found that specifically investigated VX sorption from dilute
aqueous solution onto environmental surfaces, but only a limited amount of work had been
performed, and no sorption model parameters, such as partition coefficients (K) or saturation
capacities (S_{max}), were reported.[18,19] An enhanced mechanistic understanding of how VX
interacts with environmental surfaces is critical to the development of effective countermeasures,
predictive modeling capabilities, and enhanced detection capability for illicit-use scenarios.
Information from this study will increase understanding of the fundamental principles related to
the sorption of VX with a variety of environmental surfaces. Increased understanding of the
fundamental principles of sorption will benefit multiple Department of Defense (DoD)-funded
efforts. Preliminary results from this effort were presented at the DoD-sponsored Chemical and
Biological Defense Science and Technology Conferences held in 2010 and 2011.[20,21]

          The thermodynamic characteristics and sorption isotherm factors *measured* during
this study could be used in predictive models (fate, transport, hazard mitigation) to update source
terms and potentially improve the models. In many cases, model source terms for the partition
coefficients (K) related to sorption or partitioning processes are *estimated* using organic carbon
partitioning coefficients (K_{OC}), which can be measured, but are typically estimated using
octanol–water partitioning coefficients (K_{OW}).[22–24] This estimation is based on the assumption
that a soil's organic carbon content is the only determinant of the sorption of a chemical from the
water onto the soil. However, recent studies have concluded that the use of K_{OC} values can lead
to inaccurate estimates of sorption processes in soil systems.[25–27] As examples, the System for
Hazard Assessment of Released Chemicals and PEARL models, which use K_{OC} and K_{OW} values

1

to estimate partition coefficients, could possibly be improved by incorporating measured *K* values generated during this study.[28,29]

1.2 Study Objectives

The primary objective of this study was to demonstrate the utility of isothermal titration calorimetry (ITC) as a tool for investigating the fate and transport of VX and other chemicals in soil environments. The intention was not to conduct an exhaustive investigation into the interaction, but to conduct a proof-of-concept study on the applicability of ITC as a tool to help elucidate sorption mechanisms. A secondary objective of this effort was to measure and report thermodynamic and kinetic characteristics that could be useful to the chemical defense research community.

2. EXPERIMENTAL PROCEDURES

2.1 Substrate Description

Three clay minerals were evaluated during this study: two montmorillonites and one kaolinite. Montmorillonite, a member of the smectite family, is a 2:1 clay, consisting of a single octahedral sheet between two tetrahedral sheets. Montmorillonites generally have high cation-exchange capacities (CECs) that range from 80 to 120 meq/100 g and a high shrink-swell capacity, depending on water content and exchangeable cation.[30] The shrink-swell capability and high CEC capacity are due to permanent layer charges and are not significantly influenced by bulk solution pH.[30] The shrinking and swelling of montmorillonite allows hydrated cations to exchange between the 2:1 layers. Kaolinite, a member of the kaolin family, is a 1:1 clay, consisting of a single silicon-containing tetrahedral sheet linked to a single aluminum-containing octahedral sheet via sharing of oxygen atoms. The 1:1 layers are held together through electrostatic bonding. Kaolinites generally have low CEC values that range from 1 to 10 meq/100 g.[30] The CEC of kaolinites is generally due to variable charges associated with the clay edges and is significantly influenced by the pH of the bulk solution.[30]

The first montmorillonite was a high-purity montmorillonite clay mined from bentonite deposits in Wyoming. This clay, identified as Suspengel 200, was purchased from Reade Advanced Materials (Providence, RI). Suspengel 200 was used in previous studies in which the fate of CWA was examined in a variety of sample matrices.[14,15,31] The second montmorillonite was a highly processed clay that is commonly used as a catalyst in organic chemistry reactions.[32–34] The exact procedure used to modify this clay is proprietary but consists of activating the clay with aqueous mineral acid.[32] This second montmorillonite, identified as Aldrich K10, was purchased from Sigma-Aldrich (St. Louis, MO). The reagent-grade montmorillonite was included in the current study because it has been used in other agent fate studies.[14,15,18,19] The kaolinite is a white-firing, plastic kaolinite mined from claystone deposits in Georgia. This clay, identified as no. 6 tile kaolin, was purchased from Kentucky-Tennessee Clay Company (now Imerys; Sandersville, GA). The kaolinite was used in previous studies that examined the fate of CWA in a variety of sample matrices.[14,15,31] These clays were characterized using standard soil-analysis methodologies by an outside soil-analysis laboratory. The clay characteristics are summarized in Tables 1 and 2.

Table. 1. Characteristics of Clay Substrates Used in This Study

Parameter	Substrate		
	Aldrich K10	Suspengel 200	Kaolinite
BET(N_2) surface area (m^2/g)	247.2	29.70	26.24
Bulk water pH	3.50	8.85	5.12
Bulk Adams-Evans (A-E) buffer pH[a]	5.21	8.25	7.77
Exchangeable Ca^{2+} (meq/100 g)[b]	3.6	18.6	2.1
Exchangeable Mg^{2+} (meq/100 g)[b]	3.1	7.2	1.2
Exchangeable K^+ (meq/100 g)[b]	0.27	1.31	0.10
Exchangeable Na^+ (meq/100 g)[b]	0.28	18.4	0.23
Exchangeable acidity (meq/100 g)	9.87	ND	0.64
Total CEC_{A+B} (meq/100 g)[c]	17.1	45.6	4.28
Total carbon (wt%)	0.03	0.37	0.22
Total hydrogen (wt%)	1.06	1.53	1.41
Total nitrogen (wt%)	0.04	0.08	0.02
Total sulfur (wt%)	0.28	0.45	0.32

[a] A-E buffer; initial pH was 8.00.
[b] Cation displaced from clay with pH 7.0 ammonium acetate buffer.
[c] Sum of displaced cations and exchangeable acidity.
Note: Analyses were conducted on substrates as received from the vendor.
ND, non-detect

Table 2. Composition of Clay Substrates as Determined by
X-Ray Fluorescence and X-Ray Diffraction

Type of Clay	Total Elemental Composition (wt%)[a]
Aldrich K10	73.7% SiO_2; 18.3% Al_2O_3; 3.39% Fe_2O_3; 2.17% MgO; 1.39% K_2O; 0.485% TiO_2; 0.188% CaO; 0.126% Na_2O; 0.0741% ZrO_2; 0.0371% SO_3; 0.0370% P_2O_5; 0.0145% MnO
	XRD results are consistent with this material being a montmorillonite clay. Random basal spacing of 1.49 Å, with a glycolated spacing of 17.4 Å
Suspengel 200	65.3% SiO_2; 23.4% Al_2O_3; 3.92% Fe_2O_3; 3.35% MgO; 0.450% K_2O; 0.150% TiO_2; 1.10% CaO; 1.75% Na_2O; 0.0418% ZrO_2; 0.399% SO_3; 0.0451% P_2O_5; 0.0311% MnO
	XRD results are consistent with this material being a montmorillonite clay. Random basal spacing of 1.49 Å, with a glycolated spacing of 17.2 Å
Kaolinite	51.8% SiO_2; 45.9% Al_2O_3; 0.829% Fe_2O_3; 0.181% MgO; 0.389% K_2O; 0.434% TiO_2; 0.109% CaO; 0.0210% Na_2O; 0.0238% ZrO_2; 0.0254% SO_3; 0.1920% P_2O_5; MnO (ND)
	XRD results are consistent with this material being a kaolinite clay

[a] The oxide form was assumed, not determined. In all cases, the 12 reported oxides made up >99.9 wt% of the substrate.

Note: Analyses were conducted on the substrates as received from vendors. Only the 12 most abundant elements are reported; results are reported in the oxide form typically present in soils.

ND, non-detect; XRD, X-ray diffraction

In addition to the clay minerals described earlier in this section, three additional substrates were utilized during this study. A naturally derived garden soil amendment, identified as humus, was purchased from Frey Brothers (Quarryville, PA). Two natural soils, identified as MCL lot no. 968 and HCB lot no. 969, were collected in North Dakota and provided by Battelle Memorial Institute (Columbus, OH). The collection, preparation, and characterization of these three substrates has been previously described,[35,36] and only select characteristics are summarized in this report. The humus was determined to have a bulk water pH of 7.2, moisture content of 45.0%, BET_{N2} surface area of 5.32 m^2/g, organic matter content of 16.6%, total nitrogen content of 0.9%, and organic nitrogen content of 0.9%. The MCL soil was found to have a bulk water pH of 5.8, organic matter content of 5.5%, organic carbon content of 3.1%, BET_{N2} surface area of 45.31 m^2/g, sand content of 33%, silt content of 30%, clay content of 37%, CEC of 25.4 meq/100 g, and a dry fraction of 0.8554. The HCB soil was found to have a bulk water pH of 7.2, organic matter content of 7.2%, organic carbon content of 5.2%, BET_{N2} surface area of 30.80 m^2/g, sand content of 19%, silt content of 52%, clay content of 29%, CEC of 26.4 meq/100 g, and a dry fraction of 0.7650. The MCL soil was classified as a clay loam, and the HCB soil was classified as a silty clay loam. In both soils, the predominant clay minerals were, in decreasing order of abundance, kaolinite, illite, and smectite.

2.2   Titrant Description and Preparation

        The neat VX used in this study, identified as VX-U-7330-CTF-N, was obtained from the Chemical Agent Standard Analytical Reference Material (CASARM) branch of the U.S. Army Edgewood Chemical Biological Center (ECBC). The VX was clear and colorless and was determined to have an average purity of 93.8 ± 0.4 wt% using established protocols.[37] The VX contained 0.51 ± 0.04 wt% 2-(diisopropyl)aminoethanethiol (RSH; $C_8H_{19}NS$, CAS no. 41480-75-5) and 0.56 ± 0.15 wt% *S,S*-bis-(2-diisopropylaminoethyl) methylphosphonodithioate (VX-bis; $C_{17}H_{39}N_2OPS_2$, CAS no. 16943-13-4). The bis(2-diisopropylaminoethyl) sulfide (RSR; $C_{16}H_{36}N_2S$, CAS no. 110501-56-9) and bis(2-diisopropylaminoethyl) disulfide (RSSR; $C_{16}H_{36}N_2S_2$, CAS no. 65332-44-7) were synthesized in-house, and had average purities of 89.3 ± 0.08 and 93.4 ± 1.00 wt%, respectively. The purities were determined using an established gas chromatography–thermal conductivity detector protocol.[38] Also, the RSR contained 5.63 wt% of RSSR as an impurity, and the RSSR contained 0.284 wt% of RSR as an impurity. The ethyl methylphosphonic acid (EMPA; $C_3H_9O_3P$, 98 wt%, CAS no. 1832-53-7) and methyl phosphonic acid (MPA; CH_5O_3P, 98 wt%, CAS no. 993-13-5) were purchased from Sigma-Aldrich (Milwaukee, WI) and were used as received. The RSH (98 wt%) was purchased from Cerilliant Corporation (Round Rock, TX) as the hydrochloride salt and was used as received. The chemical structures of the titrants are illustrated in Figure 1.

        Individual solutions of each titrant were prepared gravimetrically by weighing out aliquots of neat titrant into a container and then adding a known volume of pH 4.3 buffer. The concentration varied with each titrant, but VX solutions were prepared at an initial concentration of ~8 mM and diluted as required. In all cases, the final pH of each titrant solution was determined to be 4.3. Titrant solutions were refrigerated (~4 °C) when not in use and were stored in 125 mL Nalgene polypropylene bottles. VX is very stable at pH 4.3, with a reported half-life of ~3 months for solutions with pH values between 4 and 5 and maintained at 25 °C.[39] At 4 °C, the half-life of VX is considerably longer and estimated to be greater than 2 years.[39] With the exception of RSH, the other titrants are extremely stable in aqueous environments, with the half-life of EMPA in water estimated to be greater than 30 years.[40]

        The use of cosolvents to prepare titrant solutions was avoided because the addition of cosolvents can have a significant impact on adsorption of chemicals to mineral surfaces. In a study examining the interaction of pinacolyl methylphosphonofluoridate (soman, GD; $C_7H_{16}NO_3P$, CAS no. 96-64-0) with suspensions of portland cement, it was found that small amounts (1–2%) of 2-propanol added to the suspension significantly affected both sorption rate and isomeric fractionation.[41] In another study, the addition of low molecular weight alcohols to aqueous suspensions of hematite significantly affected the ionic equilibria at the hematite–water interface, which significantly affected sorption processes.[42] In a third study, the sorption of acetonitrile from water into a montmorillonite clay was found to significantly affect basal spacings, which influenced the sorptive process.[43] In addition to perturbing sorption processes, the addition of cosolvents has been found to increase hydrolysis rates of phosphorus esters by lowering the enthalpy of activation.[44]
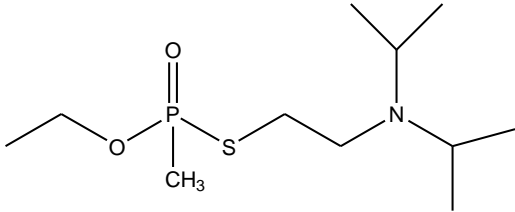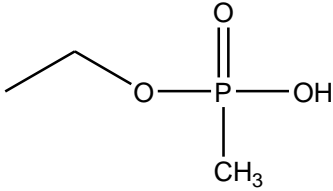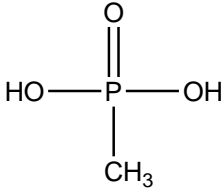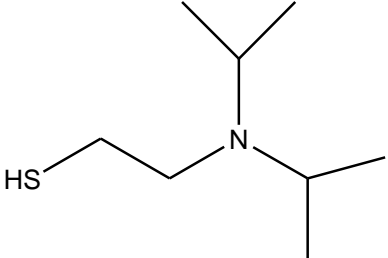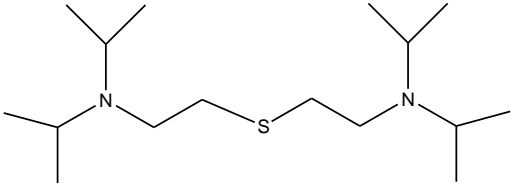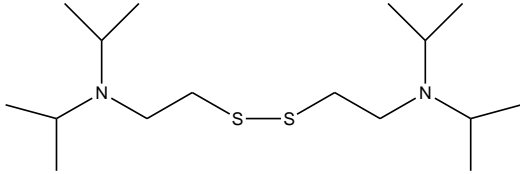
Figure 1. Chemical structures of titrants used in this study.

2.3   Reagents

        All chemicals utilized in this study were typically of American Chemical Society (ACS) reagent grade and were used as received from the manufacturers. Sodium acetate ($C_2H_3NaO_2$, CAS no. 127-09-3), sodium chloride (NaCl; 99+%, CAS no. 7647-14-5), sodium phosphate, dibasic (Na_2HPO_4, 99+%, CAS no. 7558-79-4), sodium carbonate (Na_2CO_3, CAS no. 497-19-8), sodium hydrogen carbonate ($NaHCO_3$, CAS no. 144-55-8), acetic acid (CH_3COOH, CAS no. $C_2H_4O_2$), hydrochloric acid (HCl, 37% in water, CAS no. 7647-01-0), formic acid (CH_2O_2, 99+%, CAS no. 64-18-6), acetonitrile (C_2H_3N, CAS no. 75-05-8), isopropyl alcohol (C_3H_8O, CAS no. 67-63-0), and 2-(dibutylamino) ethanol ($C_{10}H_{23}NO$, 99%, CAS no. 102-81-8) were obtained from Sigma-Aldrich (Milwaukee, WI). Sodium sulfate (Na_2SO_4, 99.0+%, pesticide residue grade, 12–60 mesh) was purchased from J. T. Baker (Phillipsburg, NJ). The proprietary capillary electrophoresis (CE) buffer was purchased from Agilent Technologies (Santa Clara, CA). The ASTM Type I deionized water (DIW) was obtained from an in-house system (18 megohm·cm; Thermo Scientific Barnstead Nanopure, Dubuque, IA).

        In addition to the substrates described in Section 2.1 of this report, 12 soil-related standard reference materials (SRMs) were obtained from the National Institute of Standards and Technology (NIST; Gaithersburg, MD). These SRMs were brick clay (SRM 679), flint clay (SRM 97b), plastic clay (SRM 98b), dolomitic limestone (SRM 88b), obsidian rock (SRM 278), basalt rock (SRM 688), estuarine sediment (SRM 1646a), Buffalo River sediment (SRM 8704), San Joaquin soil (SRM 2709), and three glass sands (SRM 165a, 81A, and 1413). A second catalyst-grade montmorillonite, KSF, was obtained from Sigma-Aldrich (Milwaukee, WI). In the screening sorption experiments, the NIST substrates were used as received from the vendor. The clays from Sigma-Aldrich had been converted to the homionic (Na^+) form as part of another project,[45] and all screening experiments were conducted with the homoionic form of the clay.

2.4   Buffer Preparation

        The buffer used in the ITC and sorption isotherm experiments was selected such that the VX would be stable in the bulk solution. In aqueous solutions with pH values ≤6, VX is reported to have a half-life of ~100 days at 25 °C.[39] In addition to being stable under acidic conditions, with reported acid dissociation constant (pK_a) values ranging from 8.60 to 9.78, VX is ~100% ionized when in acidic solution.[46,47] The buffer used in the ITC and sorption isotherm experiments was a pH 4.3, 100 mM sodium acetate buffer adjusted to a total ionic strength of 100 mM with NaCl. The buffer was prepared by dissolving 0.0689 mol of acetic acid, 0.031 mol of sodium acetate, and 0.1 mol of NaCl in 1000 mL of distilled DIW. The buffer was stirred for approximately 15 min before pH was checked; pH was consistently determined to be 4.3 after preparation. Solids were removed from the buffer by vacuum-filtration through a 0.2 μm nylon filter and stored at 4 °C in amber glass bottles.

        The buffer used to extract the samples for determination of semivolatiles was a pH 10, 500 mM carbonate/bicarbonate aqueous solution that had been used previously for the extraction of VX and VX-related products.[48,49] The buffer was prepared by dissolving 500 mmol of sodium carbonate and 500 mmol of sodium hydrogen carbonate in 1 L of distilled DIW. The buffer was stirred for approximately 1 h, and solids were removed from the buffer by vacuum-filtration through a 0.2 μm nylon filter. The buffer was stored at ambient temperature in amber

glass bottles. The initial pH of the buffer was checked, and the pH was also checked after mixing with the sample (pH 4.3 buffer) in the same proportions used during the extraction procedure (Section 2.7.1). The final pH of 10 was determined to be consistently maintained.

2.5   Substrate Suspension Preparation

In a preliminary kinetic sorption profile experiment, the Suspengel 200 substrate was used as received from the vendor, and a suspension was prepared by adding the clay directly to the pH 4.3 buffer. In this preliminary experiment, the VX degraded, as evidenced by accumulation of EMPA in solution. The pH of the bulk solution was determined to be 7.4, suggesting that the EMPA accumulation was due to hydrolysis in the bulk solution and was not related to binding with the substrate. It has been reported in the literature that the presence of carbonate impurities in reference clays accelerates the hydrolysis of carbamate pesticides.[50] A protocol was developed for removing the carbonate impurities from the reference clay.[51] Once the carbonate impurities were removed from the clay, hydrolysis of the carbamate pesticide was no longer accelerated in the presence of the clay.

The clay substrates utilized in the current study were prepared by following the referenced protocol[51] with one modification. In the original protocol, pH 5, 500 mM sodium acetate buffer was used to remove carbonate impurities. In the current study, pH 4.3, 100 mM sodium acetate buffer was used to remove the carbonate impurities. In a typical preparation, ~1000 mg of clay substrate was added to a 40 mL vial containing a stir flea, and 30 mL of pH 4.3 buffer was added. The suspension was stirred at ambient temperature for 3–4 h, and the vial was spun in a low-speed centrifuge. The supernatant was removed, and 30 mL of fresh pH 4.3 buffer was added. The suspension was then allowed to stir overnight at ambient temperature, and the centrifugation/decanting cycle was repeated. A 30 mL aliquot of fresh pH 4.3 buffer was added, and the suspension was stirred at ambient temperature for 30 min, after which the centrifugation cycle was repeated. At this stage, the pH of the supernatant was determined. If the supernatant pH was 4.3, the purification process was considered complete. If the pH was not 4.3, the washing cycles were repeated until the supernatant pH was determined to be 4.3. Typically, no more than three wash cycles were required to achieve a pH 4.3 supernatant.

Once the clay suspensions were purified, the clay fraction was obtained using a gravity sedimentation protocol.[52] The concentration of each clay suspension was determined by removing a representative 2 mL sample, transferring it to a tared glass vial, and placing the vial in a 50 °C drying oven for several days. Once dry, each vial was placed in a desiccator to cool. Once cool, the vials were weighed to obtain the dry weight of the clay/buffer salts. Concurrent controls of 2 mL, pH 4.3 buffer were also prepared and weighed to correct for the weight of the dried buffer salts. The clay suspensions were stored in amber glass jars at ~4 °C.

The humus suspension was prepared as described above for the clay substrates with one modification. After the first wash with pH 4.3 buffer, the suspension was passed through Teflon netting (Industrial Netting; Minneapolis, MN; part no. ET8120, aperture size 0.635×0.127 mm) to remove the large debris (twigs, pebbles, etc.) associated with the original humus material. After removal of the larger debris, the humus material remained noticeably heterogeneous, as evidenced by the three-layered pellet obtained after centrifugation. One of the three layers appeared to consist of a clay mineral.

The clay/humus suspension was prepared by mixing equal amounts (by weight) of the clay and humus substrates, then following the cleaning protocol as described above for the clay substrates with two modifications. After the first suspension in pH 4.3 buffer, the solids were allowed to equilibrate for 72 h instead of the 3–4 h equilibration used to prepare the clay suspensions. The second modification was that after the first wash with pH 4.3 buffer, the suspension was passed through Teflon netting to remove the large debris associated with the original humus material.

2.6 ITC Technique

2.6.1 Background

An established calorimetric technique, ITC, was used to directly determine the thermodynamic parameters of titrants interacting with substrates. The use of ITC provides sensitive, direct quantitative measurement of thermodynamic parameters as an interaction proceeds, as opposed to the collection of data at discrete points. This continuous data collection enables better elucidation of binding mechanisms, particularly when multiple binding mechanisms are occurring during the interaction. The thermodynamic foundations and principles of ITC have been extensively reviewed[53,54] and are not included in this report. The majority of ITC papers have focused on medicinal chemistry applications,[55–57] but researchers have recently been applying ITC to environmental studies.[58–61] A literature search did not reveal any studies that used ITC to investigate the binding of chemical warfare agents in nonmedical applications. An overview of the ITC process is illustrated in Figure 2.
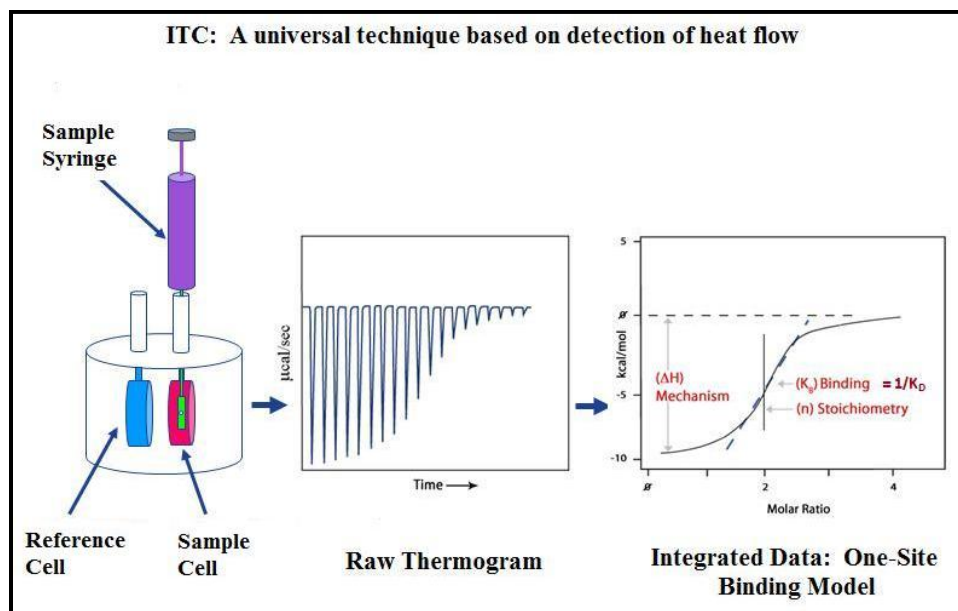
Figure 2. Overview of the ITC process. (Adapted from Frasca, 2009.[67])

9

The use of ITC allowed for direct measurement of the binding energetics and precise determination of the thermodynamics of the binding event. Thermodynamic parameters such as the observed enthalpy (ΔH_{obs}), entropy change (ΔS), Gibbs free-energy change (ΔG), and equilibrium binding constant (K_b) were determined. The simplified governing equations used in this effort were as follows, where R is the universal gas constant (8.314472 $J \cdot K^{-1} \cdot mol^{-1}$) and T is the absolute temperature in kelvins[53,54]

$$\Delta G = -RT \ln K_b = \Delta H - T\Delta S$$

Although K_b, and subsequently, the overall free energy change, can be determined using noncalorimetric techniques such as batch equilibrium sorption isotherms,[62,63] ITC directly determines both K_b and ΔH_{obs}. This allows for the determination of both the enthalpic and entropic contributions to the overall free energy change. An improved understanding of these different energetic contributions to the overall free energy change can provide a more detailed understanding of the binding event(s).

Using the isotherm approach at multiple temperatures, ΔH can be estimated using the following relationship, where R is the universal gas constant and T is the absolute temperature in kelvins[62,63]

$$\ln K_b = -(\Delta H/RT) + (\Delta S/R)$$

If a plot of $\ln K_b$ versus $1/T$ is constructed, the slope of the linear regression line is $-\Delta H/R$. Because ΔH is not always temperature-independent, this linearization approach can result in incorrect estimates of ΔH. Several studies have highlighted this issue and concluded that a calorimetric approach is superior for obtaining thermodynamic characteristics.[64–66]

2.6.2   Equipment

All ITC experiments were conducted using a MicroCal VP-ITC microcalorimeter (MicroCal; Northampton, MA) with a sample cell volume of 1.4509 mL. The reference cell was filled with degassed DIW. In all cases, the samples were vacuum-degassed for at least 5 min before being loaded into the cell or syringe. In all experiments, the substrate suspension was loaded into the sample cell, and the titrant was loaded into a 250 µL syringe. In the typical ITC experiment, 5 µL aliquots of an 8 mM titrant solution were titrated sequentially into the substrate suspension. Each injection typically lasted 10 s with a delay of 300–600 s between injections. The suspension was stirred at 502 rpm, and a total of 40 to 50 injections were titrated into the substrate suspension. Commercially available binding models (Origin, version 7; MicroCal) were used to model the integrated data with the CEC_{A+B} as the "ligand" concentration. The titrations were performed under a variety of experimental conditions, such as different substrate concentrations and temperatures ranging from 278 to 318 K.

2.7   Target Analyte Determination

2.7.1   Semivolatile Analytes

An Agilent model 6890 Plus GC with an Agilent 5975i mass-selective detector
(GC/MSD)was used to determine select semivolatile analytes (VX, RSH, RSR, and RSSR)
during this study. Helium was used as a carrier gas, at an average linear velocity of 42 cm/s, in
pressure pulse mode. All experiments utilized a capillary column with a bonded phase of 5%
phenylmethyl polysiloxane (30 m × 0.32 mm) with a 1 μm film thickness. A 4 mm single
gooseneck deactivated liner, with no packing, was utilized. Instrumental parameters are
summarized in Table 3. The linear external calibration range was established to be 0.1–100 mg/L
for each analyte.

Table 3. GC Instrument Parameters

<div style="border:1px solid black; padding:10px;">

INJECTION PARAMETERS

Injection port: 270 °C   Injection volume: 1.0 μL, pulsed splitless
Injection pulse: 20 psi for 2 min   Post injection dwell: 0.25 min
Sample washes: 1   Purge flow: 50 mL/min at 2.50 min
Sample pumps: 3   Solvent A washes: 1
Solvent B washes: 1   Viscosity delay: 1 s
Solvent A: 2-propanol   Solvent B: methanol

OVEN PARAMETERS

Initial temperature: 50 °C   Initial time: 3.00 min
Ramp: 12 °C/min to 220 °C and hold for 5 min, then 70 °C/min to 275 and hold for 5 min
Equilibration delay: 2.0 min

DETECTOR PARAMETERS

Solvent delay: 6.5 min   Scan range: 40 to 500 amu
Acquisition mode: SIM/scan   Dwell time: 100 ms
MS source: 230 °C   MS quads: 150 °C
Transfer line: 280 °C   SCAN threshold/sample rate: 50/2
SIM acquisition ions for VX: 167, 224, and 252; used m/z 252 for quantitation
SIM acquisition ions for RSH: 128, 146, and 161; qualitative only
SIM acquisition ions for RSR: 127, 144, and 160; used m/z 144 for quantitation
SIM acquisition ions for RSSR: 144, 160, and 193; used m/z 144 for quantitation

</div>

SIM, selective ion monitoring; m/z, mass-to-charge ratio

The chromatographic column selected for use in this project has been used extensively in other analytical methods and found to be rugged and reliable.[48,49,68,69] The injection parameters, such as pressure pulse, post-injection dwell time, etc., were selected based on previous experience in our laboratory.[48,49,68,69]

Extraction vials were prepared by adding 2.0 mL of pH 10 buffer, ~1 g KCl, and 2.0 mL of extraction solvent (1:1, v/v, trimethylpentane/methylene chloride) to a 7 mL glass vial. The threads of the vial were wrapped with Teflon tape to prevent leaks, and the cap had a Teflon-faced silicone liner. The extraction vials were prepared in advance and stored at ~4 °C for at least 12 h prior to use. The extraction was started by adding 0.5 mL of sample solution (filtered or unfiltered) to the vial and vortexing it for ~30 s. The layers were allowed to separate, and the vortex step was repeated for a total of three cycles. Once the layers separated, an aliquot of the organic (upper) layer was transferred to a clean vial containing ~100 mg of Na_2SO_4, and the vial was swirled. If the Na_2SO_4 was still clumping, additional Na_2SO_4 was added until the extract was dry. Once it was dried (as evidenced by free-flowing Na_2SO_4), 1000 µL of the dried extract was transferred to a deactivated amber GC vial, and 100 µL of modifier solution was added. The vial was closed with a crimp-top seal and stored at –20 °C until it was analyzed. In this extraction process, the sample was either whole substrate suspension or the recovered filtrate after pressure filtration of the suspension through a 0.2 µm nylon Acrodisc filter.

The term "matrix-induced chromatographic response enhancement" was coined in the early 1990s to describe a phenomenon whereby the instrument response per unit amount of analyte is significantly different in a sample extract than in a pure solvent.[70,71] This phenomenon has previously been documented to occur during the determination of residual VX,[48,49] and the approach of matrix-matching samples and standards was used to normalize the response differences in the current study. A modifier solution consisting of 10,000 mg/L dibutylaminoethanol in 2-propanol was used to matrix-match standards and sample extracts during this study.

Spike recovery data were generated by spiking a mixture of VX, RSR, and RSSR into pH 4.3 buffer and applying the sample preparation and analysis protocols described in the previous paragraphs. Multiple replicates ($n = 7$) were independently prepared and analyzed at a single spike level of 100 µg/L in the pH 4.3 buffer. In addition to the spiked samples, seven unspiked samples were also prepared and analyzed. In all cases, no VX, RSR, or RSSR was detected in any of the unspiked samples. The average spike recoveries and sample standard deviations (±SSDs) were 92.3 ± 4.56, 89.1 ± 6.28, and 85.4 ± 5.89 for VX, RSR, and RSSR, respectively. Overall detection limits were estimated by using the average signal-to-noise ratio and extrapolating back to the sample concentration that would yield a signal-to-noise ratio of 3. The overall detection limits were estimated to be 48, 34, and 27 µg/L for VX, RSR, and RSSR, respectively. The spike recovery data indicate the analytical method was under control and suitable for quantitative analysis of VX, RSR, and RSSR in the pH 4.3 buffer. The method will detect RSH, but quantitation was not attempted because RSH readily oxidizes to RSSR.[40,72]

2.7.2   Nonvolatile Analytes

An Agilent model 1100 liquid chromatograph (LC) with an Agilent model G1946D mass spectrometer (MS) was used to determine select nonvolatile analytes (MPA, EMPA, and EA 2192) during this study. All experiments utilized a 100×2.1 mm Hypercarb column (part no. 35005-102130; Thermo-Scientific; Bellefonte, PA) with 5 µm particle size packing. Incorporating the use of a Hypercarb column allowed the chromatographic resolution of VX and EA 2192. The use of a Hypercarb column to achieve chromatographic resolution of VX and EA 2192 was also recently reported in the open literature.[73] A 10×2.1 mm Hypercarb guard column was used prior to the analytical column. Instrumental parameters are summarized in Table 4. A novel feature of this method was the incorporation of isotopically labeled MPA and EMPA as internal standards. The working calibration range was established to be 0.005–0.500 mg/L for each targeted analyte.

Table 4. LC/MS Instrument Parameters

INJECTION PARAMETERS

Injection mode: standard	Injection volume: 25.0 µL
Draw speed: 100 µL/min	Eject speed: 100 µL/min
Draw position: 0.0 mm	Stop time: As pump
Post time: off	

FLOW PARAMETERS

Column flow: 0.350 mL/min	Column temperature: 35 °C
Stop time: 25.0 min	Post time: 7.00 min

Mobile phase A: 98% water, 2% acetonitrile, 0.1% formic acid
Mobile phase B; 99.9% acetonitrile, 0.1% formic acid
Gradient: 0.00 min, 0% B; 4.5 min, 0% B; 5.50 min, 5.0% B; 10.0 min, 5.0% B; 16.0 min, 55.0% B; 17.0 min, 100% B; 19.0 min, 100% B; 20.0 min, 0% B. NOTE: flow changed to 0.50 mL/min at 17.0 min

DETECTOR PARAMETERS

Ionization mode: API-Electrospray	Polarity: positive
Acquisition mode: SIM	Fragmenter: 60 V
Gas temperature: 300 °C	Drying gas: 3.0 L/min
Nebulizer pressure: 50 psig	Capillary voltage: 4000 V
Dry gas flow: 9 L/min	

SIM acquisition ions: 97, 100, 210, 125, 130, 240, 268, and 273

SIM, selective ion monitoring

13

The LC/MS method selected for use in this project has been used in other VX-related projects, and method details have been previously reported.[74,75] The analytes are determined directly, without derivatization or extraction. Samples were pressure-filtered through a 0.2 μm nylon Acrodisc filter, and the filtrate was diluted 1:1 with mobile-phase A prior to analysis.

An Agilent model 3D CE system (Agilent Technologies; Wilmington, DE) with an ultraviolet (deuterium lamp) diode array detector was used to determine select nonvolatile analytes (MPA, EMPA, and phosphate) during this study. The separation capillary was a piece of bare-fused silica with an external polyimide coating that was removed at the optical window. Two capillaries, each of different dimensions, were used for three distinct methods. The capillary dimensions were 64.5 cm (total length) × 50 μm i.d. for a capillary zone electrophoresis method with indirect ultraviolet detection. A proprietary Agilent buffer (part no. D-76337) was used for all analyses in this study.

The CE method selected for use in this project has been used extensively in other CWA-related projects, and method details have been previously reported.[76–78] The analytes were determined directly without derivatization or extraction. Samples were pressure-filtered through a 0.2 μm nylon Acrodisc filter, and the filtrate was diluted with CE mobile phase prior to analysis.

2.8   Batch Equilibrium Sorption Isotherms

Batch equilibrium sorption isotherms have been used extensively to evaluate binding of non-CWA chemicals to environmental matrices.[79–81] This approach was used to study the binding of CWA degradation products to soils,[82] but only one study was found in which this sorption isotherm approach was used to evaluate VX binding to soil and soil components.[18,19] This isotherm approach was also used extensively in U.S. Environmental Protection Agency studies.[83,84] The theoretical basis of batch equilibrium sorption isotherms has been extensively reviewed and is not included in this report.[83,84] The data generated in the current study was evaluated using nonlinear sorption isotherm models developed at the U.S. Department of Agriculture.[85–87]

In the current study, the batch equilibrium sorption isotherms were constructed using a variable substrate-to-solution (STS) ratio protocol.[83] In this protocol, the buffer solution has a constant solute concentration, and the mass of substrate is varied. This results in variable STS ratios in the isotherm profile. This approach generates environmentally conservative estimates of sorption and accounts for the effects of competition and other parallel processes.[83] Although the variable STS ratio protocol accounts for these effects, it does not elucidate the exact nature of these other processes. Data from the range-finding ITC runs (Section 3.1.1) were used to establish saturation levels, which allowed appropriate STS ratios to be quickly chosen for use in the sorption isotherm experiments.

2.9   Settling Rate Determination

A Varian (Agilent Technologies) Cary 300 Bio UV-visible spectrophotometer with temperature controller and multicell cuvette holder was used to determine the turbidity of select substrate suspensions during this study. All experiments were conducted in 4.5 mL, 10 mm path length, disposable polystyrene cuvettes at a temperature of 298 K. A 5×2 mm Teflon-coated stir flea was used to mix the substrate suspensions. Data was acquired in absorbance mode, at a 500 nm wavelength. In all cases, sample data acquisition was referenced against pH 4.3 buffer. This approach to determining turbidity has been reported in the literature.[88,89]

In a typical experiment, 3 mL of vacuum-degassed substrate suspension was placed in the cuvette, and the cuvette was placed into the instrument to equilibrate to 298 K while being stirred. Once equilibrated to temperature, baseline absorbance was collected for 5 min. An aliquot of 8 mM VX titrant solution that had been preequilibrated to 298 K was then added, and the absorbance was monitored for an additional 10 min. Ten minutes after the VX titrant was added, stirring was turned off, and the absorbance was monitored until the absorbance values reached a steady value. The settling rate was taken as the slope of absorbance versus time once the stirring was terminated.

3.   RESULTS AND DISCUSSION

3.1   ITC Results

During the current study, two quality-control (QC) checks were periodically performed to establish that the ITC was performing correctly. These checks were standard protocols that were recommended by the instrument manufacturer.[90,91] The first QC check was performing water-into-water titrations to determine whether the ITC was operating at optimal performance. In these water-into-water QC checks, 10 μL of DIW was injected into the sample cell, which had been filled with DIW. The DIW had been thoroughly vacuum-degassed, and all experiments were conducted at 303 K. There was no established performance standard for the water-into-water QC check, but each heat-pulse was typically less than 0.02 μcal/s. In the current study, periodic water-into-water QC checks were performed to provide insight into when components (syringe, cell, etc.) required cleaning. The second QC check involved the titration of 1.0 M calcium chloride into 0.1 M ethylenediaminetetraacetic acid (EDTA). Each solution was commercially prepared in 10 mM of pH 6.0 MES (2-(N-morpholino)ethanesulfonic acid) buffer and supplied as a kit by the instrument manufacturer. Each kit included lot-specific reference values for the thermodynamic characteristics, such as K_b and ΔH. The results obtained for all reference values for QC checks during the current study were within the acceptance criteria provided by the instrument manufacturer.[91]

3.1.1   Range-Finding Runs

An initial series of ITC runs was conducted at 298 K to establish whether any significant heat flows could be detected when various titrants (VX, EMPA, MPA, RSH, and phosphate) interacted with the three clay substrates. All clay substrate suspensions were prepared in pH 4.3 buffer with concentrations of 6200 mg/L Suspengel 200, 6600 mg/L Aldrich K10, and

6300 mg/L kaolinite. These substrate concentrations corresponded to initial STS ratios ranging from 1:161 to 1:152. The STS ratios changed during the course of the titration, with the final STS ratios ranging from 1:189 to 1:178. In addition to the runs with substrate, parallel blank runs were obtained by adding titrant solution into pH 4.3 buffer under conditions identical to those used during the runs conducted with substrate. Attempts to use RSH as a titrant were unsuccessful, due to apparent oxidation of the RSH to RSSR during the course of the titration. This oxidation was confirmed by analysis of select samples by the GC/MSD method described in Section 2.7.1.

Attempts to use RSR and RSSR as titrants were unsuccessful because of solubility issues. The aqueous solubilities of RSR and RSSR are low, being 1.2 and 9.5 mg/L, respectively.[40] In the runs with RSR and RSSR, the heat flows generated during each injection cycle were too low for the ITC to reliably detect. Thermograms in which VX, MPA, and EMPA were used as titrants are illustrated in Figures 3–5. The VX generated a significant heat signal when interacting with both the Suspengel 200 and Aldrich K10 substrates, but only a trace amount of heat was detected when VX interacted with the kaolinite. The lack of heat generation during interaction with kaolinite might have been due to the low CEC_{A+B} of kaolinite (4.28 meq/100 g) versus the CEC_{A+B} of the two montmorillonites (45.57 and 17.12 meq/100 g), neutralization of variable edge charges in the kaolinite at this pH,[30] a near-zero constant pressure heat capacity change due to binding (ΔC_p), or a combination of these three factors. There was no detectable interaction when EMPA was titrated into any of the substrate suspensions, although small heat flows were detected when MPA was titrated into the substrate suspensions. The trace-level heat flows detected during the MPA titrations are thought to have been due to phosphate, which was present as an impurity (~85 mg/L) in the MPA solution. Based on these range-finding runs and the kinetic profiles described in Section 3.2.1, it was decided to focus the current study on the two montmorillonite substrates, Suspengel 200 and Aldrich K10.

In the course of these initial range-finding ITC runs, differences in behavior between the two montmorillonites were noted. Most notably, when VX was titrated into Suspengel 200 to the point of near or total saturation, flocculation of the clay was observed when the sample was removed from the ITC sample cell. Flocculation of the clay was not observed when VX interacted with the Aldrich K10 substrate. Furthermore, the thermograms generated during the titration of the Suspengel 200 substrate were characterized by additional exothermic peaks that occurred at or near the saturation point but were not always associated with an individual titration point. These exotherms were significant in both magnitude and number and were assumed to be associated with the flocculation event. In contrast, this exothermic event was not observed when VX was titrated into the Aldrich K10 substrate. This difference is illustrated in Figure 6. In the titrations of Suspengel 200 with VX, the flocculation appeared to coincide with saturation of the substrate with VX, being in the range of 10–12 wt% VX. A titration of Suspengel 200 with VX was performed outside the ITC and was video-recorded. Select stills were extracted from the video and are illustrated in Figure 7. Scanning electron microscope (SEM) micrographs were obtained of substrate suspensions with and without the addition of RSH and are shown in Figure 8. As with the VX, titration with RSH also led to flocculation of the Suspengel 200 but not the Aldrich K10. The use of RSH was required because the samples were sent to a non-agent laboratory to obtain the SEM micrographs. These photographs clearly illustrate the changes in physical appearance and size that occurred when the clay interacted with VX and RSH.

16
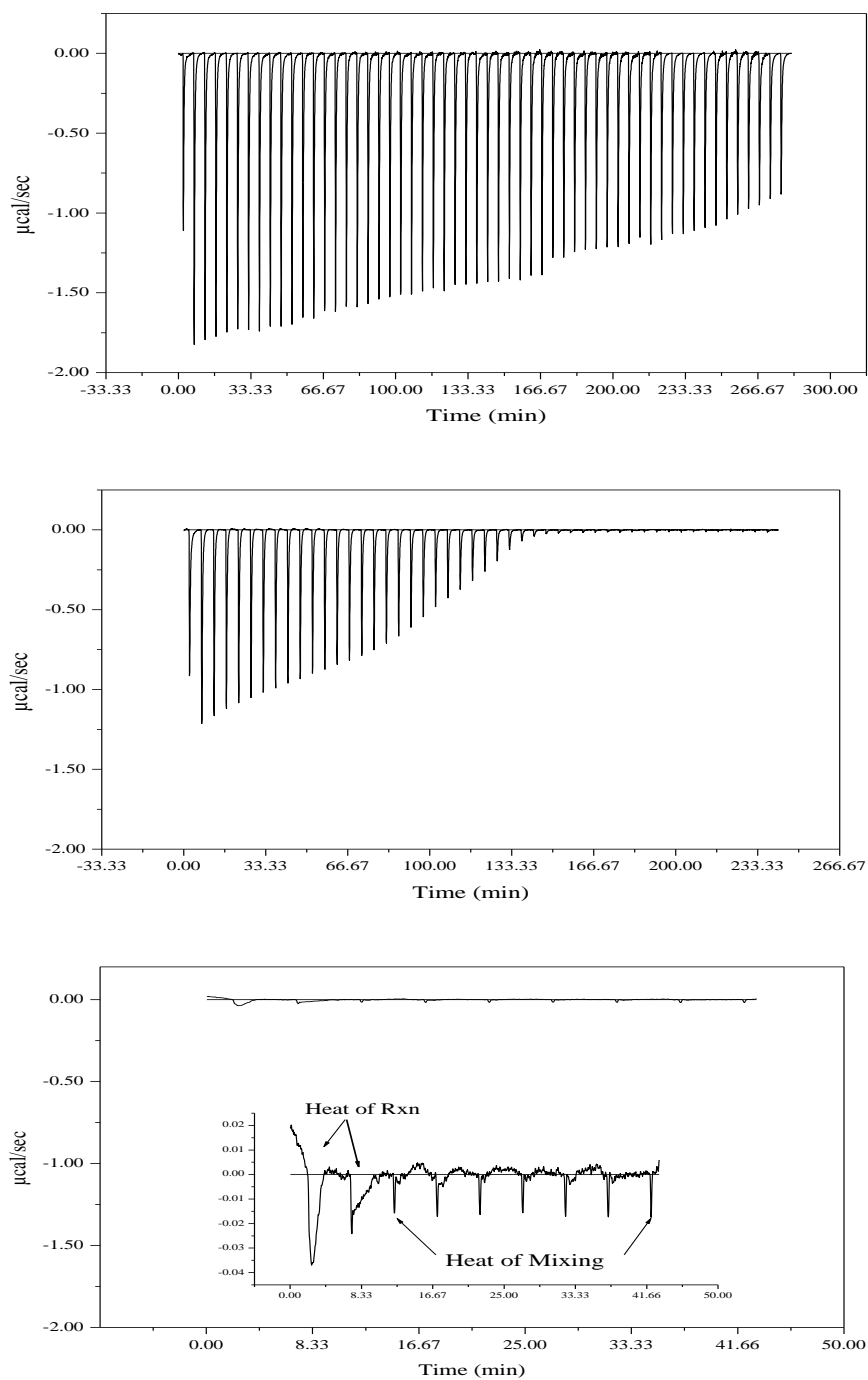
Figure 3. Thermograms generated from the titration of VX into three clay substrates. All reactions were conducted at 298 K using 4 mM VX. *Top*: 6200 mg/L Suspengel 200; *middle*: 6600 mg/L Aldrich K10; *bottom*: 6,300 mg/L kaolinite (*inset*: close-up view).
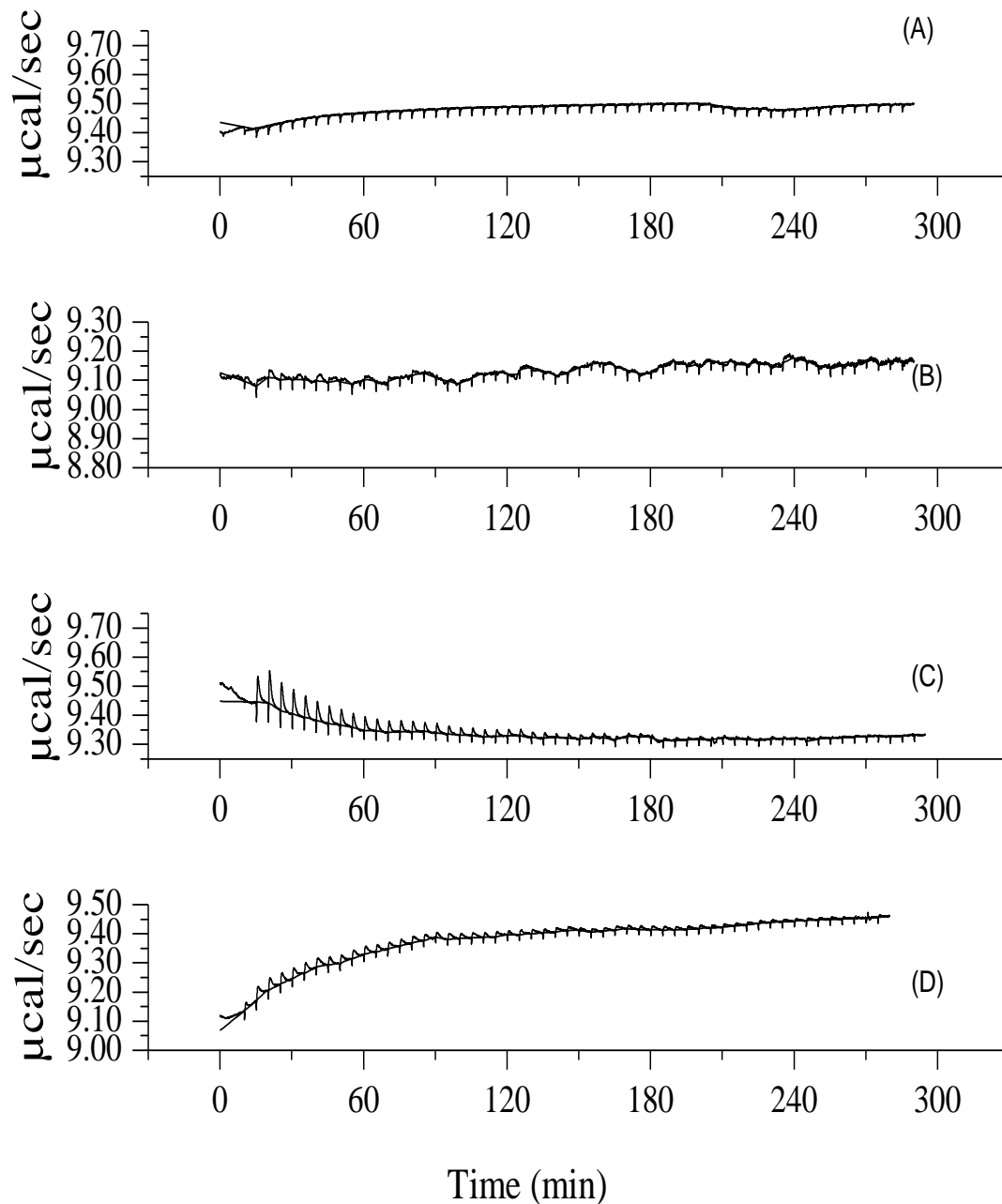
Figure 4. Thermograms generated from the titration of MPA into three clay substrates. All reactions were conducted at 298 K using 8 mM MPA. *A*: MPA into buffer blank; *B*: 6200 mg/L Suspengel 200; *C*: 6600 mg/L Aldrich K10; and *D*: 6300 mg/L kaolinite. The heat flows detected during these titrations were thought to be due to phosphate impurity in the MPA.

18
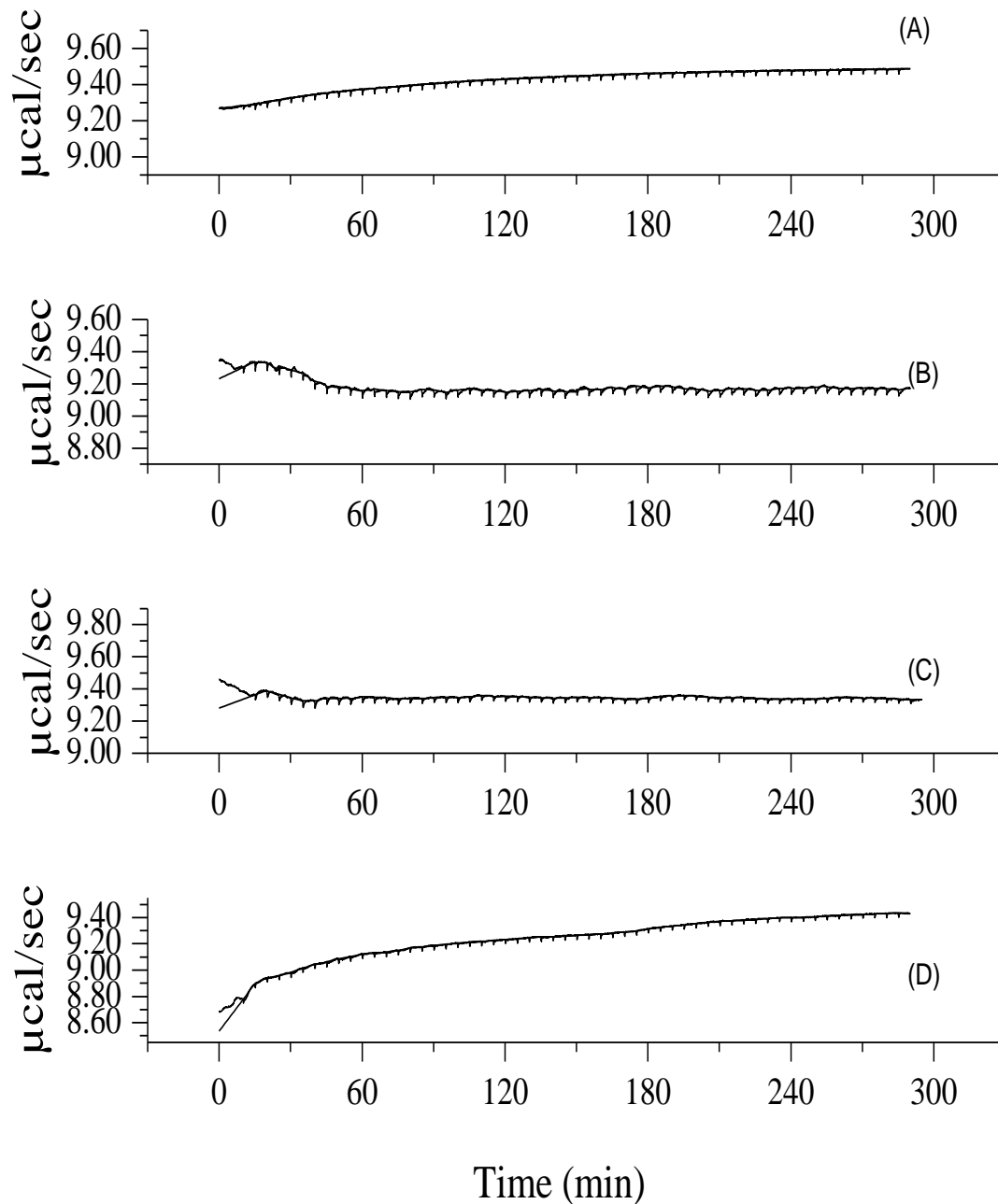
Figure 5. Thermograms generated from the titration of EMPA into three clay substrates. All reactions were conducted at 298 K using 8 mM EMPA. *A*: EMPA into buffer blank; *B*: 6200 mg/L Suspengel 200; *C*: 6600 mg/L Aldrich K10, and *D*: 6300 mg/L kaolinite.

19
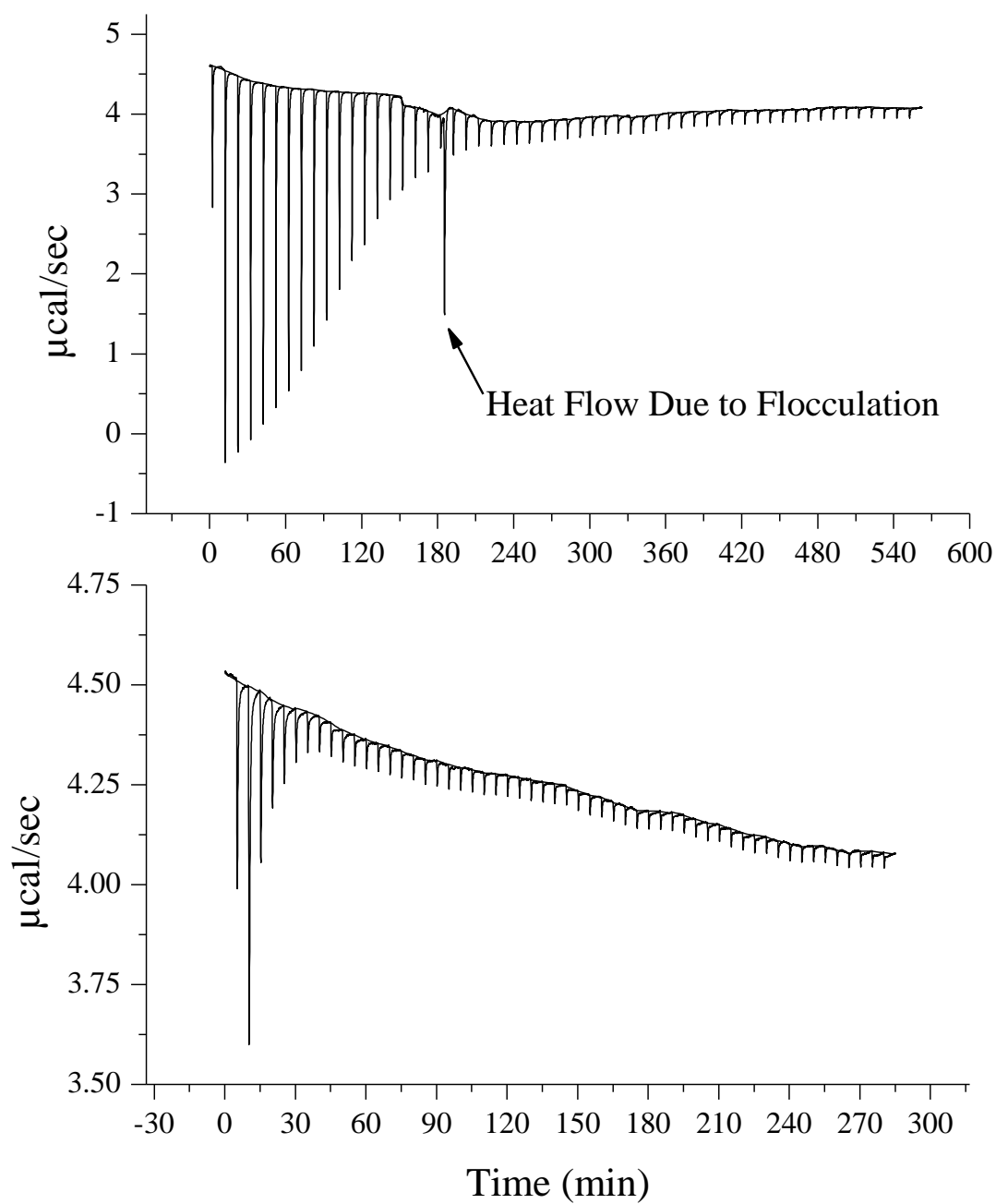
Figure 6. Flocculation event. Thermograms generated from the titration of 8 mM VX into 6200 mg/L Suspengel 200 (*top*) and 6600 mg/L Aldrich K10 (*bottom*). All reactions were conducted at 298 K.

a. No VX added; being stirred.

b. ~5 wt% VX added; being stirred.

c. ~12 wt% VX added; being stirred.

d. ~12 wt% VX added; stirring stopped.
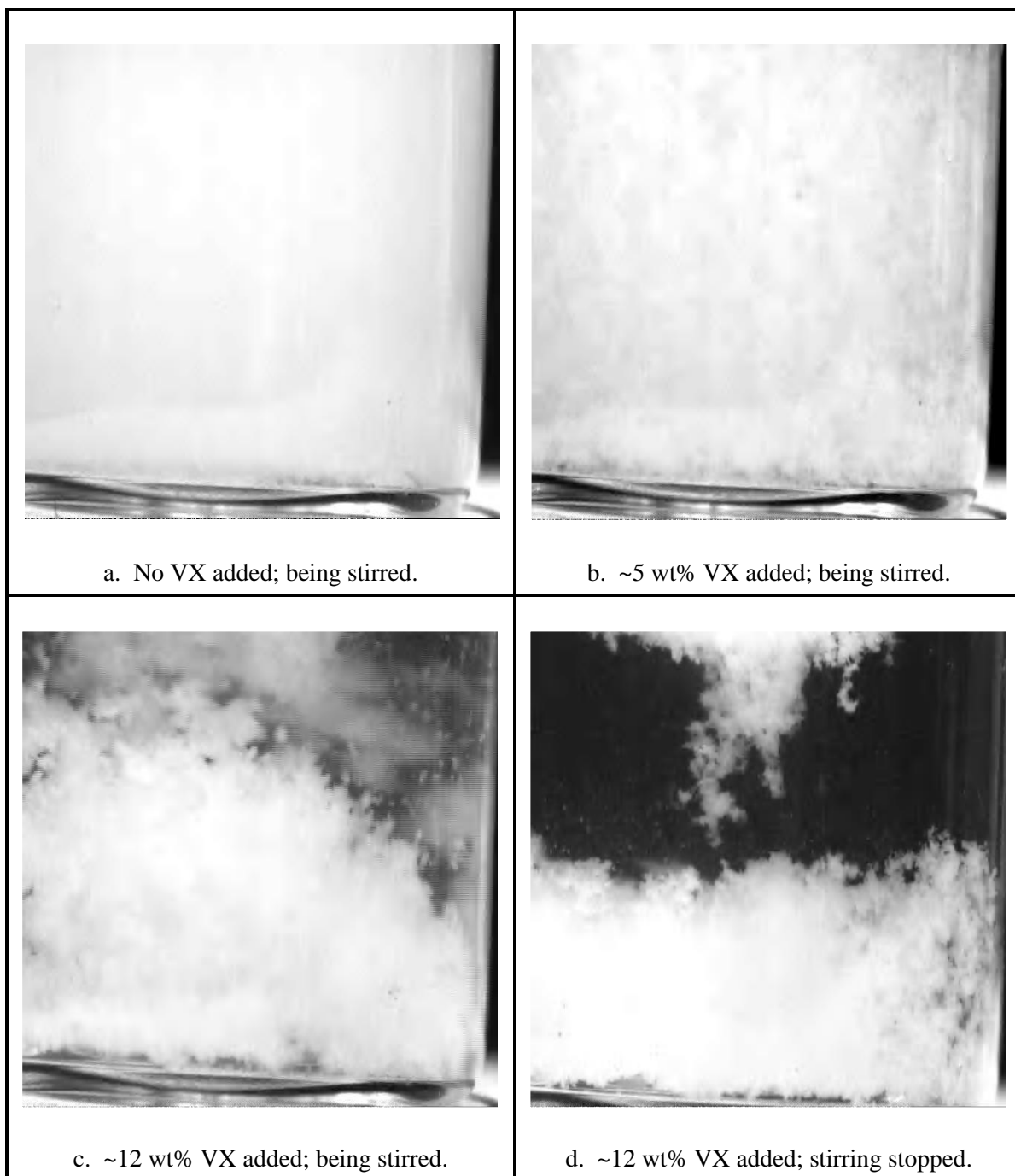
Figure 7. Flocculation of Suspengel 200 by VX. The titration was conducted in a glass vial at ambient (~295 K) temperature.

| Suspengel 200, no RSH added. | Suspengel 200, saturated with RSH. |
| Aldrich K10, no RSH added. | Aldrich K10, saturated with RSH. |

Figure 8. SEMs of clay substrates. RSH was used to saturate each substrate. Micrographs were obtained by drying the substrates onto glass slides. Magnification, ×5000; white bar, 5 µm scale.

A second series of ITC runs was conducted at 298 K, with substrate concentrations ranging from 350 to 6570 mg/L in pH 4.3 buffer. These concentrations corresponded to initial STS ratios ranging from 1:2860 to 1:152. The STS ratios changed during the course of the titration, and the final STS ratios ranged from 1:3350 to 1:178. In most cases, the substrate was Suspengel 200, but one run using Aldrich K10 was also performed. In all cases, the titrant was 8 mM VX in pH 4.3 buffer. In addition to the runs with substrate, parallel blank runs were conducted by adding VX titrant solution into pH 4.3 buffer under conditions identical to those used during the runs conducted with substrate. Example raw thermograms are provided in Figure 9. Runs in which the substrate concentration was greater than 1400 mg/L (initial STS ratio of 1:714) did not achieve heat equilibration, and the data was not modeled to obtain thermodynamic characteristics. A one-site binding model was used to reduce the data, with the acidic and basic cation-exchange capacity (CEC_{A+B}, Table 1) for each substrate used to model the heat data. The blank run was subtracted from the substrate run before the raw data was modeled. Examples of the modeled data are illustrated in Figures 10 and 11.

The thermodynamic characteristics of these runs are summarized in Table 5. When viewed as a function of substrate concentration, no significant correlation of thermodynamic parameters with substrate concentrations was found. In fact, under the conditions of this experiment, the thermodynamic data obtained for the Aldrich K10 substrate was not significantly different from the data obtained using the Suspengel 200 substrate. These results are illustrated in Figure 12. Using the regression function in Microsoft Excel, the Student's t statistics were determined for the slopes of the linear regression lines. The critical value ($t_{0.05/2,5}$) of the Student's t statistic was 2.57, and in all cases, the critical value was not exceeded. This demonstrates that the slopes of the regression lines were not significantly different ($P = 0.05$) from zero. The average (±SSD) thermodynamic characteristics across all substrate concentrations were determined to be: $\Delta H_{obs} = -10.2 \pm 1.66$; $-T\Delta S = -15.4 \pm 3.73$; and $\Delta G = -25.5 \pm 2.23$ kJ/mol. The interaction of VX with these clay substrates was exothermic, as indicated by the negative ΔH_{obs} values. The negative ΔH_{obs}, negative ΔG, and positive ΔS values indicate that the interaction was spontaneous, favored, and enthalpically driven. The ΔH_{obs} values determined in the current study are in good agreement with literature values for cation-exchange reactions at 298 K, which ranged from -20.3 to -4.10 kJ/mol for the exchange of monovalent cations (Cs^+, K^+, and NH_4^+) onto homoionic (Na^+) montmorillonite and kaolinite clays.[92,93] It is unknown if the interaction of VX with these clay substrates is truly an ion-exchange mechanism because the bulk solution was not analyzed for accumulation of counter ions such as Ca^{2+} or Mg^{2+}. The average (±SSD) K_b for Suspengel 200 in the current experiment was determined to be 2.11E4 $\pm$ 5.645E3 M^{-1}, which equates to an equilibrium dissociation constant (K_d) of 5.10E-5 $\pm$ 1.68E-6 M. The average K_b for Aldrich K10 in the current study was determined to be 5.73E4 M^{-1}, which equates to a K_d of 1.74E-5 M. The S_{max} values were estimated by visually determining the injection at which thermal equilibration was achieved, then calculating the mass of VX titrated into the cell. The average (±SSD) S_{max} for Suspengel 200 was 171,000 $\pm$ 26,800 mg/kg, and the S_{max} for Aldrich K10 was estimated to be 45,400 mg/kg.
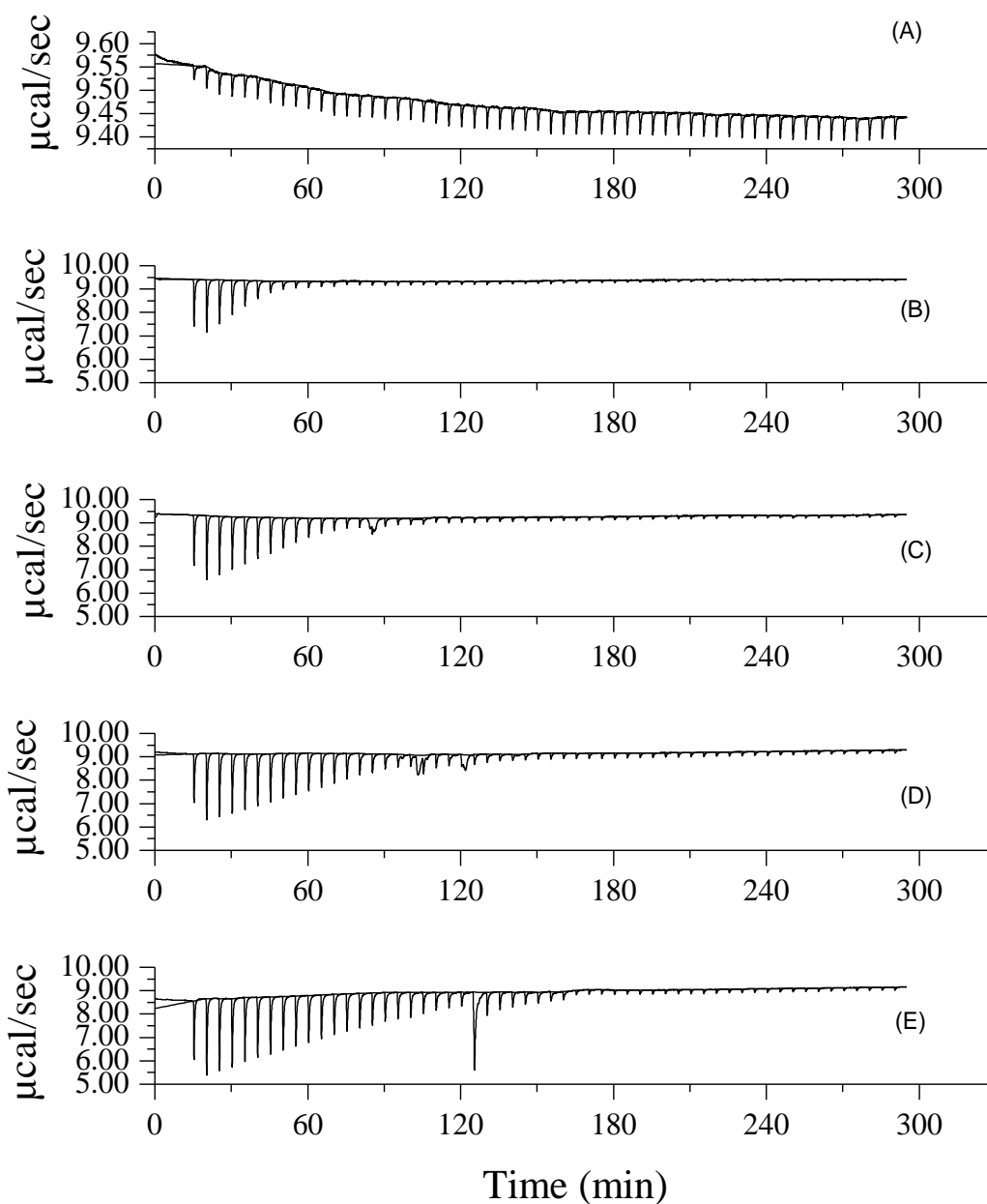
Figure 9. Thermograms generated from titration of VX into varying concentrations of Suspengel 200. All reactions conducted at 298 K using 8 mM VX. *A*: VX into buffer blank; *B*: 350 mg/L; *C*: 700 mg/L; *D*: 1050 mg/L; and *E*: 1400 mg/L. Note the scale change between the blank and samples.
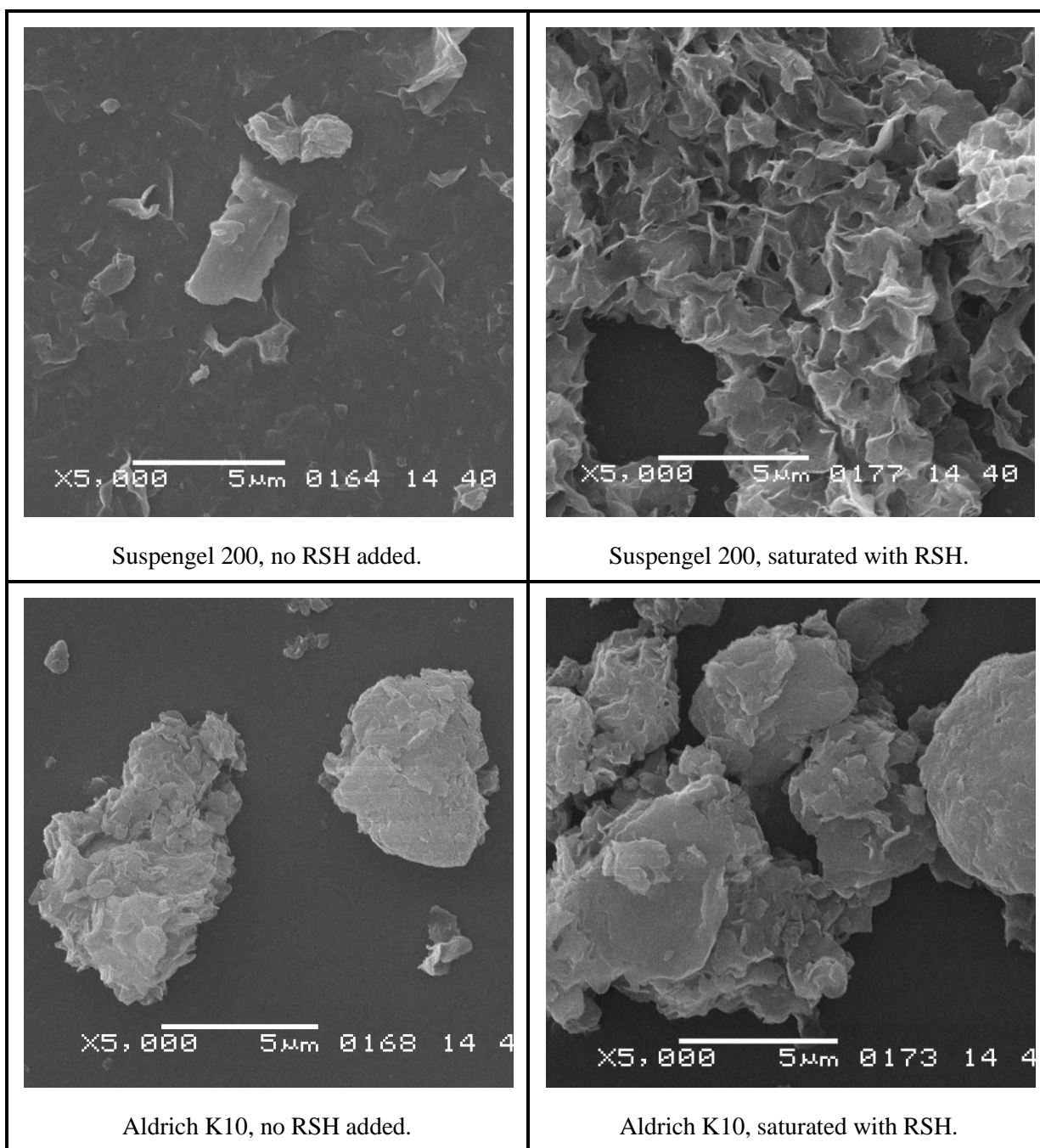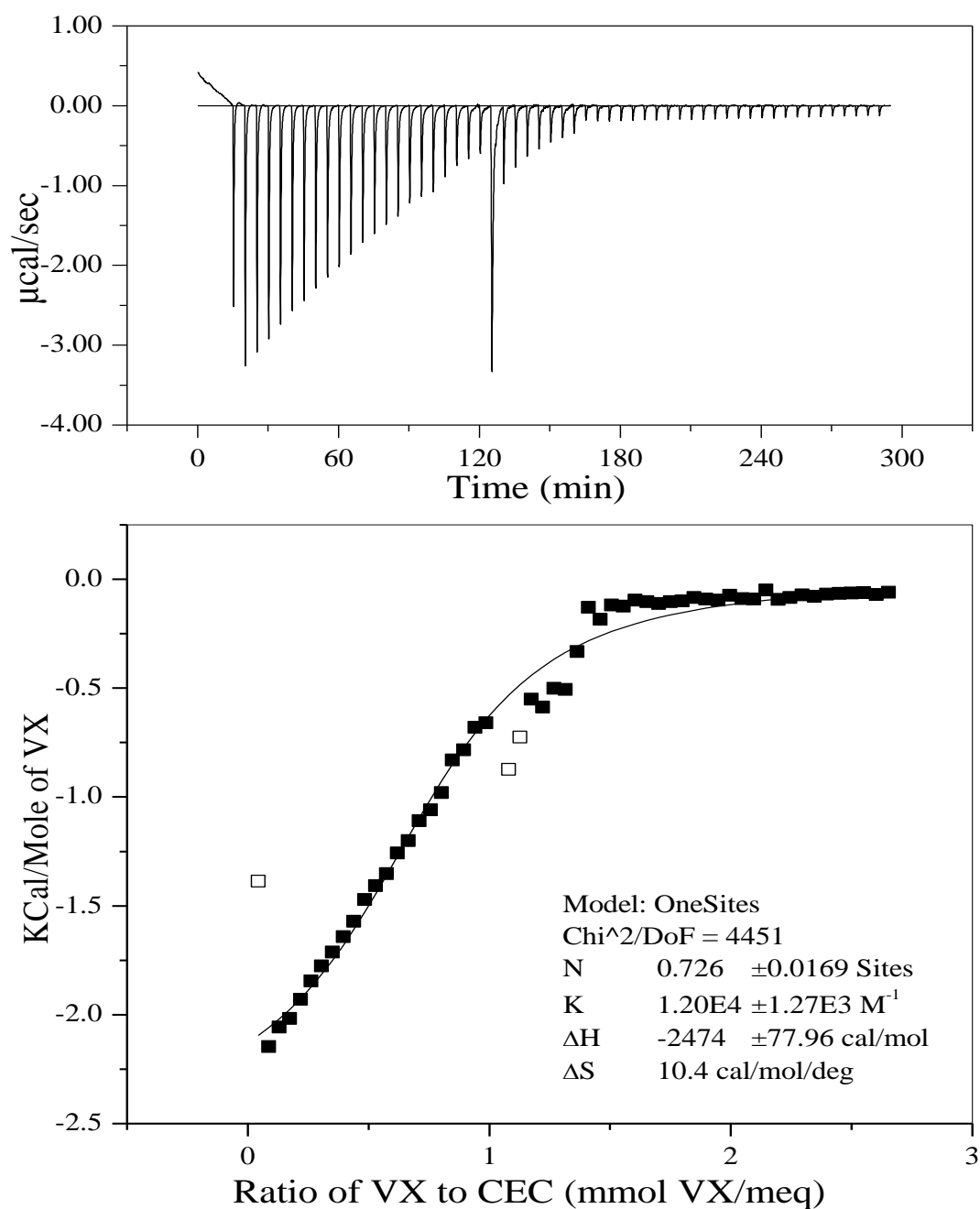
Figure 10. Titration of VX into Suspengel 200 at 298 K. Substrate concentration was 1470 mg/L and VX concentration was 8 mM. *Top*: raw data; *bottom*: modeled data. Raw data was reduced using a one-site binding model. Open symbols represent data points that were intentionally omitted from the model.
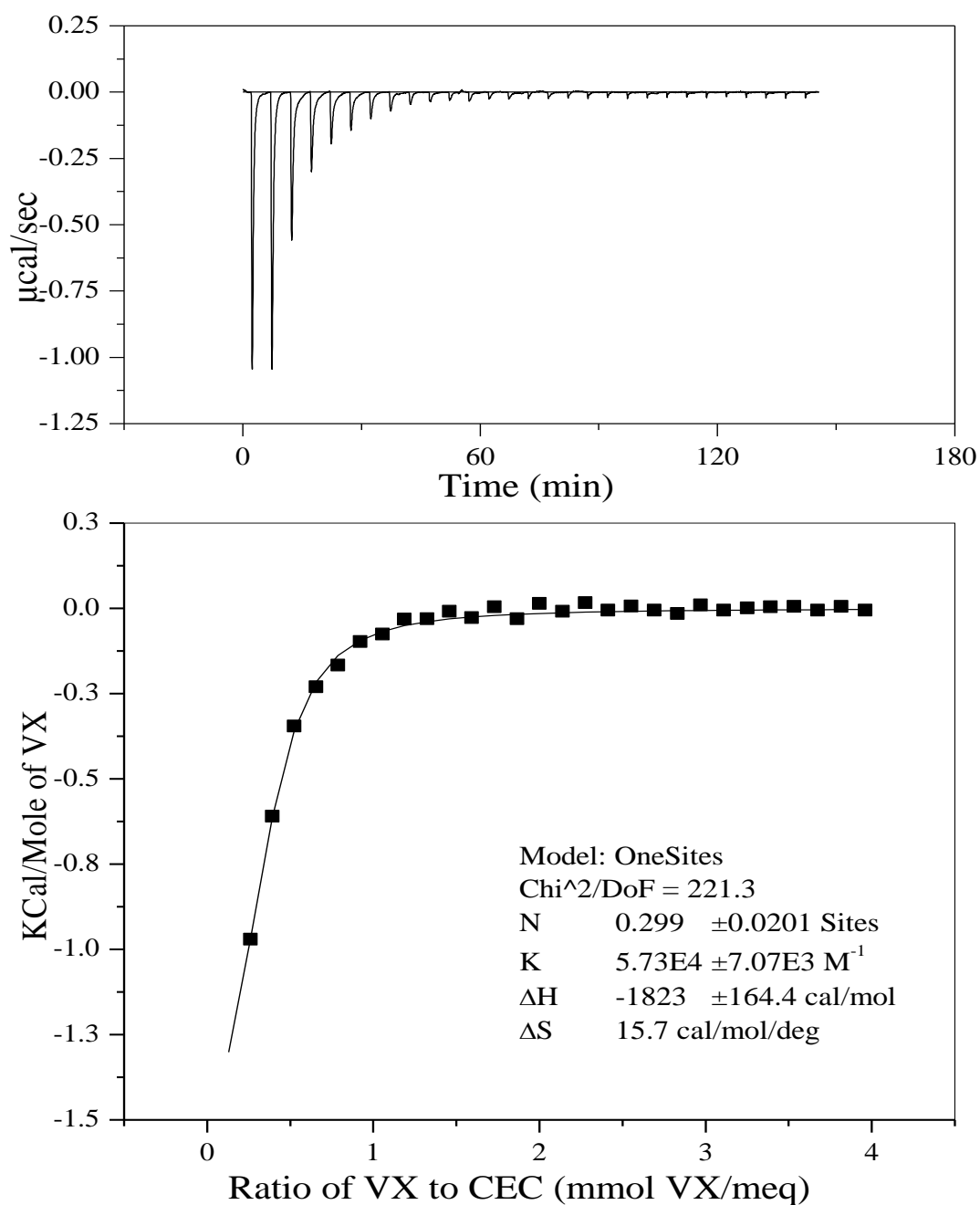
Figure 11. Titration of VX into Aldrich K10 at 298 K. Substrate concentration was 1240 mg/L, and VX concentration was 8 mM. *Top*: raw data; *bottom*: modeled data. Raw data was reduced using a one-site binding model.

Table 5. Thermodynamic Characteristics for the Binding of VX with Clay Substrates

Substrate Concentration (mg/L)	Thermodynamic Characteristic				
	Saturation Capacity (mg/kg)	K_b (M^{-1})	ΔH_{obs} (kJ/mol)	$-T\Delta S$ (kJ/mol)	ΔG (kJ/mol)
368[a]	161,000	2.97E4	−10.5	−15.7	−26.2
350[a]	204,000	2.07E4	−8.44	−20.2	−28.7
350[a]	188,000	2.24E4	−10.4	−16.0	−26.4
736[a]	131,000	2.03E4	−11.2	−13.3	−24.6
1100[a]	188,000	2.14E4	−12.6	−9.72	−22.3
1470[a]	156,000	1.20E4	−10.4	−13.0	−23.3
1240[b]	45,400[c]	5.73E4[c]	−7.63	−19.6	−27.1
Mean	171,000	2.11E4	−10.2	−15.4	−25.5
SSD	26,800	5.645E3	1.66	3.73	2.23

[a] Suspengel 200 substrate in pH 4.3 buffer.
[b] Aldrich K10 substrate in pH 4.3 buffer.
[c] Not included in calculation of mean value.
Note: All reactions were conducted at 298 K and used 8 mM VX solution as the titrant. The raw data was reduced using a one-site binding model.
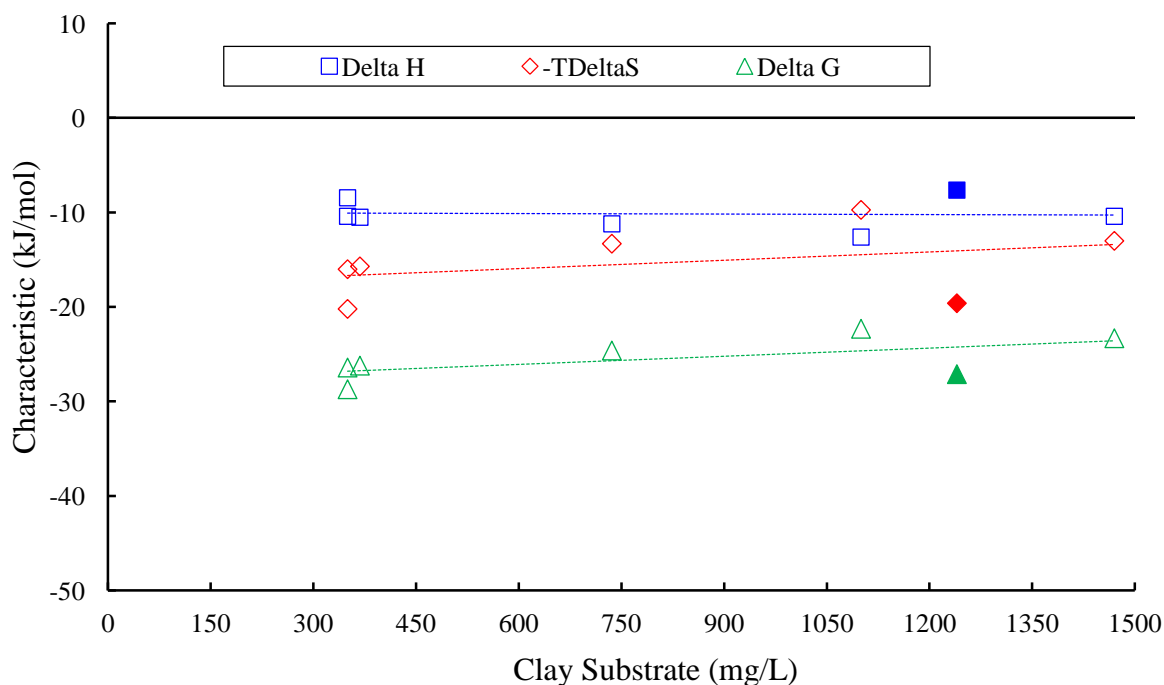
Figure 12. Thermodynamic profile as a function of clay concentration. Suspengel 200 (open symbols) and Aldrich K10 (filled symbols) data are shown. Reactions were conducted at 298 K. In all cases, the slopes of the linear regression lines were not significantly ($P = 0.05$) different from zero.

A third series of ITC runs was conducted at 278, 288, 298, and 318 K to establish whether any heat flow could be detected when phosphate interacted with suspensions of three clay substrates. The substrate concentrations were 6200 mg/L Suspengel 200, 6600 mg/L Aldrich K10, and 6300 mg/L kaolinite. All substrate suspensions were prepared in pH 4.3 buffer. These substrate concentrations correspond to initial STS ratios ranging from 1:161 to 1:152. The STS ratios change during the course of the titration, with the final STS ratios ranging from 1:189 to 1:178. In addition to the runs with substrate, parallel blank runs were obtained by adding titrant solution into pH 4.3 buffer under conditions identical to those used during the runs conducted with substrate. The thermograms are illustrated in Figure 13. The phosphate interacted with all three substrates with a predominant net endothermic reaction. The runs conducted at 278 and 288 K did not achieve saturation, but runs conducted at 298 and 318 K did reach saturation. Because phosphate is not a cation, the CEC_{A+B} could not be used to model the heat data. However, using the heat flow from the first injection, ΔH_{obs} was estimated for each clay substrate. The ΔH_{obs} values were estimated to be +3.1, +1.8, and +3.0 kJ/mol for Suspengel 200, kaolinite, and Aldrich K10, respectively. In a recent study, ΔH_{obs} values were estimated to range from –0.5 to –0.7 kJ/mol when phosphate interacted with kaolinite in pH 4.3 buffer at 298 K.[58] Although the magnitudes of the ΔH_{obs} values from both studies were reasonably close, the interaction was net endothermic in the current study but net exothermic in the reported study. The reason for this discrepancy is unknown but might be due to differences in the kaolinite used in each study.

A fourth series of ITC runs was conducted at 298 K to establish whether any heat flow could be detected when VX was titrated into suspensions of two natural soil substrates. The dry-weight substrate concentrations were 7710 mg/L HCB soil and 8920 mg/L MCL soil. All substrate suspensions were prepared in pH 4.3 buffer, and the final pH was measured to verify it remained at 4.3. These substrate concentrations corresponded to initial STS ratios ranging from 1:99 to 1:96. The STS ratios changed during the course of the titration, and the final STS ratios ranged from 1:116 to 1:113. In addition to the runs with substrate, parallel blank runs were obtained by adding titrant solution into pH 4.3 buffer under conditions identical to those used during the runs conducted with substrate. The VX interacted with both soil substrates with a predominant net exothermic reaction during most of the titration. Toward the end of each titration, the net reaction became endothermic, especially in the reaction with MCL soil substrate. These titrations did not appear to go completely to saturation. The raw thermograms and modeled data are illustrated in Figures 14 and 15. The thermodynamic characteristics for the HCB soil were determined to be as follows: $\Delta H_{obs} = -2.47$ kJ/mol, $-T\Delta S = -23.7$ kJ/mol, and $\Delta G = -26.2$ kJ/mol. The thermodynamic characteristics for the MCL soil were determined to be $\Delta H_{obs} = -2.80$ kJ/mol, $-T\Delta S = -24.7$ kJ/mol, and $\Delta G = -27.5$ kJ/mol. The initial interaction of VX with these soil substrates was net exothermic, as indicated by the negative ΔH_{obs} values. The negative ΔH_{obs}, negative ΔG, and positive ΔS values indicate that the interaction was spontaneous, favored, and enthalpically driven. The average K_b for both soils was 5.33E4 M^{-1}, which equates to a K_d of 1.88E-5 M. *It should be noted that the curves generated by the one-site model did not yield a good fit to the actual data for either of the two soil substrates.*
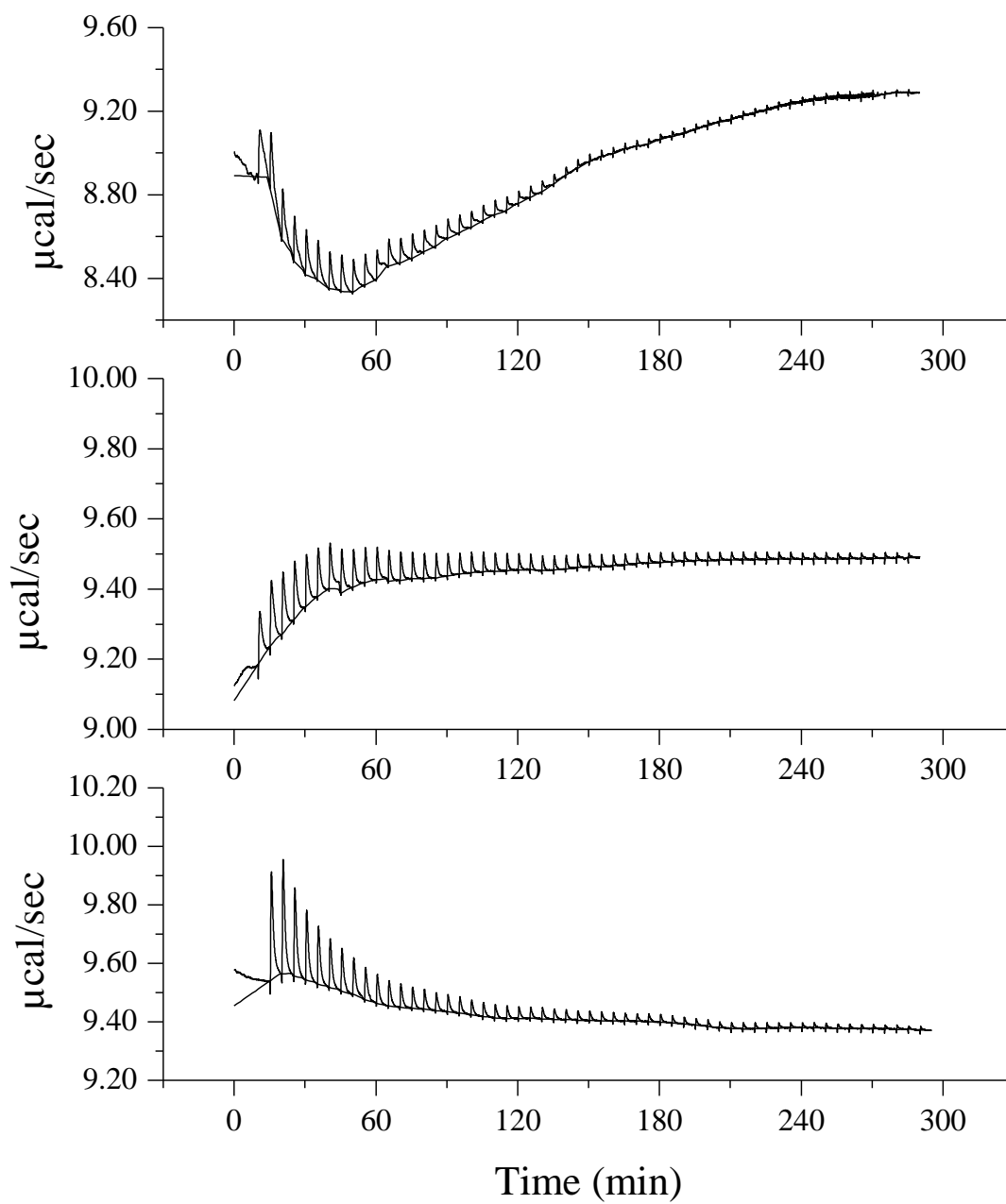
Figure 13. Thermograms generated from titration of phosphate into three clay substrates. All reactions were conducted at 298 K using 8 mM phosphate. *Top*: 6200 mg/L Suspengel 200; *middle*: 6300 mg/L kaolinite; and *bottom*: 6600 mg/L Aldrich K10.
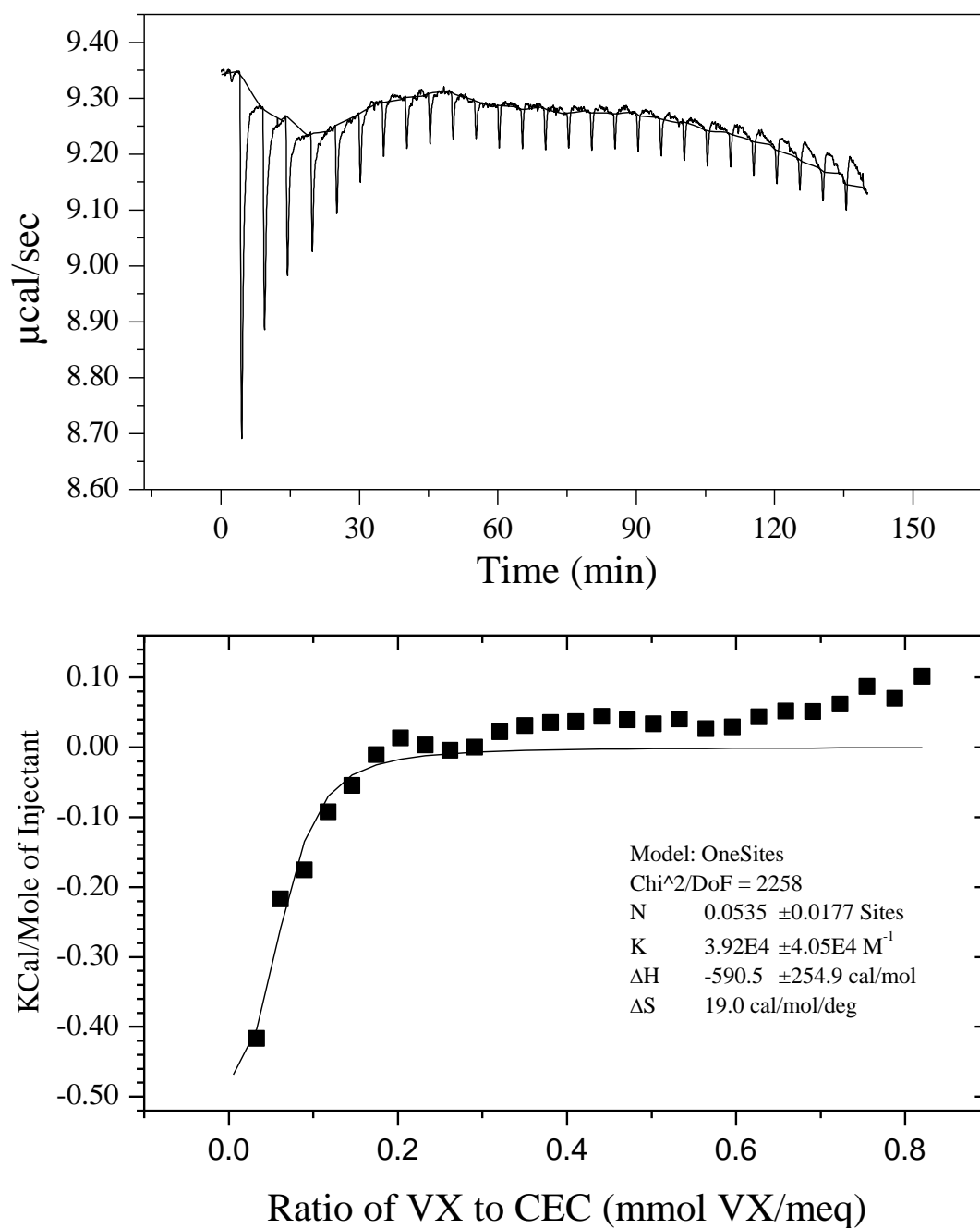
Figure 14. Titration of VX into HCB soil at 298 K. The dry-weight substrate concentration was 7710 mg/L, and the VX concentration was 8 mM. *Top*: raw data; *bottom*: modeled data. Raw data was reduced using a one-site binding model. Note the poor fit of the model, which was due to multiple processes occurring during the interaction.
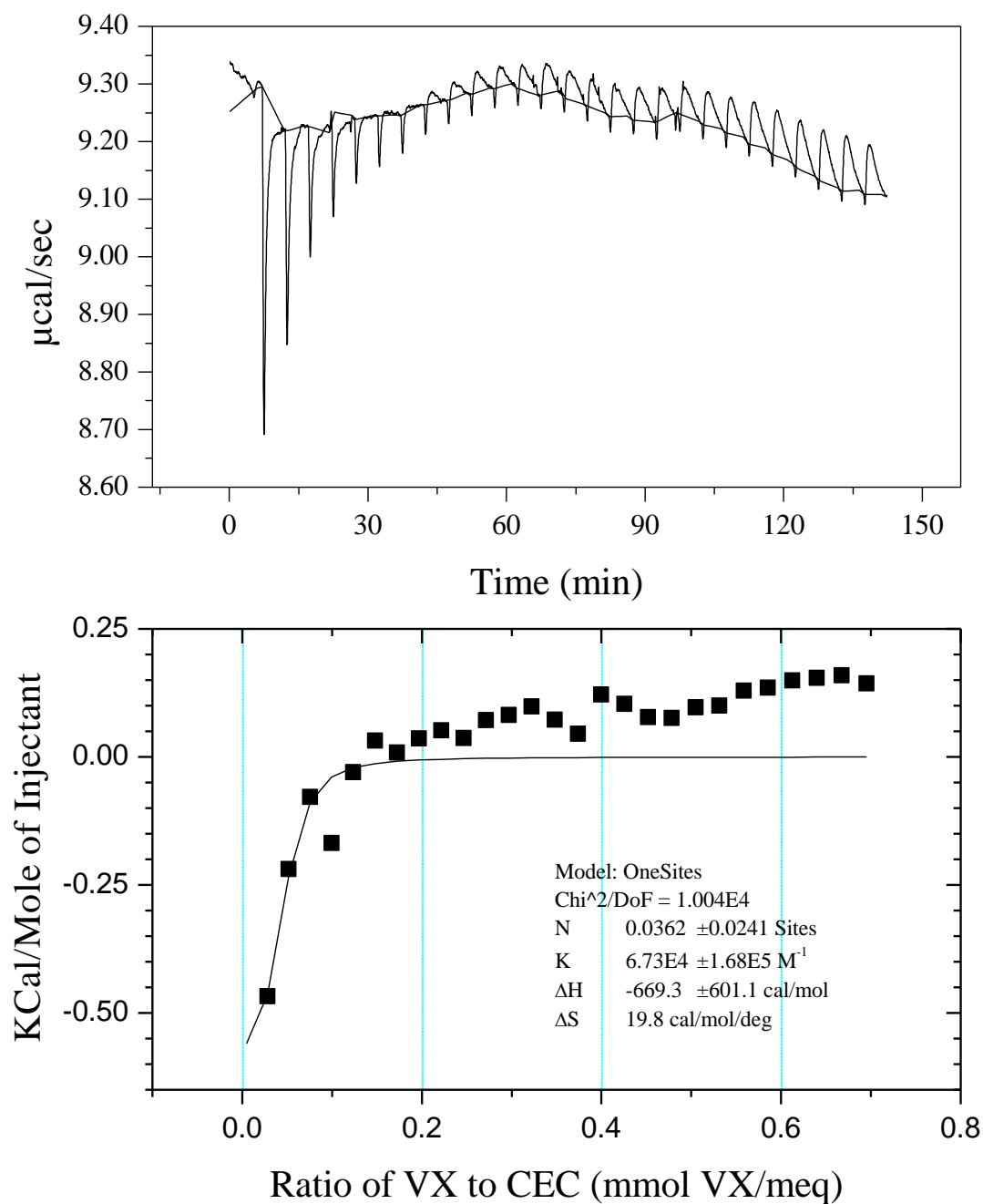
Figure 15. Titration of VX into MCL soil at 298 K. Dry-weight substrate concentration was 8920 mg/L, and VX concentration was 8 mM. *Top*: raw data; *bottom*: modeled data. Raw data was reduced using a one-site binding model. Note the poor fit of the model, which was due to multiple processes occurring during the interaction.

3.1.2　　　　　　　VX Reactions Under Saturating Conditions

　　　　　A series of ITC runs was conducted at temperatures ranging from 278 to 318 K to establish thermodynamic profiles for the sorption of VX with suspensions of Suspengel 200 and Aldrich K10 substrates. In all cases, the titrant was 8 mM VX in pH 4.3 buffer. The substrate concentrations were 1000 mg/L Suspengel 200 and 2880 mg/L Aldrich K10, with both substrates in pH 4.3 buffer. These substrate concentrations corresponded to initial STS ratios of 1:1000 and 1:347 for Suspengel 200 and Aldrich K10, respectively. The STS ratios changed during the course of the titration as titrant was added, and the final STS ratios were 1:1170 and 1:407. The substrate concentrations were chosen such that the total CEC (CEC_{A+B}, Table 1) in the ITC sample cell would be nominally the same for each substrate. In both cases, the total exchange capacity in the ITC sample cell was ~7E-4 meq. In addition to the runs with substrate, parallel blank runs were conducted by adding 8 mM VX titrant solution into pH 4.3 buffer under conditions identical to those used during the runs conducted with substrate.

　　　　　At the lower temperatures for the Suspengel 200 runs, specifically in the range of 278 to 285.5 K, the concurrent presence of both exothermic and endothermic peaks was observed in the thermogram. It should be noted that this bimodal behavior was only apparent when the reactions were conducted at or below the lower consolute temperature (LCT) of VX, which is 282.6 K (~10 °C, or ~50 °F) in pure water.[47] It has been reported the LCT can shift by up to several degrees, depending on the type and amount of added salts.[94] The specific titration with which this bimodal behavior commenced, as well as the number of titrations for which it continued, varied proportionally with reaction temperature. Retardation of the onset of the endothermic peaks as well as reduction in the magnitude of the endothermic response were observed to increase with increasing temperature. Once the reaction temperature reached 303 K, there was no longer any evidence of an endothermic process in the thermogram. Although the titrations of VX into the Aldrich K10 produced solely endothermic peaks at the lower temperatures, heat flow was monomodal. The bimodal behavior was not observed when VX was titrated into the Aldrich K10 suspension. Thermograms exhibiting the bimodal and monomodal behavior are illustrated in Figure 16.

　　　　　The raw data from the Suspengel 200 runs conducted between 278 and 283 K were modeled using a two-site binding model, whereas the raw data from Suspengel 200 runs conducted between 285 and 318 K were modeled using a one-site binding model. In both cases, CEC_{A+B} was used as the model parameter. Attempts were made to model the raw data from the Aldrich K10 runs using a variety of models; however, the curves produced were poor fits to the data and generated large errors associated with the thermodynamic parameters. For this reason, complete thermodynamic characteristics for the Aldrich K10 are not reported. Although it is beyond the scope of this report to determine why the raw data from the Aldrich K10 runs could not be successfully modeled, one hypothesis is that the titrant concentration was too high relative to the amount of substrate. This is somewhat surprising, given that the total exchange capacity in the cell for each clay was approximately the same. The Aldrich K10 substrate became saturated within a few titrations, leaving too few data points for successful application of a modeling routine.

The thermodynamic characteristics for the Suspengel 200 runs reduced by the two-site model are summarized in Table 6. An example plot of the raw data as well as a plot of the integrated data after reduction by the two-site model are illustrated in Figure 17. The thermodynamic profiles are illustrated in Figure 18. Using the regression function in Microsoft Excel, the Student's t statistics were determined for the slopes of the linear regression lines for each of the thermodynamic parameters. In all cases, the critical value ($t_{0.05/2,2}$) of the Student's t statistic was 4.30, and the critical value was not exceeded. This demonstrates that the slopes of the regression lines are not significantly different ($P = 0.05$) from zero. The average ($\pm$SSD) ΔH_{obs} for binding Site 1 was -92.9 ± 43.84 kJ/mol, while it was 260 ± 66.4 kJ/mol for binding Site 2. The average ($\pm$SSD) $-T\Delta S$ for binding Site 1 was 66.2 ± 43.72 kJ/mol, while it was -286 ± 66.3 kJ/mol for binding Site 2. The average ($\pm$SSD) ΔG for binding Site 1 was -26.6 ± 0.33 kJ/mol, while it was -26.3 ± 0.48 kJ/mol for binding Site 2. The overall average ΔG for both sites was determined to be -26.4 ± 0.42 kJ/mol. The negative ΔH_{obs}, negative ΔG, and negative ΔS values obtained for Site 1 indicate that the interaction was exothermic, spontaneous, favored, and enthalpically driven. The positive ΔH_{obs}, negative ΔG, and positive ΔS values obtained for Site 2 indicate that the interaction was endothermic, spontaneous, favored, and entropically driven. The average ($\pm$SSD) K_b for both sites in this experiment was determined to be $8.64E4 \pm 1.020E4$ M^{-1}, which equates to a K_d of $1.17E-5 \pm 1.330E-6$ M. The S_{max} values were estimated by visually determining the injection at which thermal equilibration was achieved, then calculating the mass of VX titrated into the cell. The average ($\pm$SSD) S_{max} for Suspengel 200 was $176,000 \pm 6532$ mg/kg.

The thermodynamic characteristics for the Suspengel 200 runs obtained above the LCT for VX are summarized in Table 7. An example plot of the raw data as well as a plot of the integrated data following reduction by the one-site model are illustrated in Figure 19. The thermodynamic profiles are illustrated in Figure 20. Using the regression function in Microsoft Excel, the Student's t statistics were determined for the slopes of the linear regression lines for the thermodynamic parameters. The critical value ($t_{0.05/2,10}$) of the Student's t statistic was 2.23, and in all cases, the critical value was not exceeded. This demonstrates that the slopes of the linear regression lines were not significantly different ($P = 0.05$) from zero. The average ($\pm$SSD) thermodynamic characteristics were determined to be as follows: $\Delta H_{obs} = -15.1 \pm 2.26$ kJ/mol, $-T\Delta S = -11.2 \pm 2.95$ kJ/mol, and $\Delta G = -26.4 \pm 2.16$ kJ/mol. The negative ΔH_{obs}, negative ΔG, and positive ΔS values obtained indicate that the interaction was exothermic, spontaneous, favored, and enthalpically driven. The average ($\pm$SSD) K_b was determined to be $2.69E4 \pm 4.305E3$ M^{-1}, which equates to a K_d of $3.79E-5 \pm 5.177E-6$ M. The S_{max} values were estimated by visually estimating the injection at which thermal equilibration was achieved, then calculating the mass of VX titrated into the cell. The average ($\pm$SSD) S_{max} for Suspengel 200 was $165,000 \pm 12,090$ mg/kg.
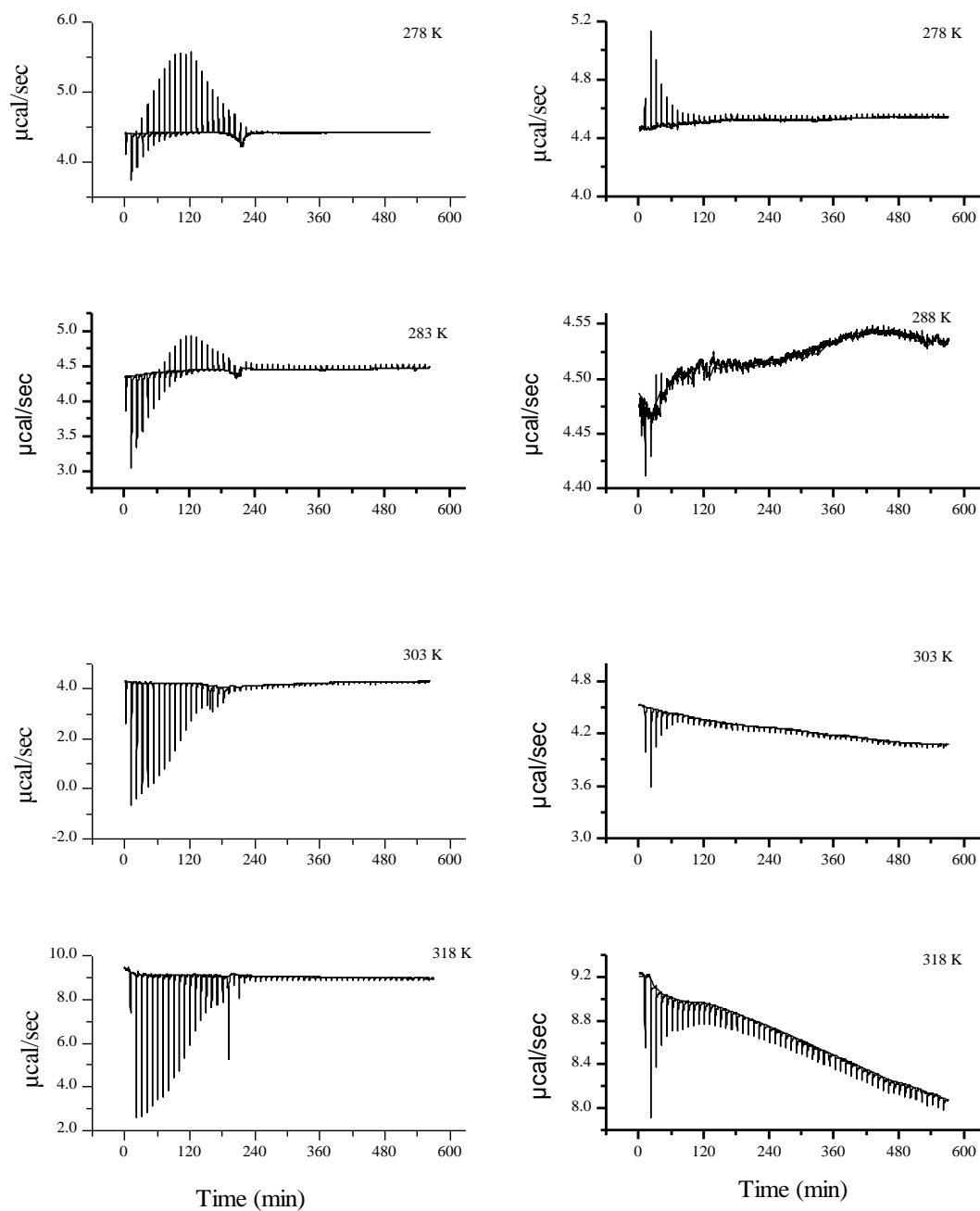
Figure 16. Bimodal behavior observed during titration of VX into clay suspensions.
Left: Suspengel 200 thermograms; *right:* Aldrich K10 thermograms. In all cases,
the titrant was 8 mM VX in pH 4.3 buffer.

Figure 17. Titration of VX into Suspengel 200 at 278 K. Substrate concentration was 1000 mg/L, and VX concentration was 8 mM. *Top*: raw data; *bottom*: modeled data. Raw data was reduced using a two-site binding model. Open symbols represent data points that were intentionally omitted from the model.

Table 6. Thermodynamic Characteristics for the Binding of VX with Suspengel 200
Below the Lower Critical Temperature

Reaction Temperature (K)	Thermodynamic Characteristic				
	Saturation Capacity (mg/kg)	K_b (M^{-1})	ΔH_{obs} (kJ/mol)	$-T\Delta S$ (kJ/mol)	ΔG (kJ/mol)
278	NA	1.04E5	−156	129	−26.8
278	NA	8.00E4	−121	63.2	−26.1
280.5	NA	8.90E4	−62.6	35.9	−26.6
283	NA	8.84E4	−63.7	36.8	−26.8
Site 2[a]					
278	184,000	9.68E4	161	−188	−26.7
278	176,000	7.33E4	176	−301	−25.7
280.5	176,000	8.00E4	298	−324	−26.0
283	168,000	7.96E4	304	−330	−26.6
Mean	176,000	8.64E4			−26.4
SSD	6,532	1.020E4			0.42

[a] CEC$_{A+B}$ was used to model Site 2 heat flows. It is unknown whether this is the correct model parameter.
NA, not applicable
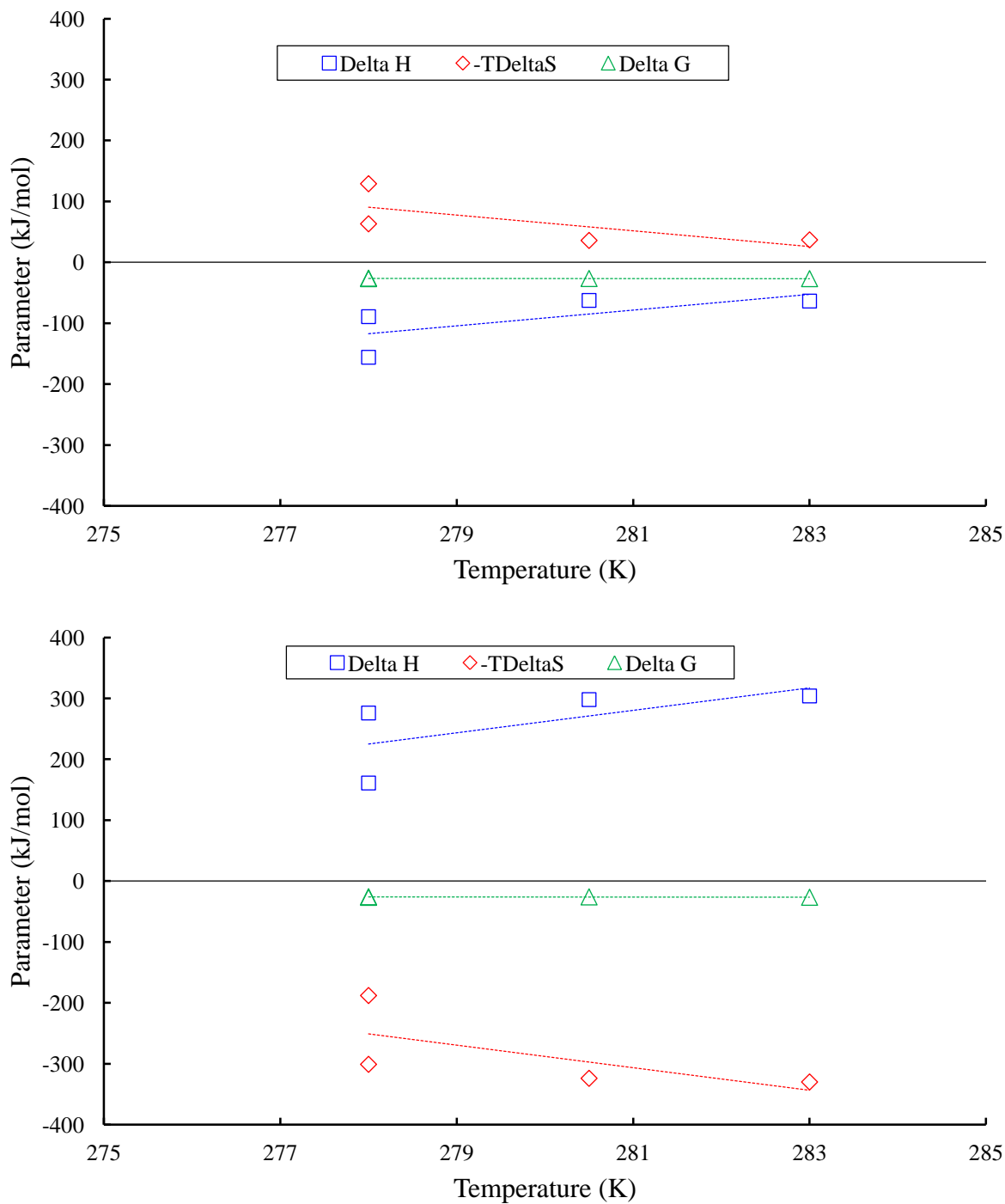
Figure 18. Thermodynamic profiles for the reaction of VX with Suspengel 200 below the lower critical temperature. Raw data were reduced using a two-site binding model. *Top*: first binding site; *bottom*: second binding site. In all cases, the slopes of the linear regression lines were not significantly ($P = 0.05$) different from zero.

A summary of thermodynamic characteristics for both binding sites on the Suspengel 200 is included as Table 8. Although the data obtained using the Aldrich K10 could not be successfully modeled, ΔH_{obs} was estimated for each reaction temperature using the first injection as described in Section 3.1.1. A comparison of ΔH_{obs} for both clay substrates is illustrated in Figure 21. It is beyond the scope of this report to determine the mechanism of the second binding site; however, one hypothesis is that when the interaction takes place at or below the LCT, a ligand exchange through the phosphorus can occur with hydroxyl groups on the clay edges.[95,96] This second mechanism was not observed in the Aldrich K10 clay, because the acid processing is reported to largely destroy binding sites associated with the clay edges.[32–34]

The ΔC_p is the slope of the linear regression line of a plot of ΔH_{obs} versus temperature, as illustrated in Figure 21.[97,98] The ΔC_p values were determined to be –0.280, –0.0533, and 12.9 kJ/mol·K for Aldrich K10, Site 1 for Suspengel 200 above the LCT, and Site 1 for Suspengel 200 below the LCT, respectively. There is a sharp break in ΔH_{obs} values that appears to correspond with the LCT for VX obtained with the Suspengel 200 clay, which is not observed in ΔH_{obs} values obtained with the Aldrich K10 clay. Negative values for ΔC_p indicate water molecules are leaving the bulk solution, and positive values indicate water molecules are moving into the bulk solution.[99–101] It is unknown whether the negative ΔC_p values were the result of solvation of the VX molecules, transfer of water into the interlaminar space of the clays, or a combination of these two processes. It is also unknown whether the positive ΔC_p value obtained for the reactions conducted below the LCT with Suspengel 200 was the result of desolvation of the VX molecules, expulsion of water from the interlaminar space of the clays, or a combination of these two processes. Another difference in the Site 1 characteristics is the strength of the binding interaction. The average K_b below the LCT is 9.04E4 M^{-1}, whereas it is 2.50E4 M^{-1} above the LCT. This indicates that the VX sorption to the Suspengel 200 was ~3.5 times stronger when the reaction was conducted below the LCT of VX.
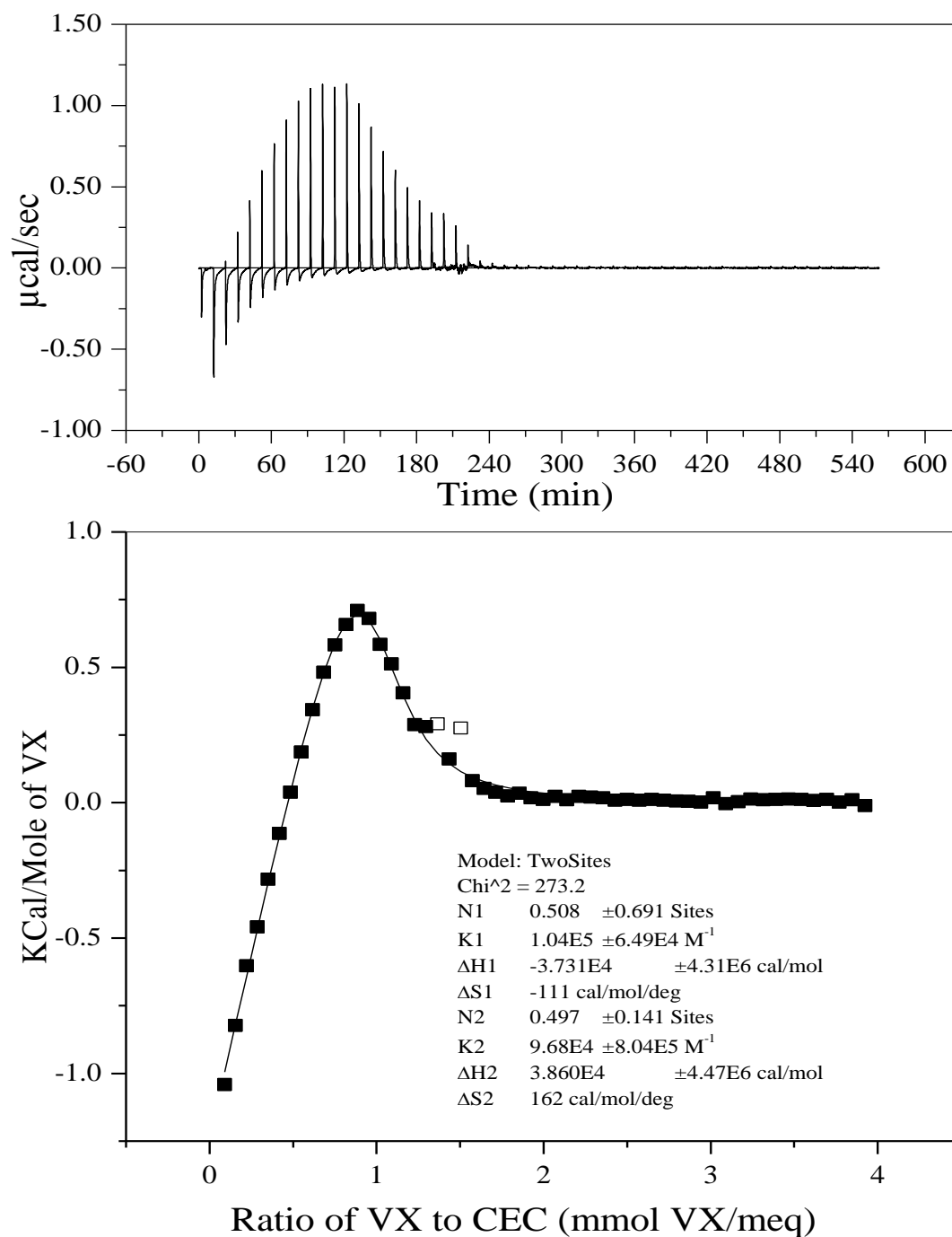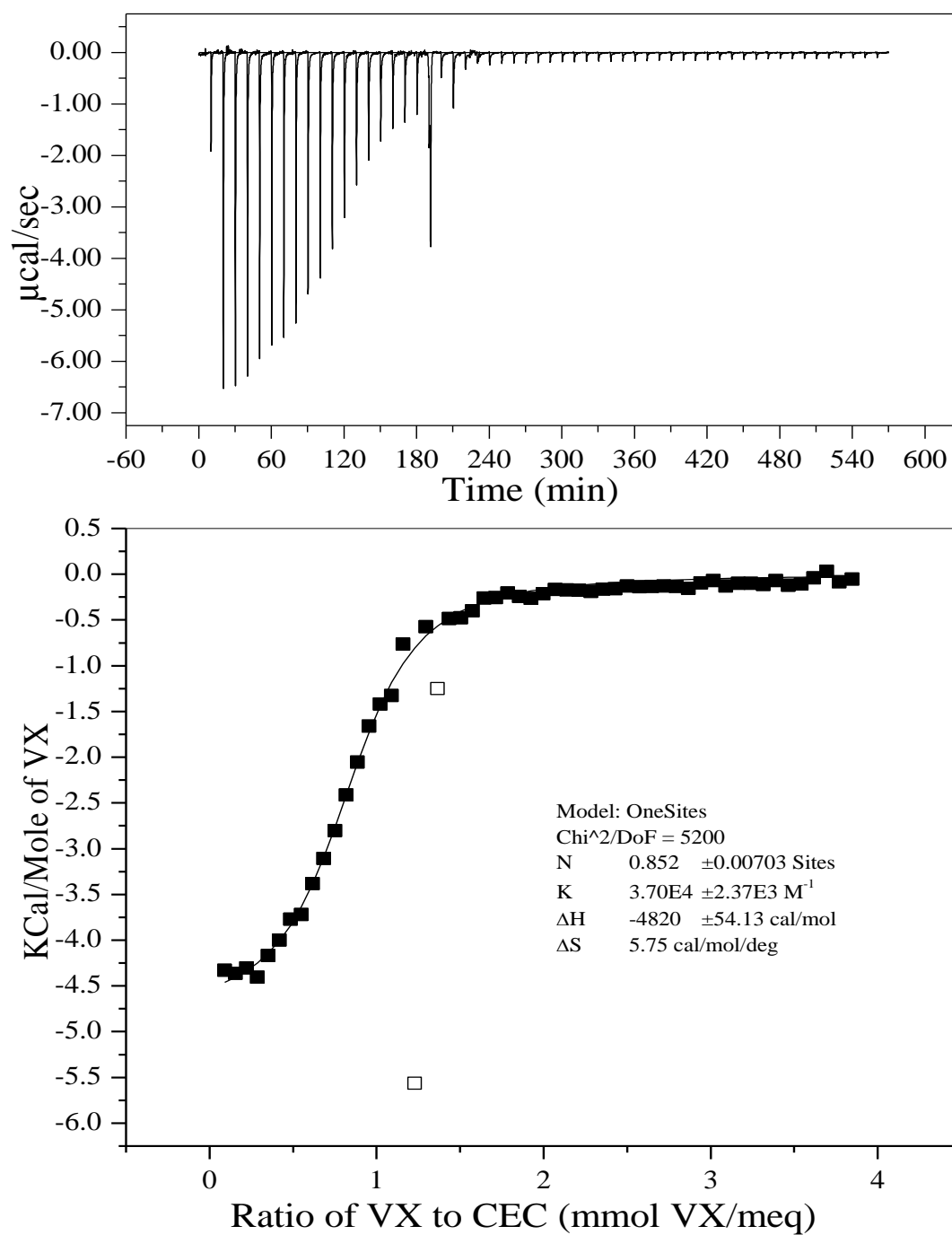
Figure 19. Titration of VX into Suspengel 200 at 318 K. Substrate concentration was 1000 mg/L and VX concentration was 8 mM. *Top*: raw data; *bottom*: modeled data. Raw data was reduced using a one-site binding model. Open symbols represent points that were not used to model the data.

Table 7. Thermodynamic Characteristics for the Binding of VX with Suspengel 200
Above the Lower Critical Temperature

Reaction Temperature (K)	Thermodynamic Characteristic				
	Saturation Capacity (mg/kg)	K_b (M^{-1})	ΔH_{obs} (kJ/mol)	$-T\Delta S$ (kJ/mol)	ΔG (kJ/mol)
285.5	160,000	2.30E4	−14.4	−8.13	−22.5
288	153,000	2.47E4	−14.0	−9.01	−23.0
303	145,000	3.27E4	−14.1	−12.1	−26.2
303	153,000	2.55E4	−17.1	−7.25	−24.3
310.5	168,000	2.98E4	−13.2	−14.2	−27.3
310.5	176,000	2.88E4	−12.6	−13.9	−26.5
310.5	168,000	2.51E4	−13.7	−12.5	−26.1
314	176,000	2.40E4	−18.1	−8.18	−26.3
318	184,000	2.44E4	−13.6	−14.6	−28.3
318	168,000	2.40E4	−15.5	−12.7	−28.3
318	176,000	2.41E4	−15.0	−14.6	−29.6
318	153,000	3.70E4	−20.2	−7.65	−27.8
Mean	165,000	2.69E4	−15.1	−11.2	−26.4
SSD	12,090	4.305E3	2.26	2.95	2.16

Note: The raw data was reduced using a one-site binding model.
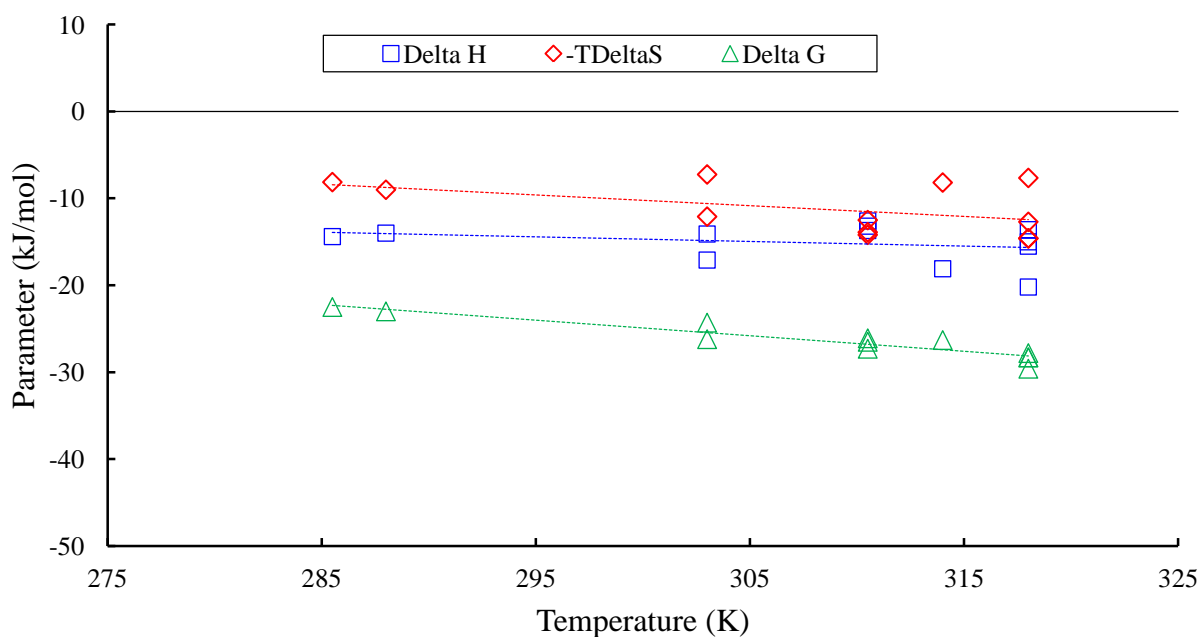
Figure 20. Thermodynamic profiles for the reaction of VX with Suspengel 200 above the lower critical temperature. Raw data was reduced with the one-site binding model. Slope of the linear regression line for ΔG was significantly ($P = 0.05$) different from zero, while slopes of the linear regression lines for ΔH_{obs} and $-T\Delta S$ were not significantly ($P = 0.05$) different from zero.

Table 8. Comparison of Thermodynamic Parameters Obtained
Above and Below the Lower Critical Temperature

Parameter	Reactions ≤ LCT		Reactions > LCT
	Site 1	Site 2	Site 1
S_{max} (mg/kg)	NA	176,000 ± 6,532	167,000 ± 17,760
K_b (M^{-1})	9.04E4 ± 9.984E3	8.24E4 ± 1.01E4	2.50E4 ± 5.421E3
K_d (M)	1.12E-5 ± 1.185E-6	1.23E-5 ± 1.388E-6	4.23E-5 ± 1.187E-5
ΔH_{obs} (kJ/mol)	−100 ± 45.8	235 ± 76.8	−13.6 ±2.94
$-T\Delta S$ (kJ/mol)	66.2 ± 43.72	−286 ± 66.3	−12.4 ± 3.47
ΔS (kJ/mol·K)	−0.237 ± 0.158	1.02 ± 0.234	0.0359 ± 0.00890
ΔG (kJ/mol)	−26.6 ± 0.33	−26.3 ± 0.48	−26.0 ± 2.22
ΔC_p (kJ/mol·K)	12.9	18.4	−0.0533

Notes: In all cases, the substrate was Suspengel 200, and the titrant was VX. Reported values are averages ± SSD. NA, not applicable

Figure 21. Observed enthalpy and entropy as a function of reaction temperature for binding Site 1. *Top*: ΔH_{obs} (Suspengel 200 and Aldrich K10 substrates); *bottom*: ΔS (Suspengel 200 substrate only). Vertical dashed lines represent the LCT for VX in pure water.

3.1.3   VX Reactions Under Pseudo-First-Order Conditions

A final series of ITC runs was conducted such that the substrate concentrations were in large excess. This allowed the assumption that the reactions were conducted under pseudo-first-order conditions, relative to substrate. The Suspengel 200 concentration was 14,000 mg/L, which corresponded to an initial STS ratio of 1:71. The Aldrich K10 concentration was 28,000 mg/L, which corresponded to an initial STS ratio of 1:36. The Suspengel 200 saturated with humus had an estimated concentrat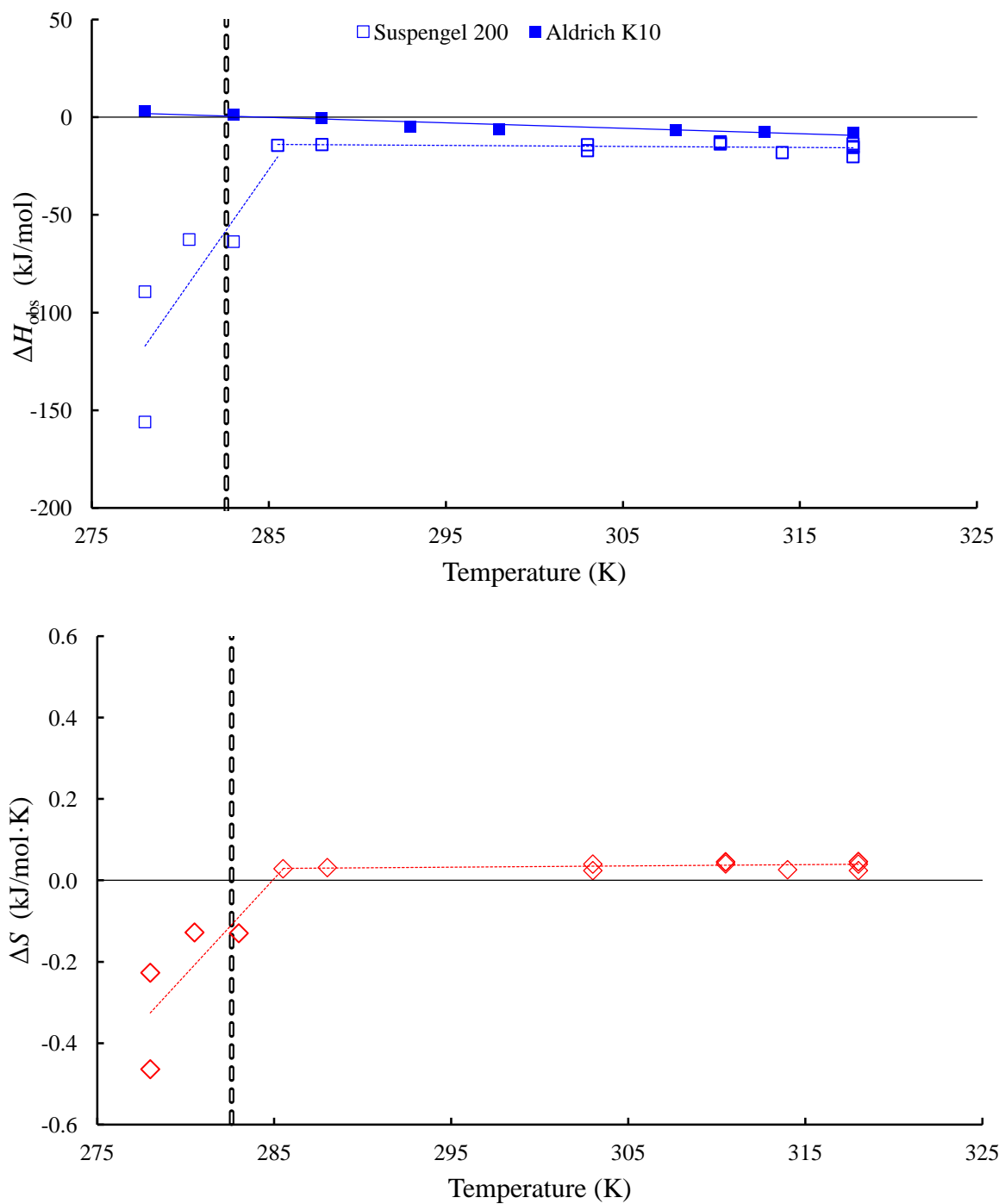ion of 8400 mg/L, which corresponded to an initial STS ratio of 1:119. The humus had a concentration of ~2200 mg/L, which corresponded to an initial STS ratio of 1:454. In these runs, the objective was to have individual peaks that did not significantly change during the course of a titration. Individual peaks were integrated and normalized against the molar amount of VX in each injection. Typically, two independent runs were conducted for each set of conditions, and the first 10 individual peaks were integrated. Typically, the lowest and highest data points were dropped, and 18 data points were used to calculate the mean response. Example raw thermograms are illustrated in Figure 22.

In addition to the runs with substrate, parallel blank runs were conducted by adding VX titrant solution into pH 4.3 buffer under conditions identical to those used during the runs conducted with substrate. Example raw thermograms are illustrated in Figure 23. A linear regression model was applied to the blank data, and results are illustrated in Figure 24. This regression model was used to correct substrate runs for the ΔH_{obs} associated with the mixing of VX titrant into pH 4.3 buffer.

The pseudo-first-order ΔH_{obs} values, corrected for blank injections, are summarized in Table 9. In the current study, ΔH_{obs} values determined at 298 K under pseudo-first-order conditions ranged from –8.67 to –6.41 kJ/mol, which is indicative of a net exothermic process. The ΔH_{obs} values obtained under pseudo-first-order conditions are in good agreement with those obtained under saturating conditions, which ranged from –12.6 to –7.63 kJ/mol at 298 K. The ΔH_{obs} values determined in the current study are in good agreement with literature values, which ranged from –20.3 to –4.10 kJ/mol for the exchange of monovalent cations (Cs^+, K^+, and NH_4^+) onto homoionic (Na^+) montmorillonite and kaolinite clays.[92,93] The reported literature values of ΔH were all determined at 298 K; there were no studies found in which thermodynamic characteristics were determined at multiple temperatures. Interestingly, one of the studies reported endothermic ΔH values ranging from +2.40 to +15.6 kJ/mol for the exchange of divalent and trivalent cations (Ba^{2+}, Ca^{2+}, La^{3+}, and Mg^{2+}) onto homoionic (Na^+) montmorillonite and kaolinite clays.[92] The ΔH_{obs} values from the current study, as a function of temperature, are illustrated in Figure 25. The ΔC_p values were determined to be –0.461, –0.323, and –0.333 kJ/mol·K for the Suspengel 200, Suspengel 200 with humus, and Aldrich K10 substrates, respectively. The average ΔC_p for all three substrates was determined to be –0.372 kJ/mol·K. Negative values of ΔC_p indicate that water molecules were leaving the bulk solution, whereas positive values indicate water molecules were moving into the bulk solution.[99–101] It is unknown whether the negative ΔC_p values were the result of solvation of the VX molecules, transfer of water into the interlaminar space of the clays, or a combination of these two processes.

The maximum heat-release rate values for each injection are summarized in Table 10. The activation energies (E_a) of binding were calculated using the Arrhenius equation,[102] and the average rates are in Table 10. This approach to estimating activation energies has been established in the literature.[103,104] The Arrhenius plots are illustrated in Figure 26, and the E_a values were calculated using both the graphical and two-point protocols.[102,105] The E_a values and pre-exponential factors (A) are summarized in Table 11. The E_a values were estimated to be 36.2, 24.7, and 13.3 kJ/mol for Suspengel 200, Suspengel 200 plus humus, and Aldrich K10, respectively. The E_a values determined in the current study are in reasonable agreement with an E_a of 23.0 kJ/mol reported in the literature for the sorption of 2,4-dichlorophenoxyacetic acid (2,4-D, $C_8H_6Cl_2O_3$; CAS no. 94-75-7) to a montmorillonite clay.[106]

Pseudo-first-order reactions using RSH as the titrant were also conducted, but did not provide valid data. In Section 3.1.1, reactions under saturating conditions were also attempted with RSH, but the results were not consistent. In these pseudo-first-order reactions, the RSH titrant solution was freshly prepared from neat material immediately prior to the experiment. This was done in an attempt to minimize the oxidation of RSH to RSSR. The ITC results with RSH were too variable from injection to injection to be useful. The relative standard deviation ranged from 45.0 to 220% across 10 injections, depending on the reaction temperature. In comparison, VX data was more reproducible, with relative standard deviations ranging from 3.07 to 30.2% across 10 injections. This comparison is illustrated in Figure 27.

A third series of ITC runs was conducted at 278, 298, and 318 K to determine whether any significant interactions were occurring when VX interacted with the humus substrate. The substrate concentration was ~2200 mg/L to ensure the reaction was occurring under pseudo-first-order in substrate. This substrate concentration corresponded to an initial STS ratio of 1:454. In addition to the runs with substrate, parallel blank runs were conducted by adding titrant solution into pH 4.3 buffer, under conditions identical to those used during the runs conducted with substrate. In all cases, no heat flow was detected in any of the titrations. This apparent lack of interaction was confirmed during the kinetic profile experiments described in Section 3.2.1.
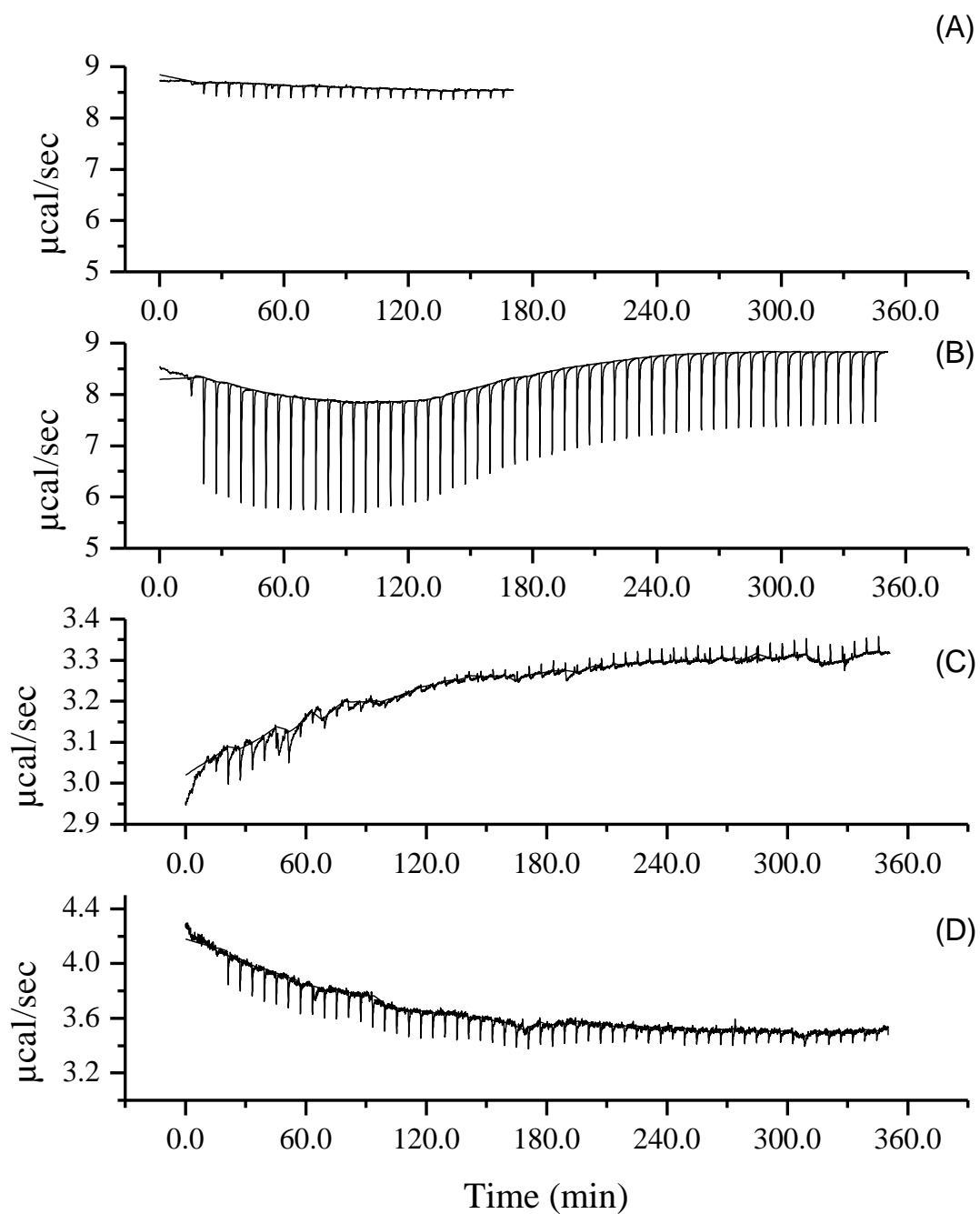
Figure 22. Pseudo-first-order raw thermograms using VX as the titrant. *A*: Suspengel 200 at 278 K; *B*: Suspengel 200 at 318 K; *C*: Aldrich K10 at 278 K; *D*: Aldrich K10 at 318 K.
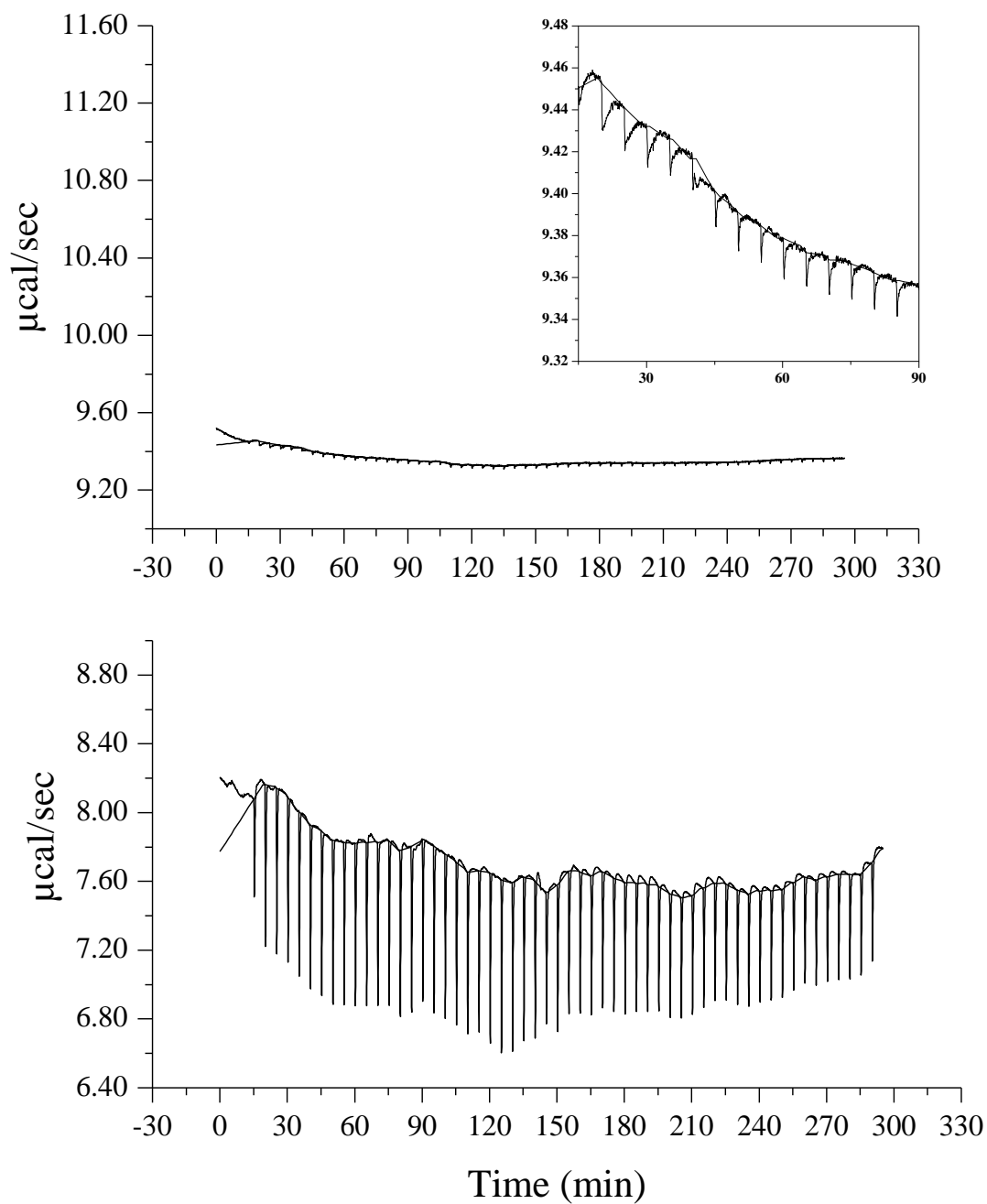
Figure 23. Thermograms comparing a blank and a sample. *Top*: VX being titrated into pH 4.3 buffer (*inset*: close-up view to show detail); *bottom*: VX titrated into Suspengel 200. All runs were conducted at 298 K with a 5 μL injection volume.

$$y = -2\text{E-}10x + 7\text{E-}08$$
$$R^2 = 0.4382$$
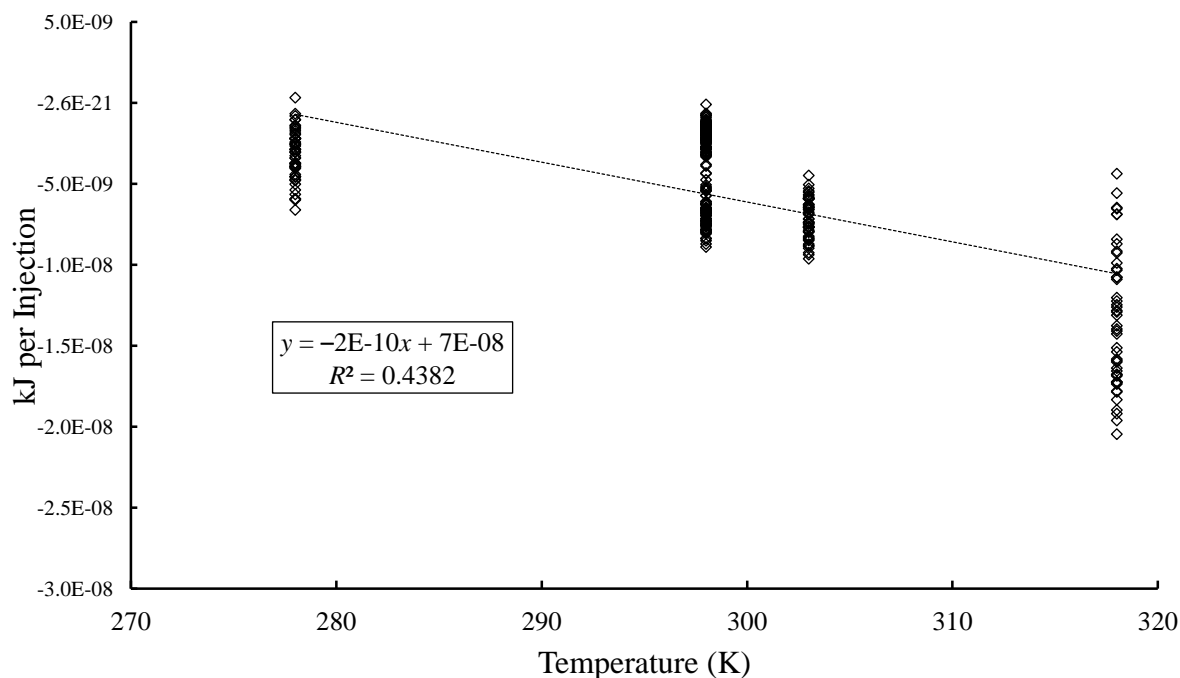
Figure 24. Estimation of blank correction.

Table 9. Enthalpy of Binding Under Pseudo-First-Order Conditions

Substrate Suspension	Titrant Solution (mM VX)	ΔH_{obs} (kJ/mol, Mean ± SSD)			
		Reaction Temperature			
		278 K	288 K	298 K	318 K
14,000 mg/L Suspengel 200	2	−3.08 ± 0.8305	−5.05 ± 0.981	−8.18 ± 1.010	−21.1 ± 1.72
Suspengel 200 Saturated with humus[a]	2	~0[b]	NA	−6.41 ± 0.662	−12.9 ± 0.88
28,000 mg/L Aldrich K10	0.4	~0[b]	NA	−8.67 ± 2.746	−13.3 ± 8.00

[a] Concentration was 8400 mg/L.
[b] No significant heat flow was detected; ΔH_{obs} = ~0 kJ/mol.
Notes: Reactions conducted first-order in substrate. Reported values are averages of 18 peaks. Corrected for titrant solution into pH 4.3 buffer.
NA, not applicable

Table 10. Maximum Heat Release Rates Under Pseudo-First-Order Conditions

Substrate Suspension	Titrant Solution (mM VX)	Maximum Heat Rate (kJ/s/mol, Mean ± SSD)			
		Reaction Temperature			
		278 K	288 K	298 K	318 K
14,000 mg/L Suspengel 200	2	−0.104 ± 0.0083	−0.177 ± 0.0071	−0.389 ± 0.0095	−0.846 ± 0.0751
Suspengel 200 saturated with humus[a]	2	~0[b]	NA	−0.272 ± 0.0083	−0.509 ± 0.0133
28,000 mg/L Aldrich K10	0.4	~0[b]	NA	−0.354 ± 0.0625	−0.496 ± 0.0436

[a] Concentration was 8400 mg/L.
[b] No significant heat flow was detected; ΔH_{obs} = ~0 kJ/mol.
Notes: Reactions conducted first-order in substrate. Reported values are averages of 18 peaks. These rates were not corrected for a blank titration.
NA, not applicable
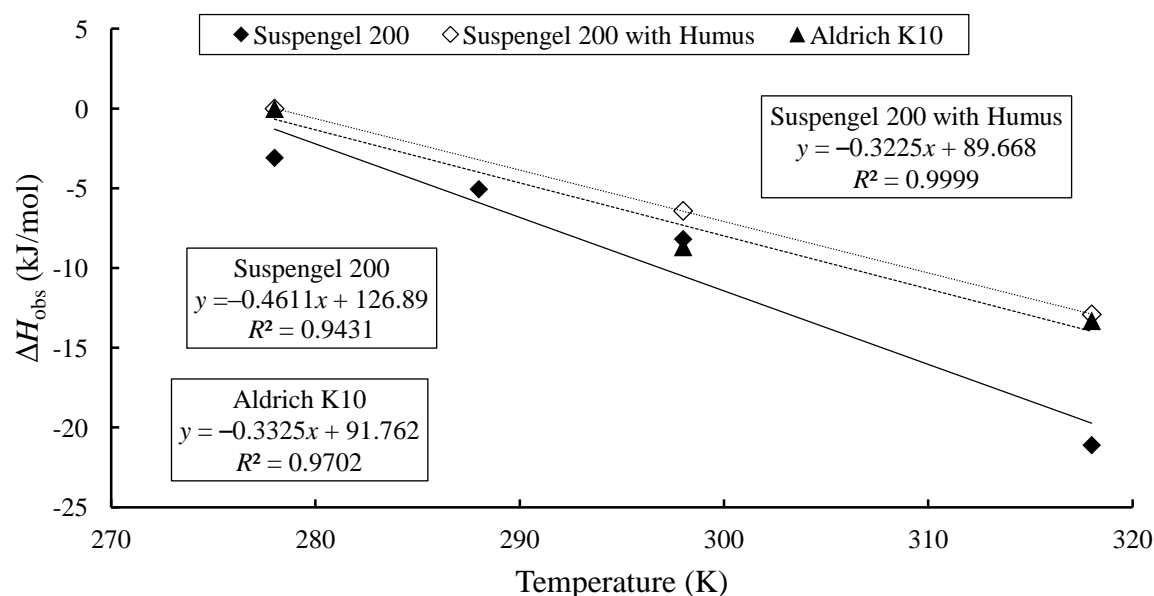
Figure 25. Estimation of heat capacity change of binding under pseudo-first-order conditions.

Table 11. Estimation of Arrhenius Activation Parameters
Under Pseudo-First-Order Conditions

Substrate Suspension	Titrant Solution (mM VX)	Arrhenius Parameters		
		E_a[b] (kJ/mol)	A[b] (kJ/s·mol)	E_a[c] (kJ/mol)
14,000 mg/L Suspengel 200	2	39.4	2.62E6	30.6[d] 38.5[e]
Suspengel 200 saturated with humus[a]	2	24.7	5.78E3	24.7[d]
28,000 mg/L Aldrich K10	0.4	13.3	75.5	13.3[d]

[a] Concentration was 8400 mg/L Suspengel 200.
[b] Estimated using graphical protocol.
[c] Estimated using two-point equation.
[d] Estimated using 298 and 318 K.
[e] Estimated using 278 and 318 K.
Note: Reactions conducted first-order in substrate.
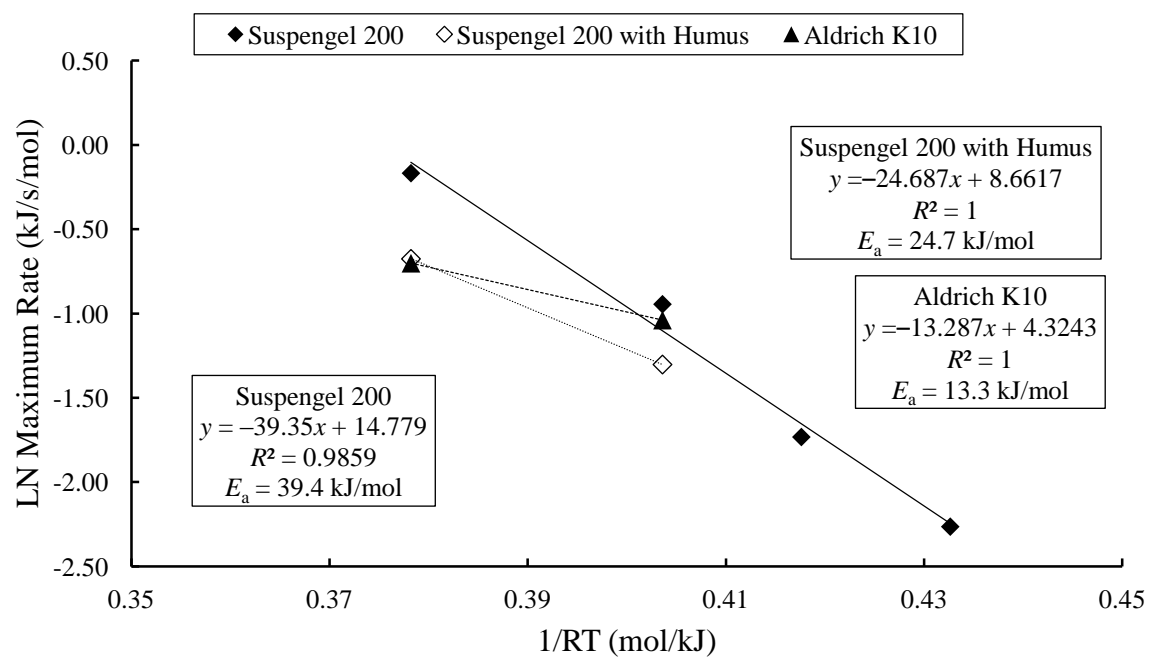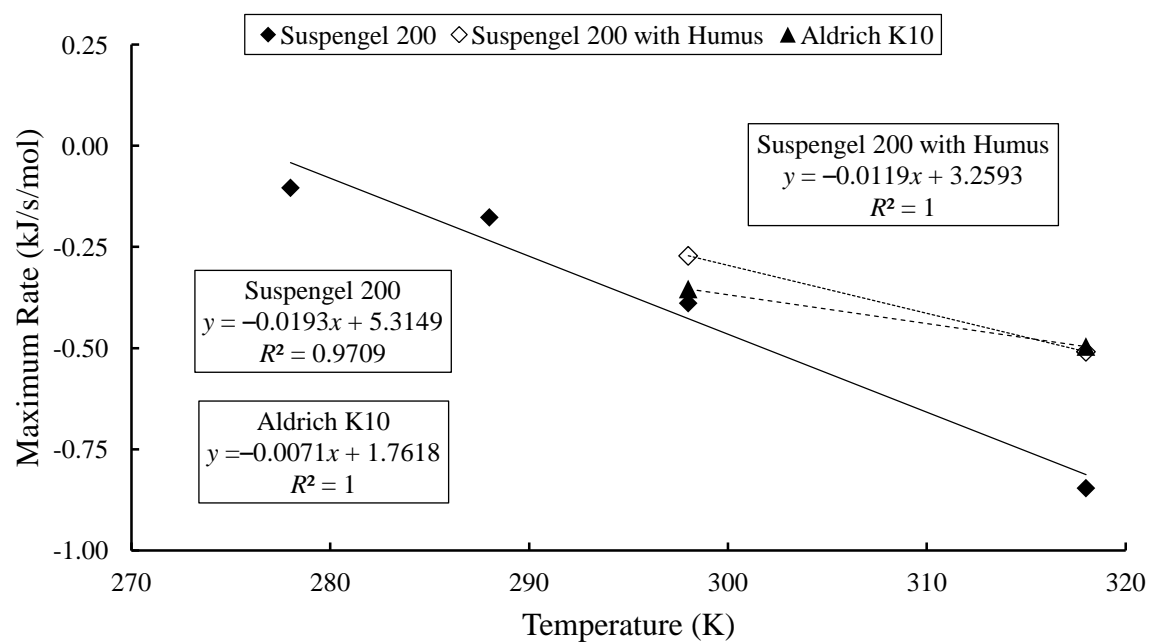
Figure 26. Estimation of E_a of binding.
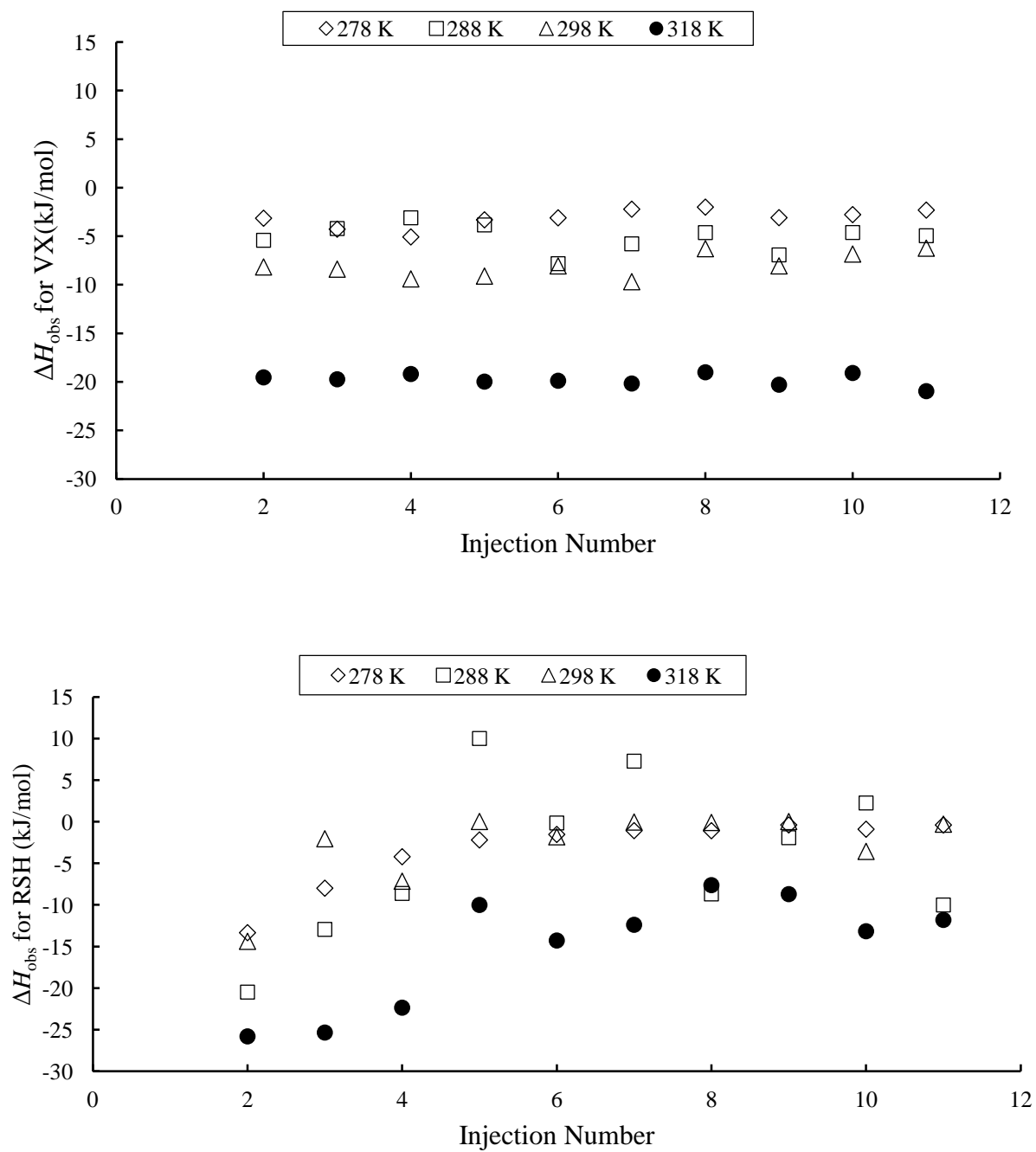
Figure 27. Injection-to-injection repeatability during pseudo-first-order reactions.
Top: VX; *bottom*: RSH. In both cases, the substrate was Suspengel 200.

3.2   Batch Equilibrium Sorption Isotherms

3.2.1   Kinetic Profiles

Prior to selection of substrates to be used in this study, a screening experiment was conducted with the twofold purpose of providing operator experience and some preliminary sorption data. In this screening effort, 12 NIST SRMs and 2 reagent-grade montmorillonite clays were evaluated. The NIST SRMs are described in Section 2.3, and the two reagent-grade clays were Aldrich KSF and K10 montmorillonite clays. The NIST SRMs were used as received, but the Aldrich clays had been converted to the homoionic Na^+ form for another project.[45] Substrate suspensions were prepared in a formulated source water (FSW) at a concentration of 250 mg/L. This FSW has been used in other agent fate studies and is well characterized.[74,107] The FSW has a pH of 7.7, total hardness of 25.7 mg/L, total dissolved solids of 100 mg/L, total organic carbon of 1.1 mg/L, and a specific conductance of 172 µmho/cm. These suspensions were allowed to equilibrate in the FSW for 72 h before being used. A mixed solution of MPA, EMPA, EA 2192, and VX was prepared in FSW at a concentration of ~1.6 mg/L and equilibrated to 298 K. The substrate suspensions were also equilibrated to 298 K prior to the start of the experiment. Once equilibrated, 10 mL of substrate suspension was mixed with 10 mL of analyte solution. Resulting suspensions were 125 mg/L in substrate and 0.8 mg/L in analyte, which is a 1:8,000 STS ratio. In addition to the samples, a control (no substrate) was also prepared. Samples were stirred, and time-point samples were removed at 0.25, 2, 6, and 48 h. Samples were immediately filtered (0.2 µm nylon Acrodisc) and analyzed by the LC/MS method described in Section 2.7.2. Relative to the control, there was no apparent loss of MPA, EMPA, or EA 2192 from solution when it was exposed to any of the 14 substrates. In the two Aldrich clay substrates, there was a significant decrease in VX solution concentration over time, with a slight increase in EMPA concentration. The increase in EMPA was similar to that observed in the FSW control reaction. The VX also degraded in the FSW, with a first-order half-life ($t_{1/2}$) of 248 h. The $t_{1/2}$ values in the Aldrich clay suspensions were 34.1 and 5.74 h for Aldrich KSF and Aldrich K10, respectively. The increases in EMPA concentration in the clay suspensions were equivalent to the increase observed in the control, suggesting that VX was being sorbed to the clay.

Once the substrate cleaning protocol described in Section 2.5 was established, preliminary kinetic sorption profiles were obtained at 298 K to investigate sorption of EMPA, MPA, and VX with three different clay substrates. The substrate suspensions were prepared in pH 4.3 buffer, and in all cases, the pH of the final suspension was determined to be 4.3. The substrate concentrations were 7350 mg/L for Suspengel 200, 7200 mg/L for Aldrich K10, and 7500 mg/L for kaolinite. The STS ratios ranged from 1:133 to 1:139 with an average of 1:136. The initial analyte concentrations were 699 ± 22.2 mg/L for MPA and 852 ± 21.9 mg/L for EMPA. In the phosphonic acid experiments, all samples were filtered and analyzed by the CE method described in Section 2.7.2. In the VX experiment, samples were analyzed unfiltered and filtered, to distinguish sorptive processes from degradation in bulk solution. The initial VX concentration in the filtered treatment was 97.4 ± 2.20 mg/L, and the unfiltered was 103 ± 1.8 mg/L. Because there was no significant difference between the filtered and unfiltered VX values, the overall average ($n = 14$) initial concentration of 100 ± 3.5 mg/L was used. The samples from the VX experiment were immediately extracted and analyzed using the GC/MSD method described in Section 2.7.1. The phosphonic acid results are illustrated in Figure 28. In all

cases, there was no loss of either phosphonic acid from solution, which indicates that neither phosphonic acid was sorbed by any of the substrates. Additional evidence for lack of sorption was also obtained during the ITC experiments, as summarized in Section 3.1.1. In a reported study, both MPA and EMPA were determined to bind with three different soils.[82] In that study, the STS ratio was 1:40, the samples were equilibrated for 24 h at 298 K, and the solution pH values ranged from 4.4 to 4.7. The reported S_{max} values ranged from 159 to 512 mg/kg for MPA and 2.1 to 3.9 mg/kg for EMPA. The reported distribution coefficients (K values) ranged from 0.00006 to 0.00016 L/kg for MPA and 0.0010 to 0.0080 L/kg for EMPA. The apparent discrepancy in results between the current study and the reported values is most likely due to differences in STS ratios and substrates (the reported study used soils) and the reported instability of EMPA in some soil extracts.

The initial kinetic sorption profiles for VX are illustrated in Figure 29. There was no significant sorption of VX by the kaolinite substrate, with the average ($n = 7$) filtered concentration being 93.1 ± 2.13 mg/L and the unfiltered concentration being 99.4 ± 5.37 mg/L. In both the filtered and unfiltered treatments, there were no trends observed in the concentrations over the 24 h experiment. The lack of sorption in the kaolinite kinetic sorption profiles was supported by the ITC experiments, as described in Section 3.1.1. There was significant loss of VX from solution in both the Suspengel 200 and Aldrich K10 suspensions. In the case of Suspengel 200, the average ($n = 7$) VX concentrations were 0.504 and 14.1 mg/L for filtered and unfiltered treatments, respectively. There was no trend in the filtered treatment, but a downward trend over time was observed in the unfiltered treatment. In the case of Aldrich K10, the average ($n = 7$) VX concentrations were 0.408 and 33.3 mg/L for the filtered and unfiltered treatments, respectively. There was no trend in the filtered treatment, but a downward trend over time was observed in the unfiltered treatment. In both cases, the fast loss of VX from solution was consistent with data from a previous study[18,19] and with the ITC results summarized in Section 3.1.1.

An initial kinetic sorption profile was obtained at 298 K to investigate sorption of VX with humus. The substrate suspension was prepared by mixing 4 mL of the humus stock suspension (Section 2.5) with either 16 mL of pH 4.3 buffer (control) or 16 mL of VX solution in pH 4.3 buffer. The samples were analyzed unfiltered and filtered (0.2 μm nylon Acrodisc) to help distinguish sorptive processes from degradation in the bulk solution. The average ($n = 7$) VX concentration in the filtered control was 27.9 ± 1.54 mg/L, and the average ($n = 7$) unfiltered control was 29.0 ± 0.67 mg/L. There was no significant difference between the filtered and unfiltered VX values, so the overall average ($n = 14$) initial VX concentration of 28.4 ± 1.27 mg/L was used. The samples from the VX experiment were immediately extracted and analyzed using the GC/MSD method described in Section 2.7.1. The results are illustrated in Figure 30. In all cases, there was no loss of VX from solution, which indicates that no significant sorption/degradation of VX by the humus substrate took place under the experimental conditions evaluated. As summarized in Section 3.1.3, additional evidence for lack of sorption was also obtained during the ITC experiments.
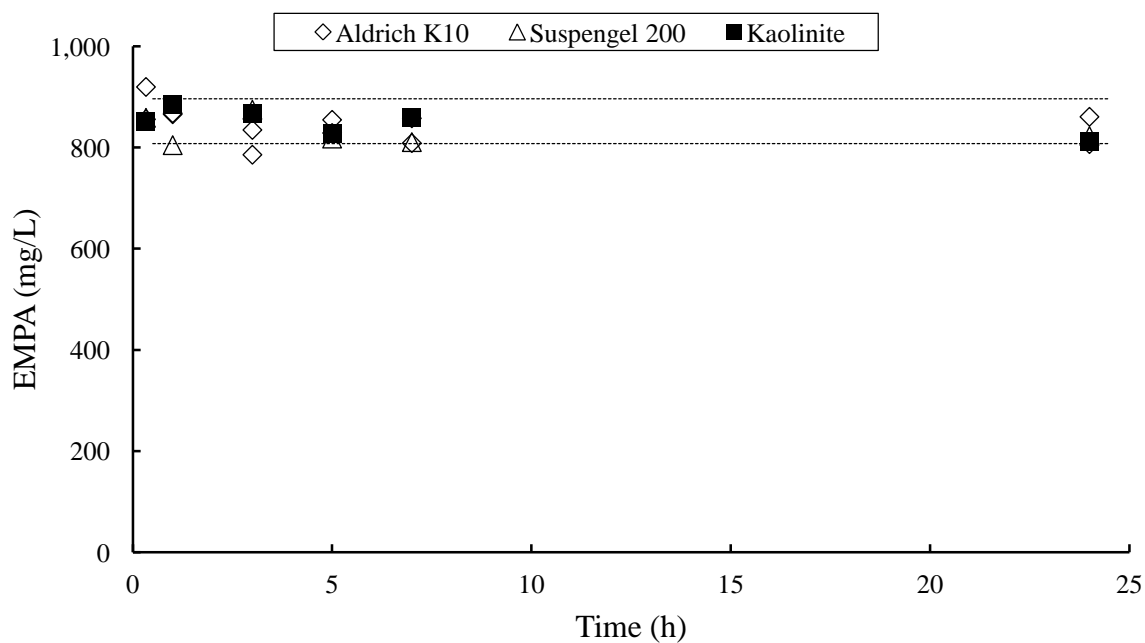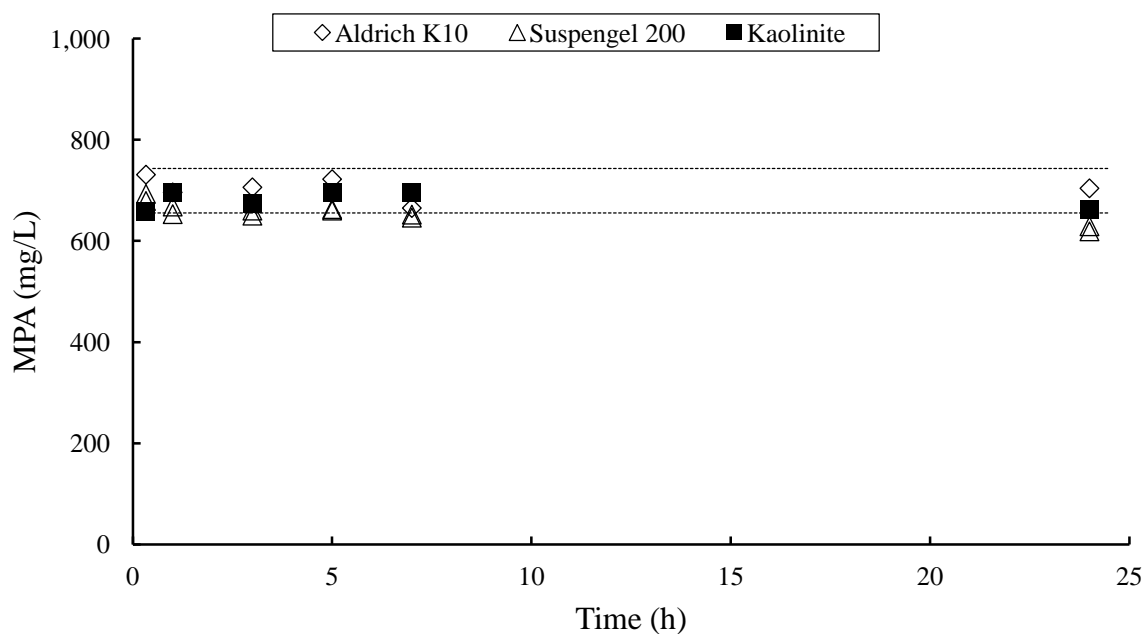
Figure 28. Initial kinetic sorption profiles for phosphonic acid degradation products.
Top: MPA; *bottom*: EMPA. Dashed lines indicate the estimated 95% confidence intervals for the control (no substrate) samples. Profiles were obtained at 298 K, and all samples were filtered.

Figure 29. Initial kinetic sorption profiles for VX with clay substrates.
Top: filtered; *bottom*: unfiltered. Dashed lines indicate the estimated 95% confidence
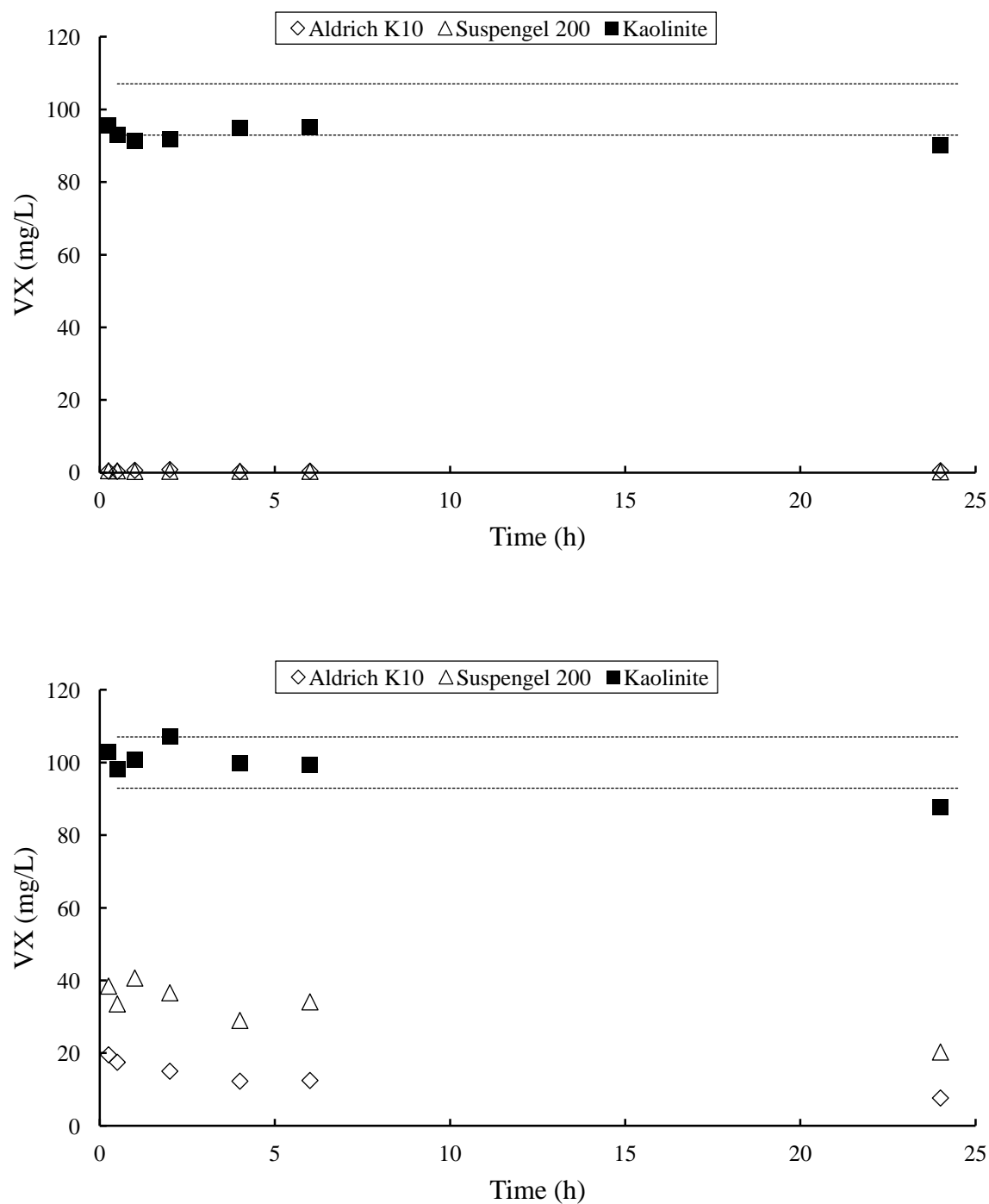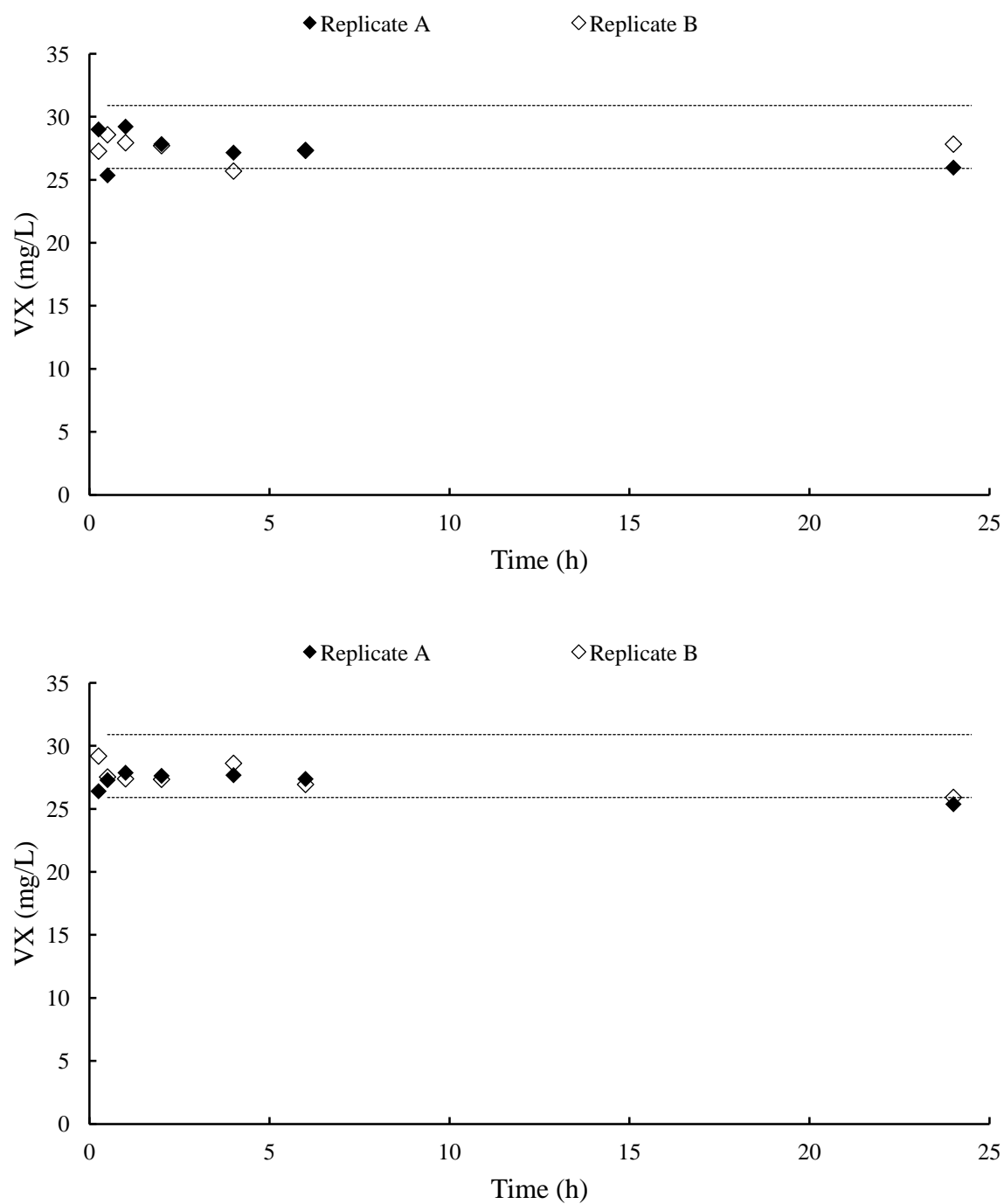intervals for the control (no substrate) samples. Profiles were obtained at 298 K.

Figure 30. Initial kinetic sorption profiles for VX with humus substrate. *Top*: filtered; *bottom*: unfiltered. Dashed lines indicate the 95% confidence intervals for the control (no substrate) filtered and unfiltered samples. Profiles were obtained at 298 K.

Once the baseline conditions were established, definitive kinetic sorption profiles were obtained at 298 K to investigate sorption of VX with Suspengel 200. It was decided to focus the definitive study on the natural clay substrate and not the highly processed catalyst clay identified as Aldrich K10. The substrate suspensions were prepared in pH 4.3 buffer, and in all cases, the pH of the final suspension was determined to be 4.3. The substrate concentrations were 100, 200, 400, and 1000 mg/L, which corresponded to STS ratios of 1:10,000, 1:5,000, 1:2,500, and 1:1,000, respectively. The clay concentrations utilized in this experiment corresponded to VX loadings as a percentage of S_{max} (Table 12) of 173, 86.6, 43.3, and 17.3%. Results are illustrated in Figures 31 through 34. The VX control samples exhibited no trending with time, with average ($n = 10$, ±SSD) VX concentrations of 20.5 ± 0.96 and 20.9 ± 0.99 mg/L for filtered and unfiltered samples, respectively. There was no significant difference between the filtered and unfiltered control samples, so the overall average ($n = 20$, ±SSD) VX concentration of 20.7 ± 0.97 mg/L was used in all calculations.

The loss of VX from solution was very fast, with no change in dissolved VX (VX_F) concentration between the first (15 min) and last (8640 min) sampling points. This fast sorption of VX from dilute solution was also observed in a previous study.[18,19] In calculations, the average ($n = 10$) dissolved VX concentration for each Suspengel 200 loading was used because no trending was observed over time. The average initial VX (VX_{INT}) added to each vial was 1.04 mg. Similarly, no trending was observed for the RSSR concentrations, and the average initial RSSR in each vial was 0.0369 mg. The RSSR was not added to the clay suspensions but was present as an impurity in the VX. Using the following relationships, the recovery of VX (or RSSR) from the clay substrate at each time point was calculated. The VX recovered in the dissolved (filtered) fraction was identified as VX_F, and the whole (unfiltered) VX recovered was identified as VX_{UF}. The total amount of VX bound to the substrate was identified as VX_{TOT}, and the VX recovered from the substrate was identified as VX_{REC}.

$$VX_{INT} - VX_F = VX_{TOT}$$

$$VX_{UF} - VX_F = VX_{REC}$$

Recoveries of VX and RRSR from the Suspengel 200 substrate as a function of aging time and VX loading are illustrated in Figures 35 and 36. In addition, the initial recovery at 15 min and the minimum modeled recoveries are also illustrated. The minimum recoveries were estimated using a nonlinear Langmuir model.[85–87] Recovery of both VX and RSSR from the Suspengel 200 decreased with aging time. This phenomenon of recovery loss with aging is well documented in the pesticide literature.[108–110] In addition to recovery loss as a function of aging time, there was a significant decrease in recovery based on the substrate concentration. The loss of recovery appears to be biphasic, in which the initial loss rate (in the first hour) is fast and is followed by a slower secondary loss rate. Overall, for both VX and RSSR, the initial recovery loss rate was determined to be ~0.5 %/min, and the slower secondary-recovery loss rate was determined to be ~100 times slower.

Once the baseline conditions were established, a definitive kinetic sorption profile was obtained at 298 K to investigate sorption of EMPA with Suspengel 200. The substrate suspensions were prepared in pH 4.3 buffer, and in all cases, the pH of the final suspension was

determined to be 4.3. The substrate concentrations were 100, 200, 400, and 1,000 mg/L, which corresponded to STS ratios of 1:10,000, 1:5,000, 1:2500, and 1:1,000. Results are illustrated in Figure 37. The EMPA control samples exhibited no trending with time, with an average ($n = 6$) EMPA concentration of 77.2 ± 1.80 mg/L. There was no loss of EMPA from solution under any of the substrate loadings. These results support those from previous experiments and demonstrate that no VX degradation occurred in these sorption profiles.

After the sorption profiles were completed, a kinetic desorption profile was obtained at 298 K to investigate desorption of VX from Suspengel 200. The substrate suspensions were prepared in pH 4.3 buffer, and in all cases, the pH of the final suspension was determined to be 4.3. The substrate concentrations were 100, 200, 400, and 1000 mg/L, which corresponded to solid–liquid ratios of 1:10,000, 1:5000, 1:2500, and 1:1000, respectively. Once the substrate and VX solutions were mixed, the suspensions were allowed to stir for 8 days while being maintained at 298 K. Once the 8 day sorption phase was completed, the vials were centrifuged, and the supernatant was discarded. The clay pellet was then resuspended in 40 mL of fresh pH 4.3 buffer and stirred for 1 h; then the centrifugation was repeated. The supernatant was discarded. The clay pellet was then resuspended in 20 mL of 2-propanol, and stirring was started. The 2-propanol was chosen as the desorption solvent because a previous study had demonstrated the ability of 2-propanol to effectively desorb VX from a variety of sorbent materials.[49] Time-point samples were obtained and analyzed by GC/MSD. Results are illustrated in Figure 38. There was an upward trend observed with increasing desorption time, and the maximum amount of VX desorbed was estimated using a nonlinear Langmuir model.[85–87] These results are also illustrated in Figure 38. The results of the desorption experiment clearly demonstrated that VX did not degrade during the sorption process and was stable for at least 8 days under the conditions evaluated. In a reported study, hexadecyltrimethylammonium bromide (CTAB; $C_{19}H_{42}BrN$; CAS no. 57-09-0) was found to be stable for at least 5 months when sorbed to a natural montmorillonite clay.[111] In that study, the CTAB was sorbed from dilute aqueous solution, then the modified clay was isolated, air-dried, and stored dry at ~293 K. In both the current and reported studies, the reported stabilities should be considered lower limits, because the experiments were terminated after 8 days or 5 months, respectively.
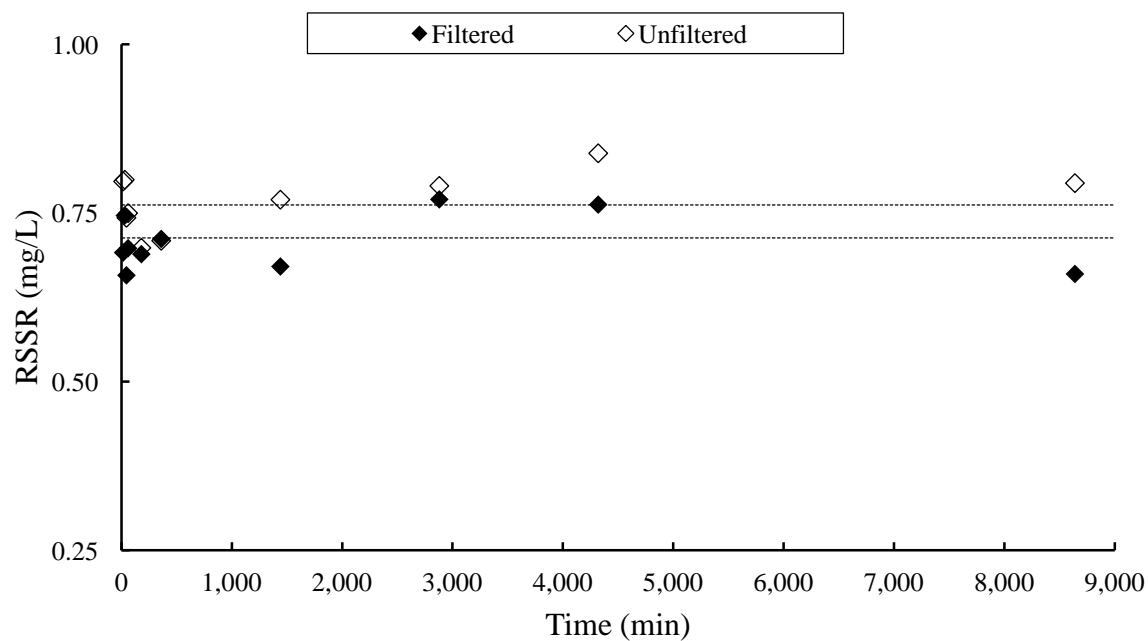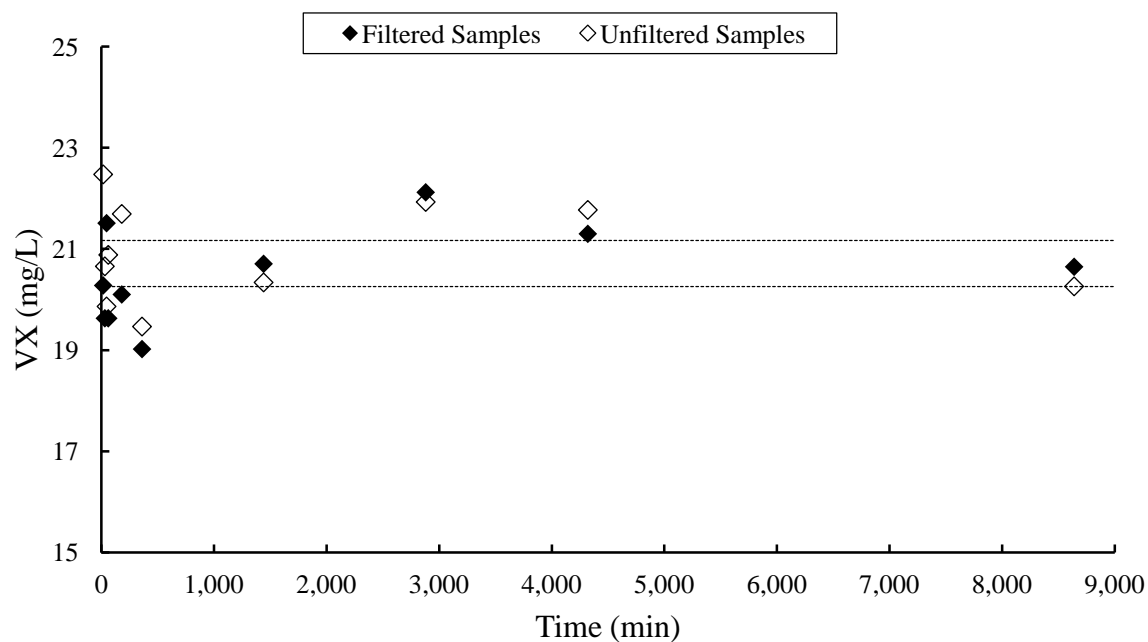
Figure 31. Kinetic profiles of filtered and unfiltered control samples. *Top*: VX; *bottom*: RSSR. Dashed lines indicate the 95% confidence intervals for the average values. RSSR was present as an impurity in the VX. Profiles were obtained at 298 K. Note: *y*-scales are shown close up to clarify detail.
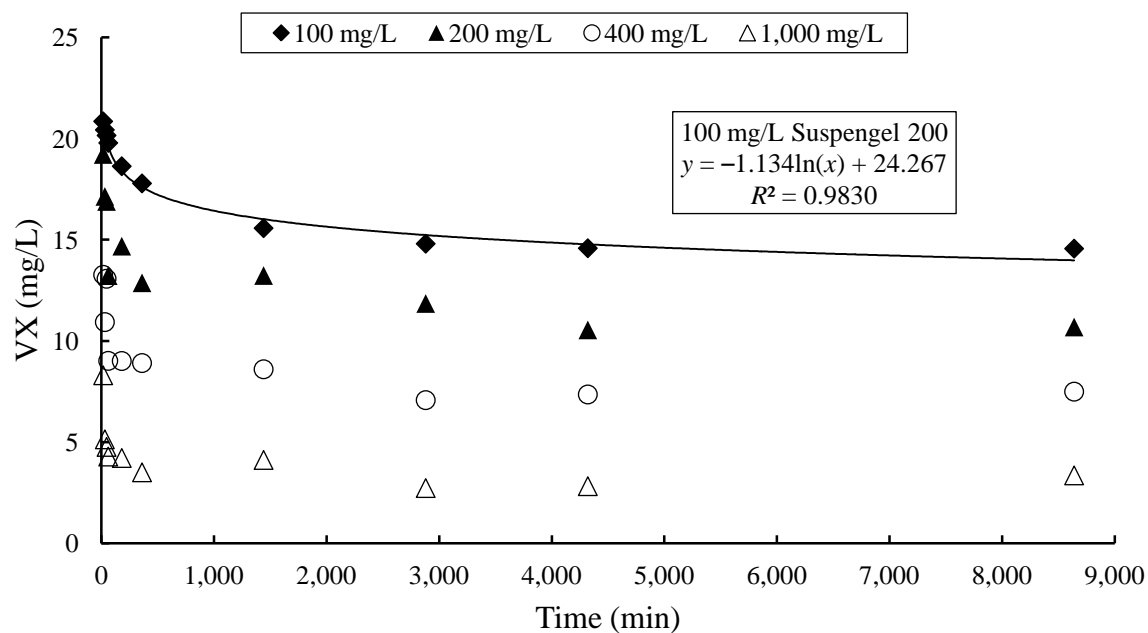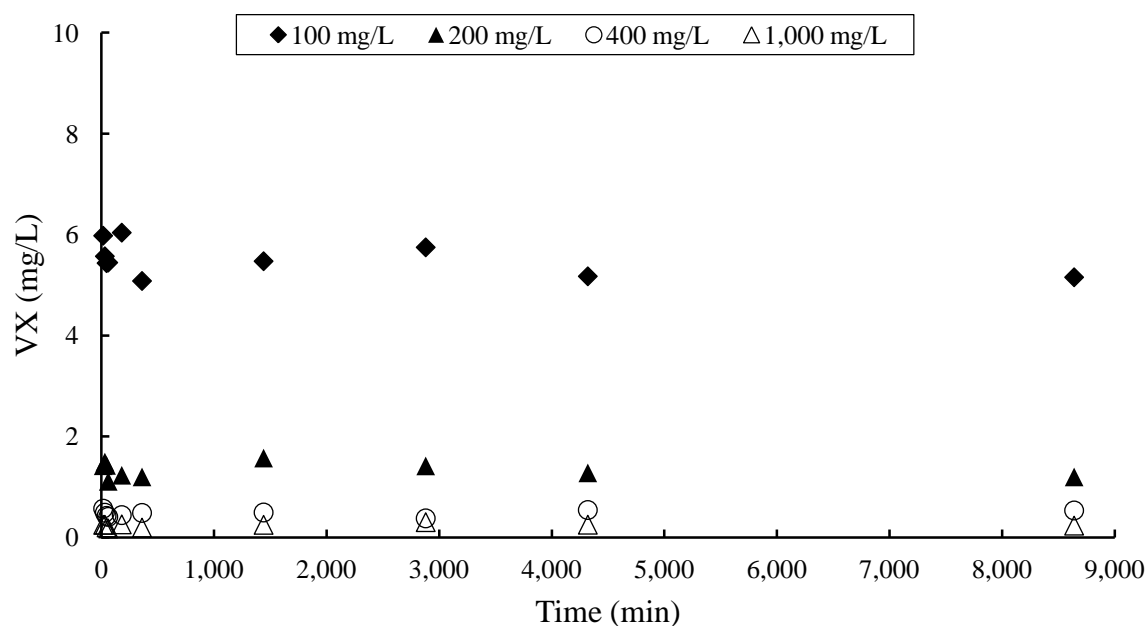
Figure 32. Kinetic profiles of filtered and unfiltered VX samples. *Top*: filtered; *bottom*: unfiltered. In all cases, the substrate was Suspengel 200. Profiles were obtained at 298 K.
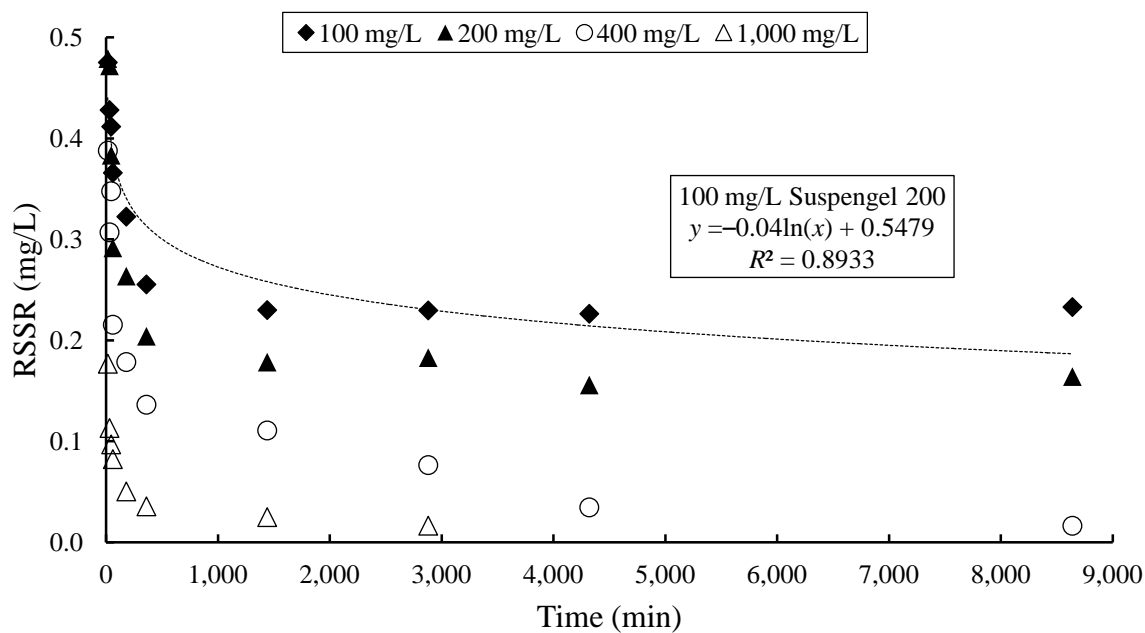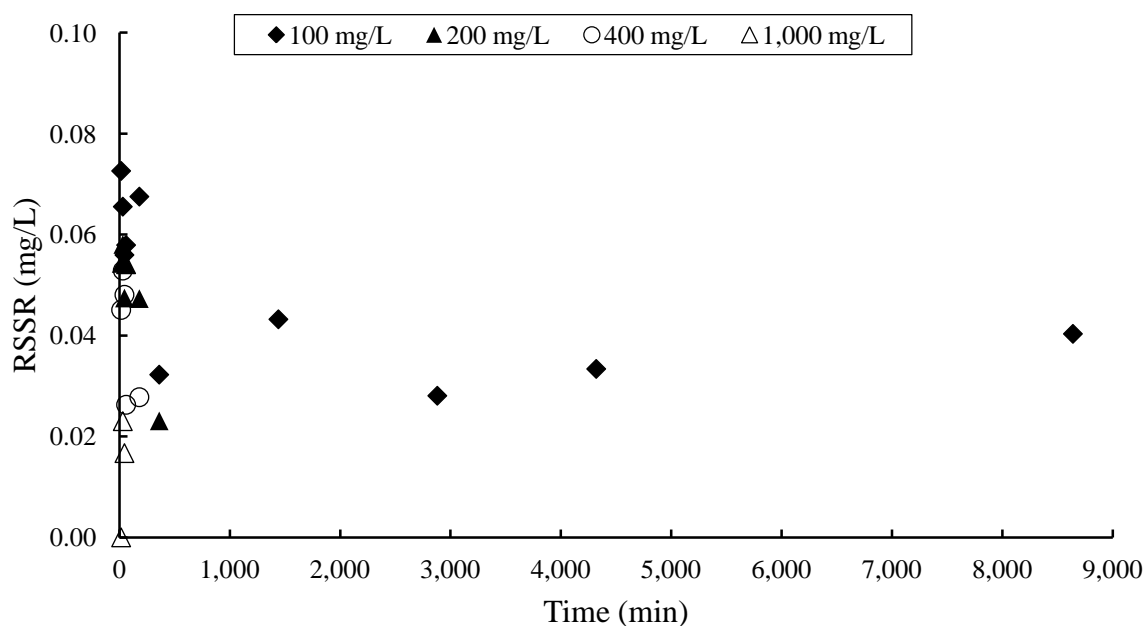
Figure 33. Kinetic profiles of filtered and unfiltered RSSR samples. *Top*: filtered; *bottom*: unfiltered. RSSR was present as an impurity in the VX. In all cases, the substrate was Suspengel 200. Profiles were obtained at 298 K.
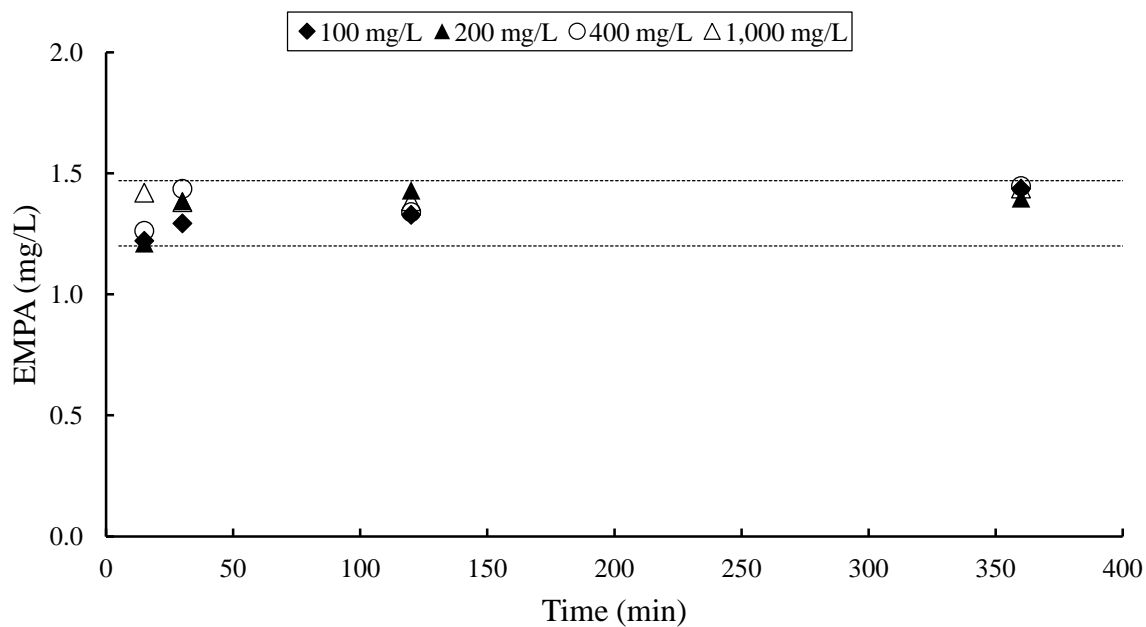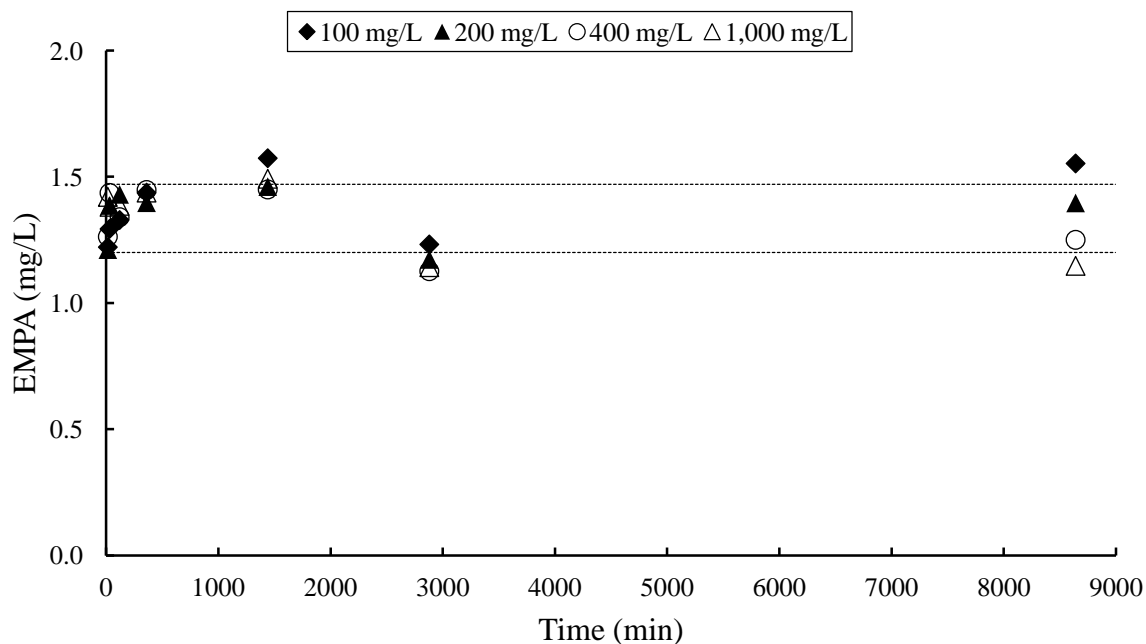
Figure 34. Kinetic profiles for EMPA impurity with different substrate loadings. Dashed lines indicate the estimated 95% confidence intervals for the control samples. *Top*: full-time range; *bottom*: close-up view to show to first 400 min. EMPA was present as an impurity in the VX. In all cases, the substrate was Suspengel 200. Profiles were obtained at 298 K.
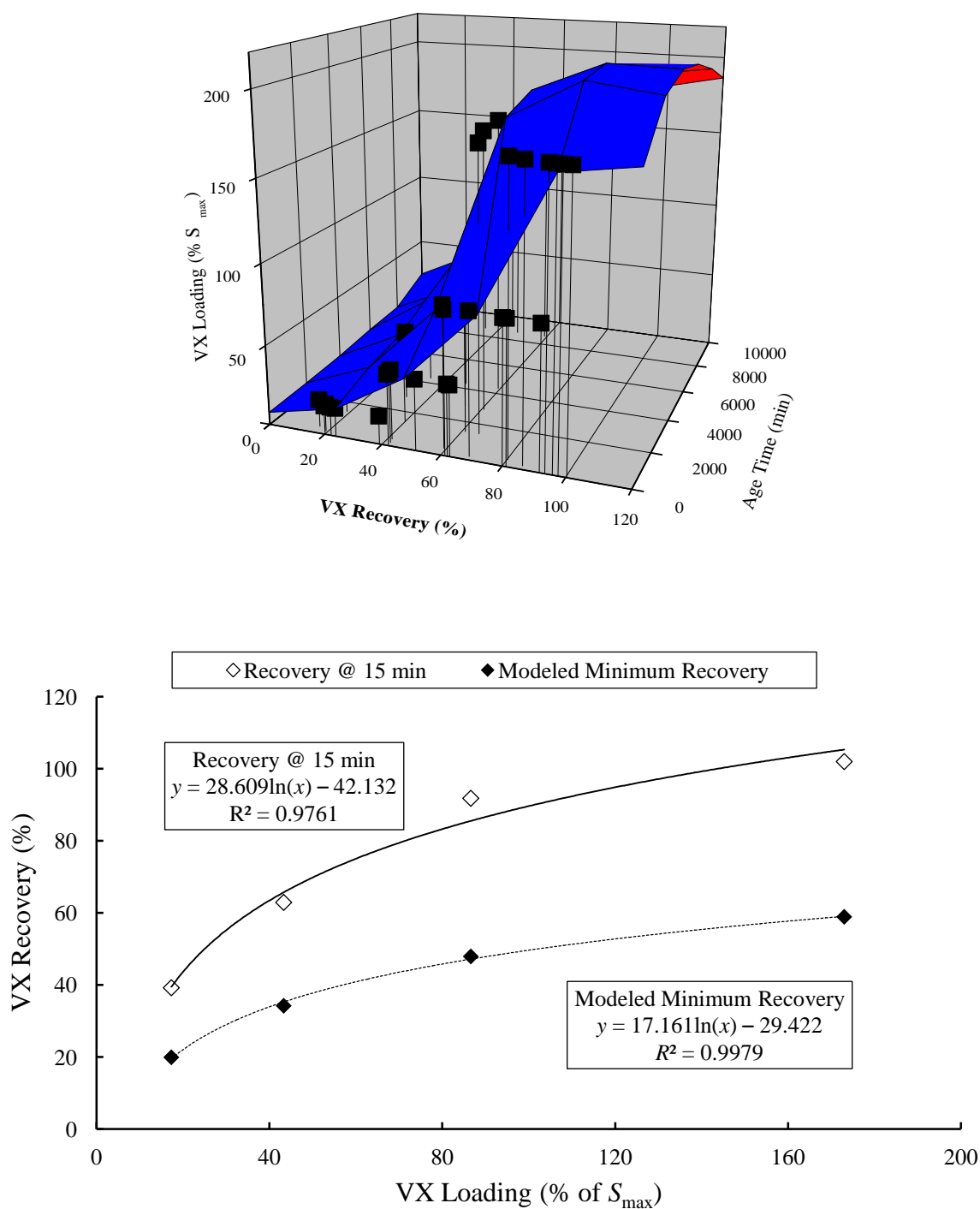
Figure 35. Recovery of VX from Suspengel 200 as a function of aging time and VX loading. *Top*: recovery versus aging time and VX loading. *Bottom*: initial recovery at 15 min and modeled minimum recovery as a function of VX loading. Profiles were obtained at 298 K.
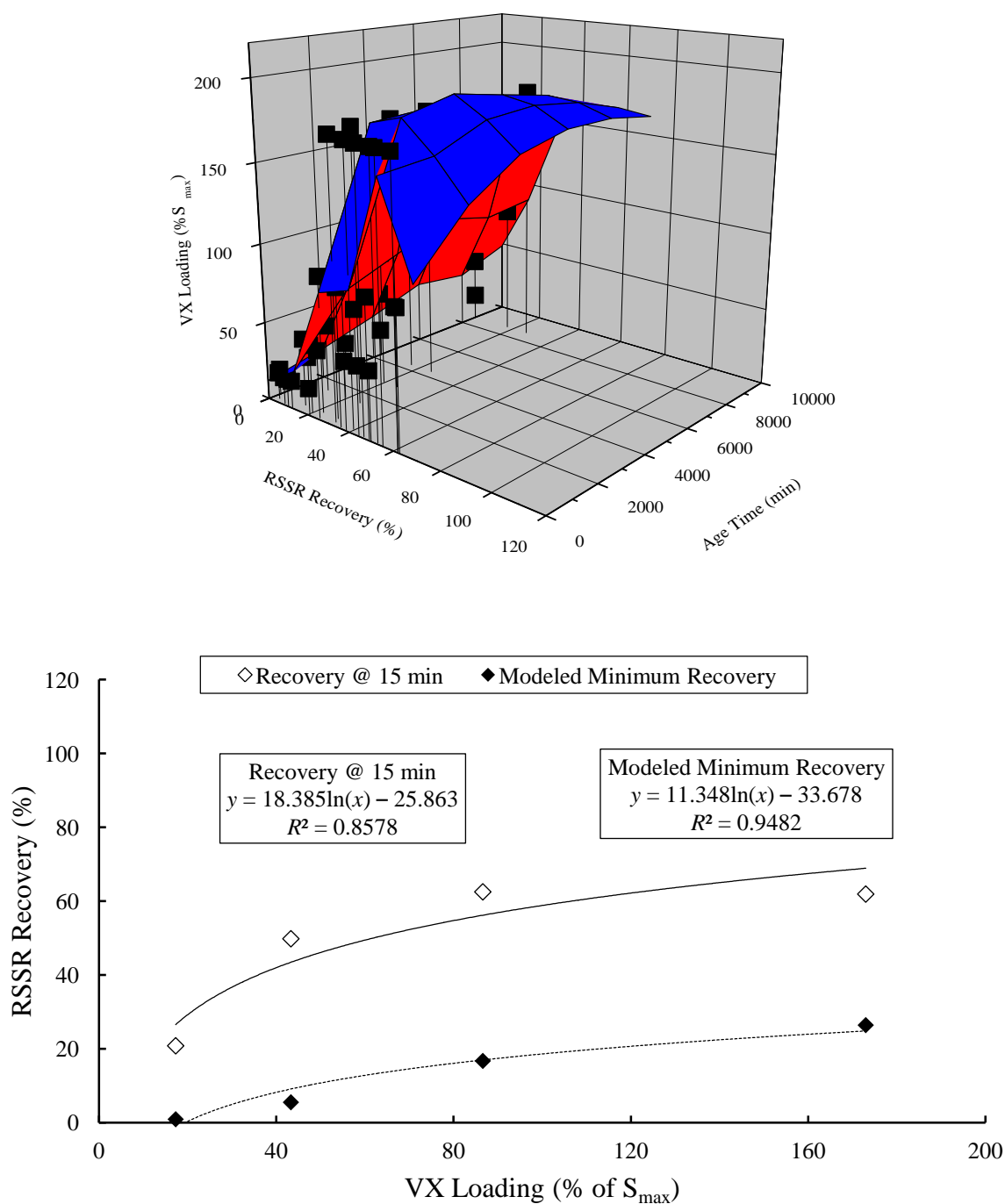
Figure 36. Recovery of RSSR from Suspengel 200 as a function of aging time and VX loading. *Top*: recovery versus aging time and VX loading. *Bottom*: initial recovery at 15 min and modeled minimum recovery as a function of VX loading. Profiles were obtained at 298 K. RSSR was present as an impurity in the VX.
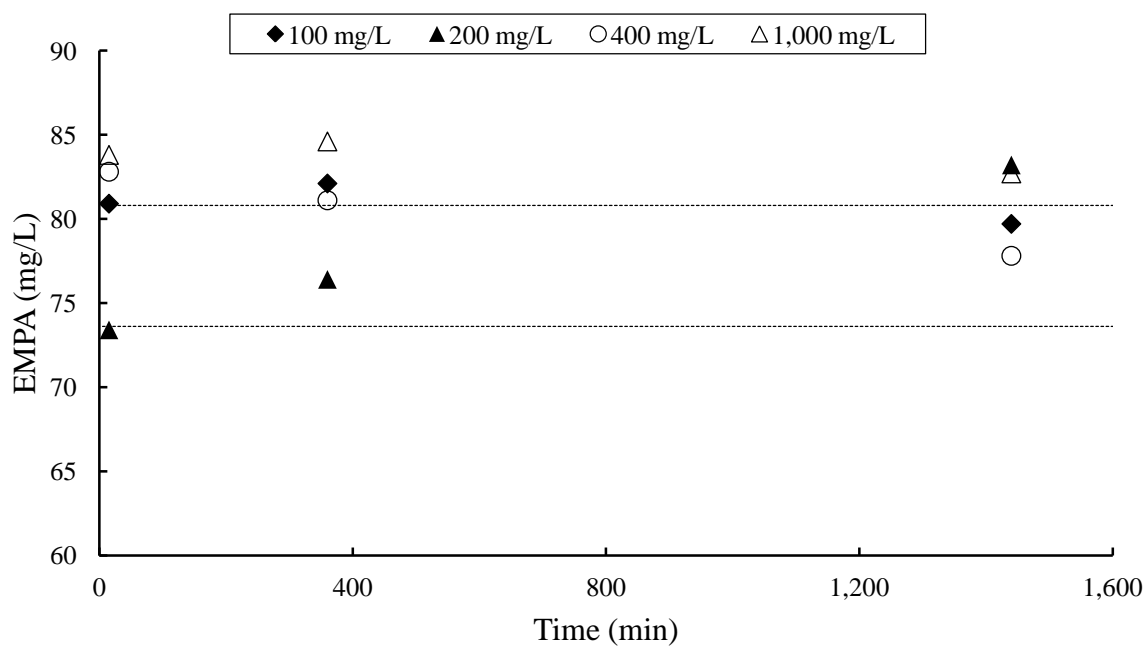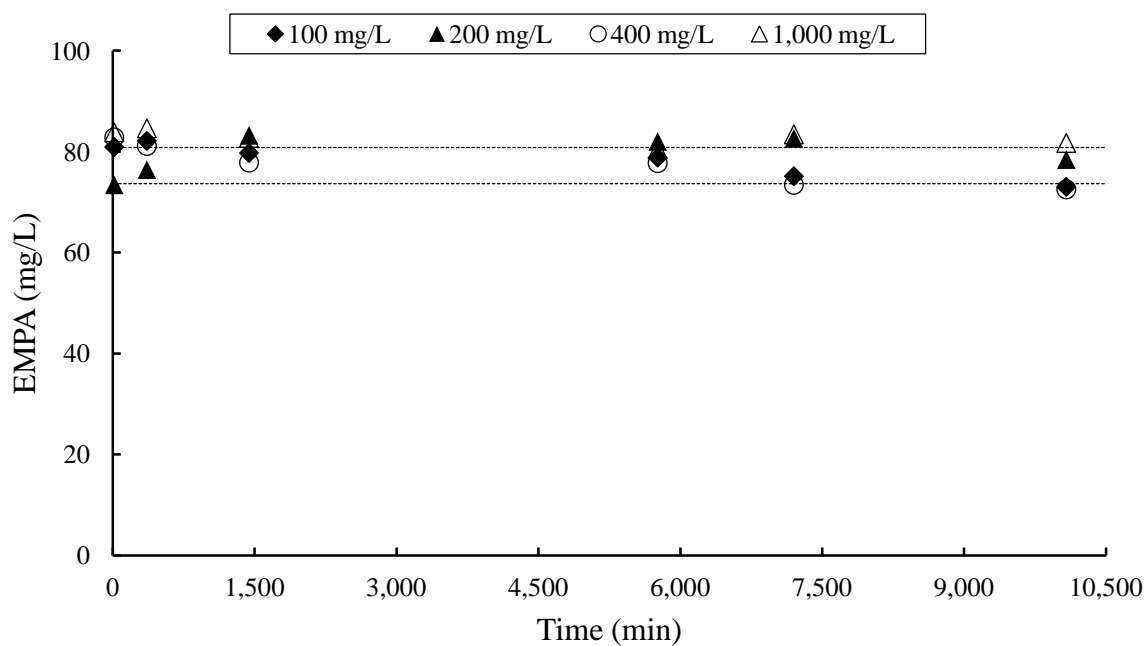
Figure 37. Kinetic sorption profiles for EMPA with different Suspengel 200 concentrations. Dashed lines indicate the estimated 95% confidence intervals for the control samples. *Top*: full time range; *bottom*: close-up view to show the first 1600 min. Profile was obtained at 298 K.
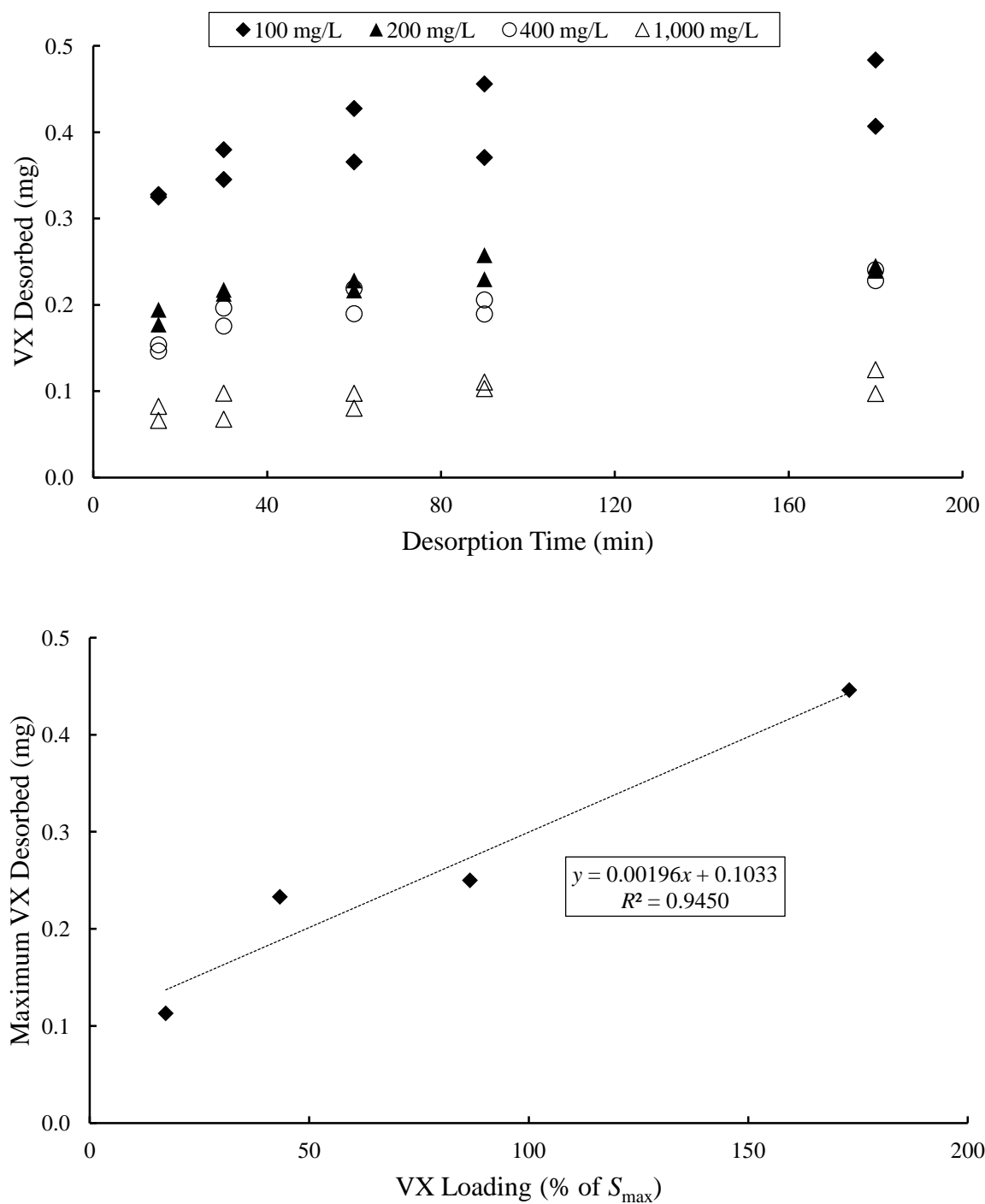
Figure 38. Kinetic desorption profiles for VX with different Suspengel 200 concentrations. *Top*: kinetic profile; *bottom*: modeled maximum amount of VX desorbed as a function of clay loading. Profiles were obtained at 298 K.

3.2.2   Batch Equilibrium Sorption Isotherms

            Batch equilibrium sorption isotherms for VX on clay substrates were obtained at
298 K, using an equilibration time of 60 min. The 60 min equilibration time was chosen based on
the kinetic profiles described in Section 3.2.1. The isotherms were constructed using a variable
STS approach[83] with STS ratios ranging from 1:1,000 to 1:10,000. In all cases, the substrates
were suspended in pH 4.3 buffer, and pH was maintained at 4.3 through all STS ratios. The VX
batch equilibrium sorption isotherms for the Aldrich K10 and Suspengel 200 montmorillonite
clay substrates are illustrated in Figure 39. The initial VX concentrations were determined to be
30.9 and 30.5 mg/L for runs 1 and 2 of the Aldrich K10 clay, respectively. The initial VX
concentrations were determined to be 20.3 and 22.8 mg/L for runs 1 and 2 of the Suspengel 200
clay, respectively. Combined data from both runs for each substrate was evaluated using
nonlinear isotherm models.[85–87] In both cases, only the Langmuir model was able to converge on
a solution. The model parameters are summarized in Table 12. The modeled S_{max} values were
45,000 and 119,000 mg/kg for Aldrich K10 and Suspengel 200, respectively. These S_{max} values
were still significantly different when normalized to BET_{N2} surface area, being 0.182 and
4.01 mg/m^2 for Aldrich K10 and Suspengel 200, respectively. When normalized to the CEC_{A+B},
the S_{max} values became 262 and 261 mg/meq for Aldrich K10 and Suspengel 200, respectively.
Because the molecular weight of VX is 267, these CEC_{A+B} normalized S_{max} values translated to
0.981 and 0.978 meq_{VX}/meq_{clay} for Aldrich K10 and Suspengel 200, respectively. This indicates
that within experimental error, VX interacted with both clay substrates on a 1:1 basis, and the
interaction appeared to be an ion-exchange process. The average S_{max} value of 119,000 mg/kg
obtained for the Suspengel 200 using the isotherm approach was significantly lower (by ~30%)
than the value obtained during the ITC experiments (Section 3.1.2). It is thought that the S_{max}
value from the ITC results was overestimated due to inclusion of heat flows associated with
flocculation events.

            In one study found in the literature (referred to as the 2004 LLNL study), the
sorption of VX to montmorillonite clay (and other environmental matrices) in dilute suspensions
was examined.[18,19] The results from this study are compared with results from the current study
in Figure 40. In the 2004 LLNL study, the clay was an Aldrich montmorillonite clay, but the
authors did not provide details on which type of clay was used. Data from the 2004 LLNL study
was evaluated using nonlinear isotherm models.[85–87] Only the Freundlich-Langmuir model was
able to converge on a solution. The model parameters are summarized in Table 13. Because few
experimental details were provided in the 2004 LLNL paper, it is difficult to directly compare
results from the two studies.

            Batch equilibrium sorption isotherms for VX on soil substrates were obtained at
298 K using an equilibration time of 60 min. The 60 min equilibration time was chosen based on
the kinetic profiles described in Section 3.2.1. The isotherms were constructed using a variable
STS approach[83] with STS ratios ranging from 1:189 to 1:27,000. In all cases, the substrates were
suspended in pH 4.3 buffer, and pH was maintained at 4.3 through all STS ratios. The VX batch
equilibrium sorption isotherms for the HCB and MCL soil substrates are illustrated in Figure 41.
The initial VX concentrations were both determined to be 18.4 mg/L. Isotherm data from each
run was evaluated using nonlinear isotherm models.[85–87] In the case of the HCB soil, none of the
four models evaluated were able to successfully converge on a solution. In the case of the MCL

soil, only the Freundlich-Langmuir model was able to converge on a solution. The model parameters are summarized in Table 13.

In many cases, model source terms for the K values related to sorption or partitioning processes were *estimated* using K_{OC} values.[22–24] Although K_{OC} values can be measured, they are typically estimated using K_{OW} values.[22–24] This estimation is based on the assumption that the organic carbon content of the soil is the only determinant of the sorption of a chemical from the water onto the soil. However, recent studies have concluded that the use of K_{OC} values can lead to inaccurate estimates of sorption processes in soil systems.[25–27] In the literature, reported log K_{OW} values for VX ranged from 0.675 to 2.13.[18,19,24,40,46,112,113] The reported log K_{OW} values can be sorted into two groups: measured and estimated. The single measured log K_{OW} value of 0.675 was determined using a shake-flask approach with DIW as the aqueous phase.[113] The estimated log K_{OW} values ranged from 1.992 to 2.13, with an average value of 2.06. Following an established methodology,[24] K_d values were estimated using the reported log K_{OW} values and the organic carbon fraction (f_{OC}) for the MCL soil determined in the current study. The *estimated* K_d value for the MCL soil was 3.30 L/kg when the reported log K_{OW} of 0.675 was used in the calculation. The *estimated* K_d value for the MCL soil was 10.1 L/kg when the average reported log K_{OW} of 2.06 was used in the calculation. In the current study, the *measured* K_d value for the MCL soil was 0.0729 L/kg, with a 95% confidence interval of 0.0696 to 0.0762 L/kg. The estimated K_d values ranged from 45 to 138 times higher than the measured value, depending on which log K_{OW} value was used in the calculation. Using the *estimated* K_d values will significantly underestimate the mobility of VX in the MCL soil.
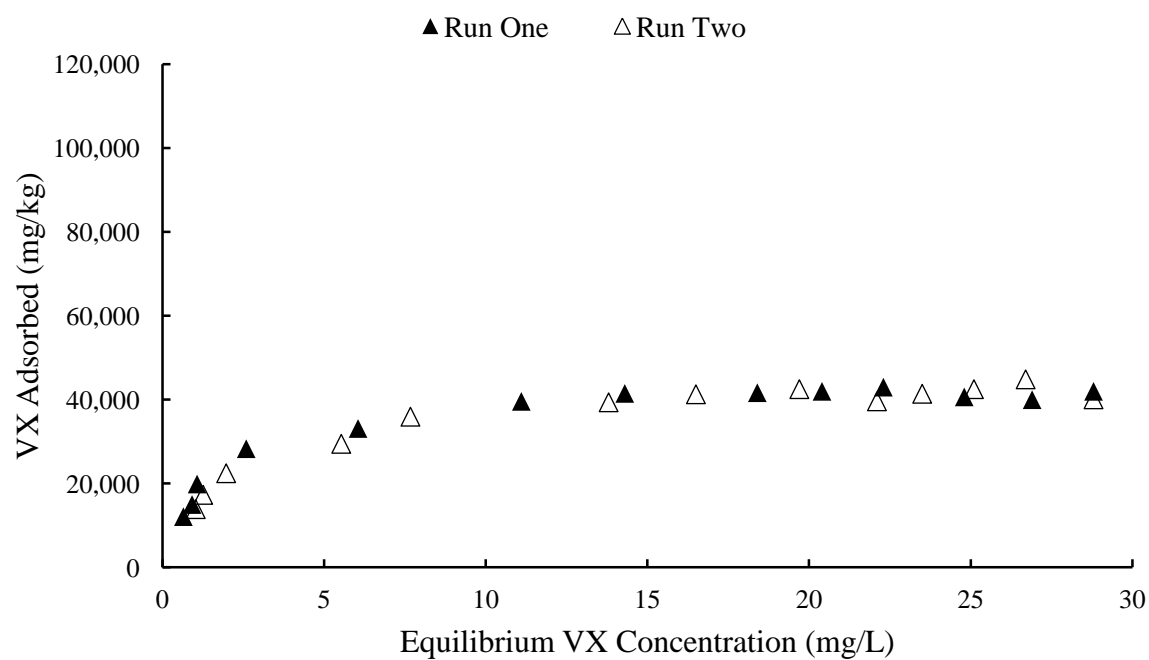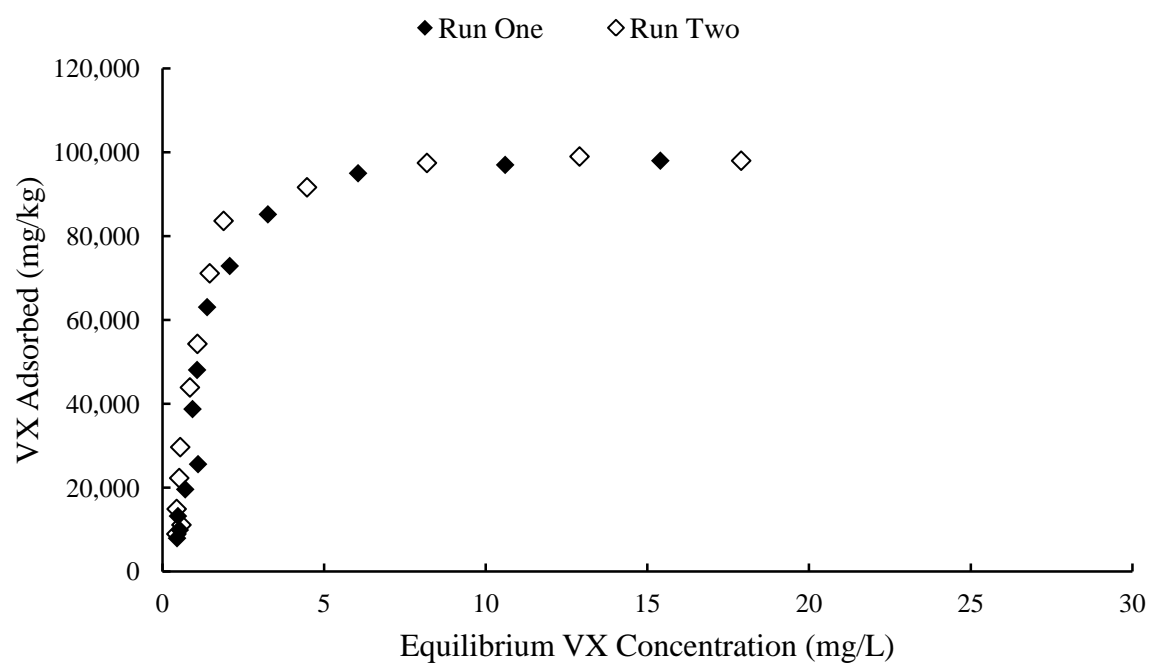
Figure 39. Batch equilibrium sorption isotherms for VX interacting with montmorillonites. *Top*: Suspengel 200; *bottom*: Aldrich K10. Isotherms were obtained at 298 K.

Table 12. Results of Nonlinear Langmuir Modeling of VX Equilibrium Isotherm Data

Model Parameter	Clay Substrate	
	Aldrich K10	Suspengel 200
S_{max} (mg/kg)	45,000 (43,700–46,300)	119,000 (104,000–134,000)
K_d (L/kg)	0.536 (0.453–0.618)	0.570 (0.371–0.768)
Goodness of fit	0.974	0.897

Notes: Results were modeled using the combined data of both runs. Runs were obtained at 298 K. Results are reported as fitted values; estimated 95% confidence intervals are in parentheses.
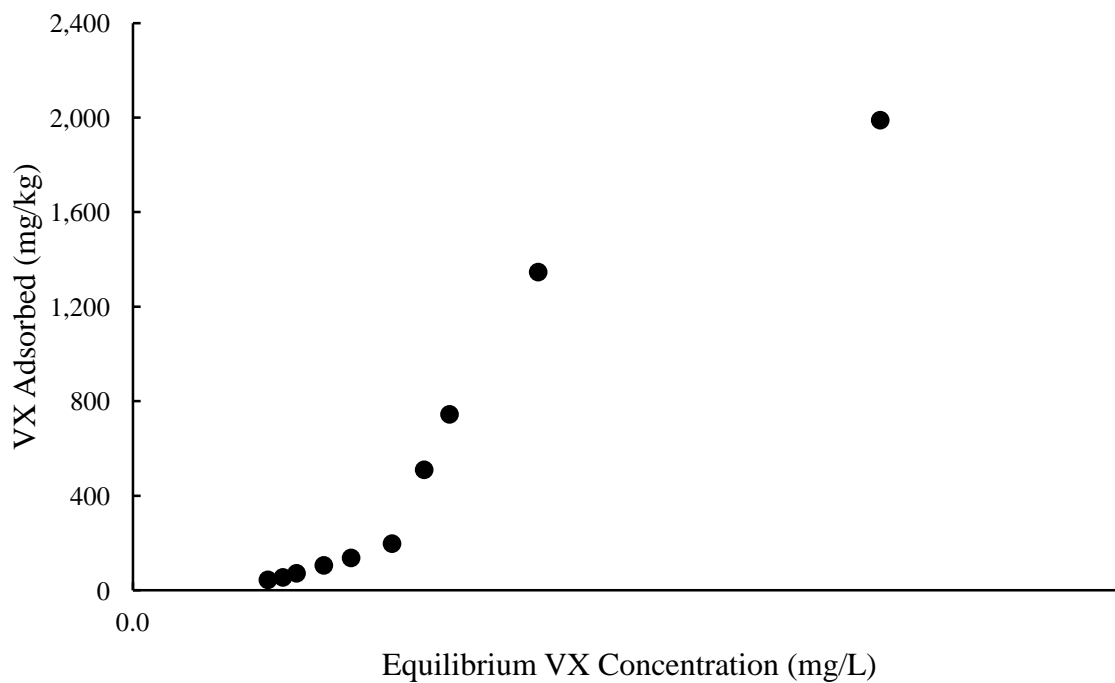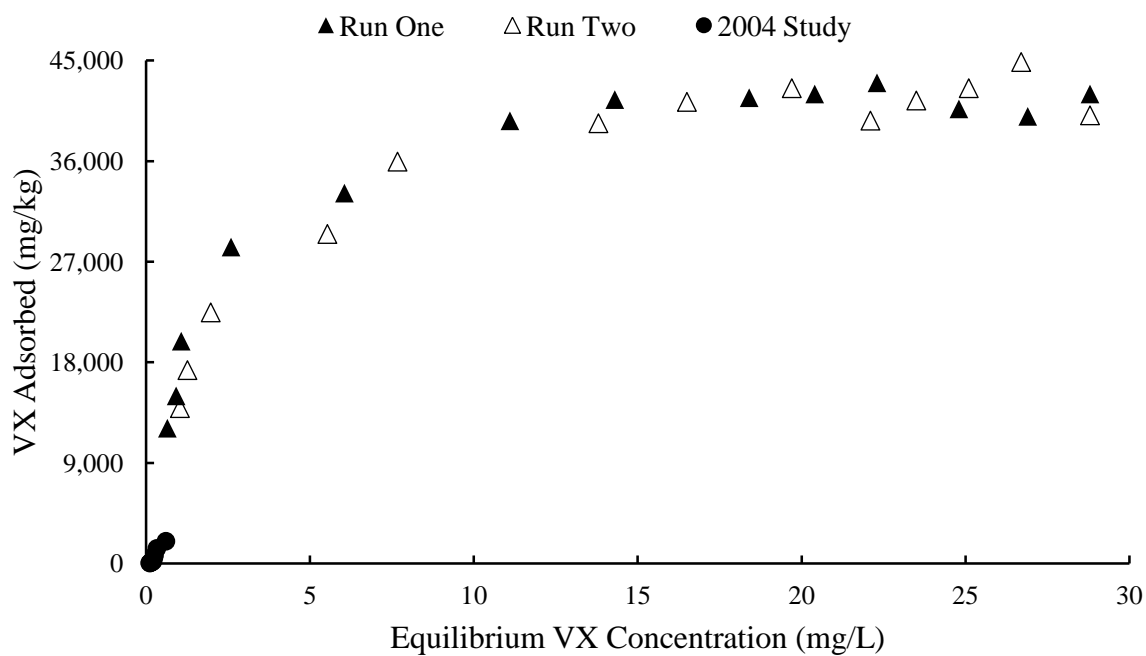
Figure 40. Comparison of batch equilibrium sorption isotherms for VX from two different studies. *Top*: Aldrich K10 results from the current study compared with data from a reported study. *Bottom*: close-up view to illustrate data from Davisson et al.[19] and Morrissey et al.[20]
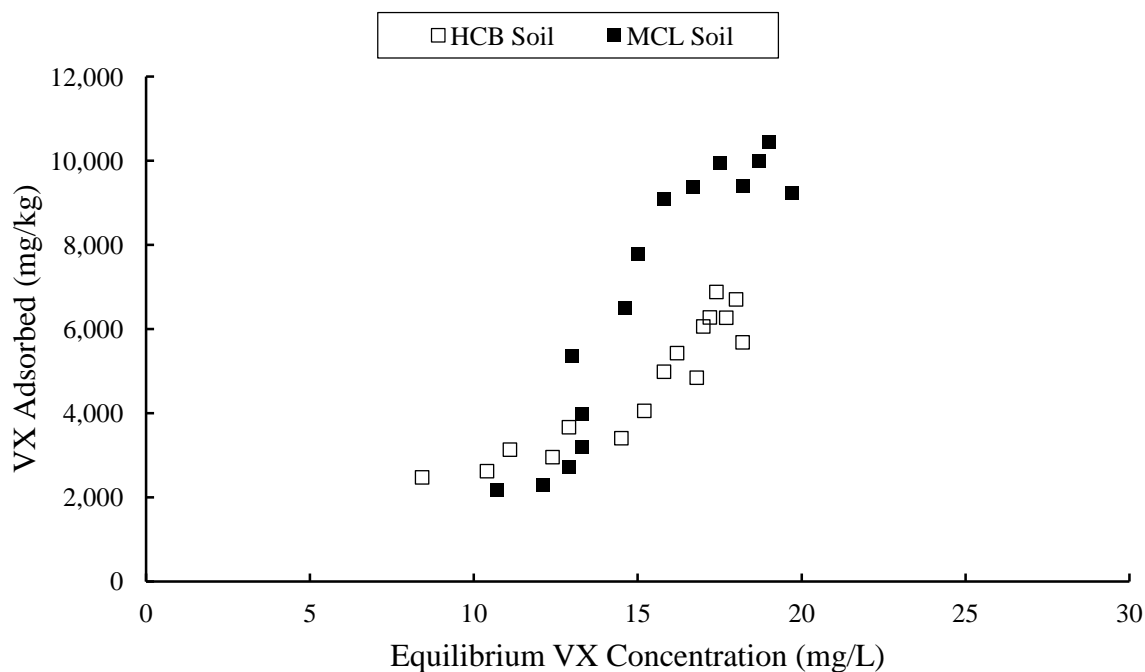
Figure 41. Batch equilibrium sorption isotherms for VX interacting with two natural soils.
Isotherms were obtained at 298 K.

Table 13. Results of Nonlinear Freundlich-Langmuir Modeling
of VX Equilibrium Isotherm Data

Model	Substrate	
Parameter	LLNL 2004 Study	MCL Soil
S_{max} (mg/kg)	2,020 (1,880–2,160)	10,400 (9,000–11,700)
K_d (L/kg)	3.49 (3.32–3.65)	0.0729 (0.0696–0.0762)
n	5.53 (4.51–6.56)	10.2 (5.53–15.0)
Goodness of fit	0.995	0.937

Notes: Results were modeled using dry soil weights. Runs were obtained at 298 K. Results are reported as
fitted values; estimated 95% confidence intervals are in parentheses.

3.3   Settling Rates

A series of experiments were conducted to obtain preliminary information on the settling rates of Suspengel 200 and Aldrich K10 substrates in pH 4.3 buffer at 298 K. The substrate concentrations were 1470 and 1440 mg/L for Suspengel 200 and Aldrich K10, respectively. In all cases, 8 mM VX in pH 4.3 buffer was used as the titrant, with titrant volumes ranging from 0 to 250 µL. This resulted in VX loadings ranging from 0 (control) to 12.1 wt% relative to the mass of substrate.

The settling results are illustrated in Figure 42. The average ($n = 2$) settling rate for Suspengel 200 without VX was 0.174 AU/min, and it was 0.0430 AU/min for the Aldrich K10 substrate. This indicates that the Suspengel 200 without any VX will settle out of solution approximately 4-fold faster than uncontaminated Aldrich K10. Overall, the addition of VX to Aldrich K10 substrate did not significantly affect settling rate, with an overall average ($n = 19$, ±SSD) settling rate of 0.0496 ± 0.00586 AU/min at 298 K. The addition of VX to the Suspengel 200 substrate had a significant effect on settling rate: the settling rate initially increased, then it dramatically decreased once the Suspengel 200 flocculated. The settling rate increased approximately 1.5-fold during the initial phase, then decreased approximately 3-fold once the flocculation occurred. Once flocculated, the Suspengel 200 settled at approximately the same rate as the Aldrich K10. In the course of preparing the Suspengel 200 samples for elemental analyses, the suspensions with and without VX added were photographed; these images are shown in Figure 43. Note how clear the liquid became above the flocculated Suspengel 200, and how the flocculated Suspengel 200 clay crept up the sides of the glass vial.
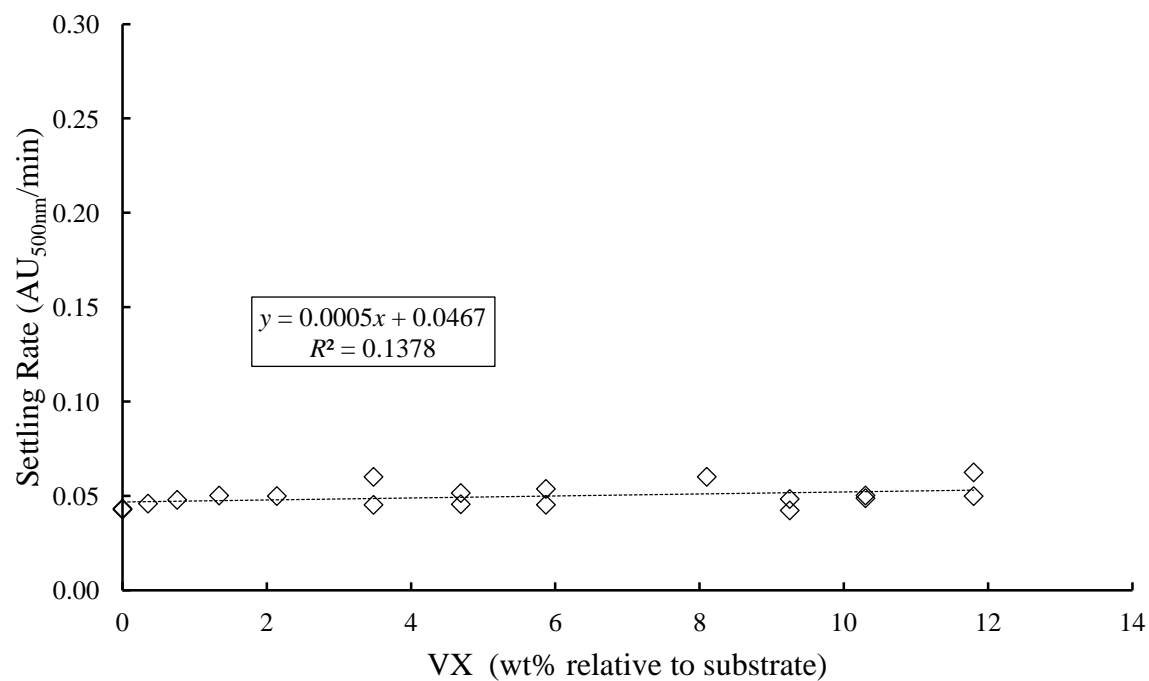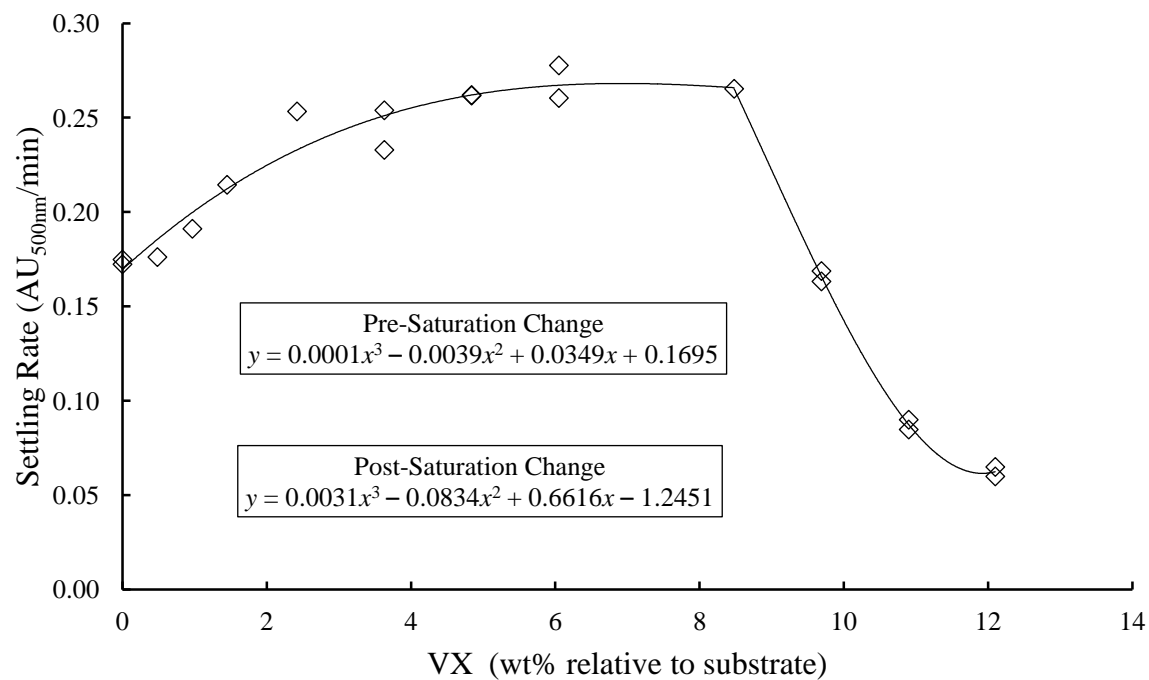
Figure 42. Settling rates as a function of VX loading. All reactions were conducted at 298 K.
Top: Suspengel 200; *bottom*: Aldrich K10.

Figure 43. Effect of VX on settling of Suspengel 200. Photographs were obtained immediately after stirring (*top*) and 30 min after stirring was stopped (*bottom*). VX was added to vials at *right* but not to vials at *left*.

4.   CONCLUSIONS AND DATA GAPS

ITC was found to be a useful technique for elucidating the sorption of VX to environmental substrates. This calorimetric technique is particularly useful when coupled with both kinetic profiling and equilibrium sorption isotherms. The current study is the first to examine VX sorption from dilute aqueous solution onto environmental sample matrices for which thermodynamic and sorption parameters were reported.

The sorption of VX to a natural montmorillonite clay at temperatures *above* the lower critical temperature of VX (~10 °C) was determined to occur rapidly (<15 min) and be a physisorption type of process, consistent with an ion-exchange mechanism. The reaction of VX with the clay is exothermic, as indicated by the negative enthalpy values. The negative enthalpy, negative Gibbs free energy, and positive entropy values indicate that the sorption is spontaneous, favored, and enthalpically driven. The enthalpy values measured at 298 K (~25 °C) in the current study (−12.6 to −8.44 kJ/mol) are consistent with literature values for cation exchange on clays.[92,93]

The sorption of VX to a natural montmorillonite clay at temperatures *below* the lower critical temperature of VX (~10 °C) was bimodal with both exothermic and endothermic heat flows. The initial interaction (Site 1) was determined to occur rapidly (<15 min) and to be a physisorption type of process, consistent with an ion-exchange mechanism. The interaction of VX with Site 1 is exothermic, as indicated by the negative enthalpy values. The negative enthalpy, negative Gibbs free energy, and negative entropy values indicate the interaction is spontaneous, favored, and enthalpically driven. The second interaction (Site 2) occurred once the Site 1 interaction was complete and was endothermic, as indicated by the positive enthalpy values. The positive enthalpy, negative Gibbs free energy, and positive entropy values indicate that the interaction is spontaneous, favored, and entropically driven. *The interaction of VX with Site 2 is thought to be a ligand-exchange mechanism via the phosphorus, but this has not been confirmed.* Additional studies are required to further understand the interactions of VX and other CWAs with environmental matrices.

The overall average equilibrium binding constant for VX sorption to binding Site 1 (apparent ion-exchange mechanism) of a natural montmorillonite clay at temperatures *above* the lower critical temperature was determined to be 25,000 M^{-1}, whereas it was determined to be 90,400 M^{-1} at temperatures *below* the lower critical temperature of VX. This indicates that the strength of binding of VX to this clay will be ~3.5 times stronger when the reaction occurs below ~10 °C. The apparent temperature dependence of binding strength has significant implications for fate studies, especially those conducted at lower temperatures. Additional studies are required to determine whether this apparent temperature dependence is unique to this clay or will occur across a wide range of sample matrices.

Batch equilibrium sorption isotherms for VX on clay and soil substrates were obtained at 298 K, and *measured* sorption model parameters reported for the first time. Using a standard modeling approach, K_d values for one soil were estimated and found to be up to 138 times higher than the measured value. Using these *estimated* K_d values will result in significant underestimation of the mobility of VX in the soil. Additional studies are required to achieve a better understanding of how VX and other CWAs are retained by natural soils.

The sorption of VX to two natural soil substrates was determined to occur rapidly and to be initially dominated by a physisorption type of process. When VX reacted with the two soils, the interaction was initially net exothermic but became net endothermic as the titration proceeded. This is indicative of at least two sorption processes taking place during the titration. Additional studies are required to elucidate the other mechanism(s).

Sorption of VX from dilute aqueous solution to humus and kaolinite was determined not to occur. Sorption of MPA and EMPA from dilute aqueous solution to kaolinite and two montmorillonites was also determined not to occur. This lack of interaction was confirmed by both ITC and kinetic profile experiments.

The process of sorption of VX onto a natural montmorillonite clay was found to preserve the VX, as was demonstrated by quantitative recovery of VX from the clay after 8 days of storage at room temperature. In a reported study, an amine was found to be stable for at least 5 months when sorbed to a natural montmorillonite clay.[111] In both the current and reported studies, the reported stabilities should be considered as the lower limits, because the experiments were terminated after 8 days or 5 months, respectively. The process of sorptive preservation of VX and other CWAs is not well understood and needs further study.

The settling rate of a natural montmorillonite clay was significantly affected by VX sorption. The settling rate initially increased, then dramatically decreased once the Suspengel 200 flocculated. The settling rate increased approximately 1.5-fold during the initial phase, then decreased approximately 3-fold once the flocculation occurred. This change in settling rate should be accounted for in hazard-transport models.

The sorptive behavior of VX onto a natural montmorillonite clay was significantly different from that of a highly processed montmorillonite clay that is typically used as a catalyst in organic synthesis. These catalyst-grade montmorillonites have been used in previous environmental fate studies. It is recommended that these catalyst-grade clays not be used in future environmental fate studies.

Blank

LITERATURE CITED

1.   Draoui, K.; Denoyel, R.; Chgoura, M.; Rouquerol, J. Adsorption of Paraquat on Minerals: A Thermodynamic Study. *J. Therm. Anal. Cal*. **1999**, *58*(3), 597–606.

2.   Li, H.; Sheng, G.; Teppen, B.J.; Johnston, C.T.; Boyd, S.A. Sorption and Desorption of Pesticides by Clay Minerals and Humic Acid-Clay Complexes. *Soil Sci. Soc. Am. J.* **2003**, *67*(1), 122–131.

3.   Charles, S.M.; Li, H.; Teppen, B.J.; Boyd, S.A. Quantifying the Availability of Clay Surfaces in Soils for Adsorption of Nitrocyanobenzene and Diuron. *Environ. Sci. Technol*. **2006**, *40*(24), 7751–7756.

4.   Wagner, G.W.; O'Connor, R.J.; Edwards, J.L.; Brevett, C.A.S. Effect of Drop Size on the Degradation of VX in Concrete. *Langmuir* **2004**, *20*(17), 7146–7150.

5.   Wagner, G.W.; O'Connor, R.J.; Procell, L.R. Preliminary Study on the Fate of VX in Concrete. *Langmuir* **2001**, *17*(14), 4336–4341.

6.   Mizrahi, D.M.; Columbus, I. ^{31}P MAS NMR: A Useful Tool for the Evaluation of VX Natural Weathering in Various Urban Matrices. *Environ. Sci. Technol*. **2005**, *39*(22), 8931–8935.

7.   Gura, S.; Tzanani, N.; Hershkovitz, M.; Barak, R.; Dagan, S. Fate of the Chemical Warfare Agent VX in Asphalt: A Novel Approach for the Quantitation of VX in Organic Surfaces. *Arch. Environ. Contam. Toxicol*. **2006**, *51*(1), 1–10.

8.   Waysbort, D.; Manisterski, E.; Leader, H.; Manisterski, B.; Ashani, Y. Laboratory Setup for Long-Term Monitoring of the Volatilization of Hazardous Materials: Preliminary Test of *O*-Ethyl *S*-2-(*N,N*-diisopropylamino)ethyl]methylphosphonthioate on Asphalt. *Environ. Sci. Technol*. **2004**, *38*(7), 2217–2223.

9.   Brevett, C.A.S.; Sumpter, K.B.; Pence, J.; Nickol, R.G.; King, B.E.; Giannaras, C.V.; Durst, H.D. Evaporation and Degradation of VX on Silica Sand. *J. Phys. Chem. C* **2009**, *113*(16), 6622–6633.

10.   Gershonov, E.; Columbus, I.; Zafrani, Y. Facile Hydrolysis-Based Chemical Destruction of the Warfare Agents VX, GB and HD by Alumina-Supported Fluoride Reagents. *J. Org. Chem*. **2009**, *74*(1), 329–338.

11.   Wagner, G.W.; Chen, Q.; Wu, Y. Reaction of VX, GD, and HD with Nanotubular Titania. *J. Phys. Chem. C* **2008**, *112*(31), 11901–11906.

12. Columbus, I.; Waysbort, D.; Shmuel, L.; Nir, I.; Kaplan, D. Decomposition of Adsorbed VX on Activated Carbons Studied by ^{31}P MAS NMR. *Environ. Sci. Technol*. **2006**, *40*(12), 3952–3958.

13. Wagner, G.W.; Procell, L.R.; O'Connor, R.J.; Munavalli, S.; Carnes, C.L.; Kapuor, P.N.; Klabunde, K.J. Reaction of VX, GB, GD, and HD with Nanosize Al_2O_3. Formation of Aluminophosphonates. *J. Am. Chem. Soc.* **2001**, *123*(8), 1636–1644.

14. Brevett, C.A.S.; Hall, M.G.; Sumpter, K.B. Degradation of VX and RVX on a Variety of Environmental Surfaces. U.S. Army Edgewood Chemical Biological Center: Aberdeen Proving Ground, MD. In progress. UNCLASSIFIED Report. (Footnote only; 2500 SN 103453).

15. Brevett, C.A.S.; Sumpter, K.B. Degradation of VX and GB on Moist and Ambient Sand, Sand/Clay and Sand/Clay/Humus Substrates. U.S. Army Edgewood Chemical Biological Center: Aberdeen Proving Ground, MD. In progress. UNCLASSIFIED Report. (Footnote only; 2500 SN 103352).

16. Verweij, A.; Boter, H.L. Degradation of *S*-2-diisopropylaminoethyl *O*-ethyl methylthioate in Soil: Phosphorus Containing Products. *Pestic. Sci*. **1976**, *7*(4), 355–362.

17. Kaaijk, J.; Frijlink, C. Degradation of *S*-2-diisopropylaminoethyl *O*-ethyl methylthioate in Soil. Sulphur Containing Products. *Pestic. Sci*. **1977**, *8*(5), 510–514.

18. Love, A.H.; Vance, A.L.; Reynolds, J.G.; Davisson, M.L. Investigating the Affinities and Persistence of VX Nerve Agent in Environmental Matrices. *Chemosphere* **2004**, *57*, 1257–1264.

19. Davisson, M.L.; Love, A.H.; Vance, A.L.; Reynolds, J.G. Environmental Fate of Organophosphorus Compounds Related to Chemical Weapons. UCRL-TR-209748; Lawrence Livermore National Laboratory: Livermore, CA, February 2005; UNCLASSIFIED Report.

20. Morrissey, K.M.; Schenning, A.M.; Sumpter, K.B. "Interaction of VX and VX Degradation Products with Environmental Matrices: A Thermodynamic Perspective", presented at the 2010 Chemical and Biological Defense Science and Technology Conference, Orlando, FL, 15–19 November 2010.

21. Morrissey, K.M.; Schenning, A.M.; Cheicante, R.C.; Sumpter, K.B. "Sorption of VX to Clay Minerals and Soils: Thermodynamic and Kinetic Studies", presented at the 2011 Chemical and Biological Defense Science and Technology Conference, Las Vegas, NV, 14–18 November 2011.

22. *RBCA Fate and Transport Models: Compendium and Selection Guidance*; American Society for Testing and Materials: West Conshohocken, PA, 1998.

23. Imoff, J.C.; Stoddard, A.; Buchak, E.M. *Evaluation of Contaminated Sediment Fate and Transport Models*: *Final Report*. Contract number 68-C-01-037, National Exposure Research Laboratory, U.S. Environmental Protection Agency: Athens, GA, 2003.

24. Small, M.J. *Compounds Formed from the Chemical Decontamination of HD, GB, and VX and Their Environmental Fate*. USAMBRDL-TR-8304, U.S. Army Medical Research and Development Command: Fort Detrick, MD, June 1984; UNCLASSIFIED Report (ADA149515).

25. Mingelgrin, U.; Gerstl, Z. Reevaluation of Partitioning as a Mechanism of Nonionic Chemical Adsorption in Soils. *J. Environ. Qual.* **1981**, *12*(1), 1–11.

26. Xing, B.; McGill, W.B.; Dudas, M.J. Cross-Correlation of Polarity Curves to Predict Partition Coefficients of Nonionic Contaminants. *Environ. Sci. Technol*. **1994**, *28*(11), 1929–1933.

27. Simpson, M.J. Nuclear Magnetic Resonance Based Investigation of Contaminant Interactions with Soil Organic Matter. *Soil Sci. Soc. Am. J.* **2006**, *70*(3), 995–1004.

28. Smith, J.; Muller, A.; Ward, M.; Cragan, J.; Cary, C.; Kapuschansky, C. *Validation of Model Predictions for the Dispersion and Fate of Reactive Chemical Releases in a Sub-Estuary of the Chesapeake Bay*. Presented at the 2011 Chemical and Biological Defense Science and Technology Conference, Las Vegas, NV, 14–18 November 2011.

29. Homepage of the PEARL and GeoPEARL models; http://www.pearl.pesticidesmodels.eu/home.htm (accessed February 2013).

30. Hinrich, B.; McNeal, B.; O'Connor, G. *Soil Chemistry*, 2md ed.; John Wiley and Sons: New York, 1985. ISBN 0-471-82217-5.

31. Savage, J.J.; D'Onofrio, T.G.; Durst, H.D.; Kilpatrick, W. *Environmental Fate of Chemical Agents: Final Report for Defense Technology Objective CB.42*. ECBC-TR-532; U.S. Army Edgewood Chemical Biological Center: Aberdeen Proving Ground, MD, 2007. UNCLASSIFIED Report (ADB333475).

32. Milone, C.; Dhanagopal, M.; Santangelo, S.; Lanza, M.; Galvagno, S.; Messina, G. K10 Montmorillonite Based Catalysts for the Growth of Multiwalled Carbon Nanotubes through Catalytic Chemical Vapor Deposition. *Ind. Eng. Chem. Res*. **2010**, *49*, 3242–3249.

33. Bigi, F.; Chesini, L.; Maggi, R.; Sartori, G. Montmorillonite KSF as an Inorganic, Water Stable, and Reusable Catalyst for the Knoevenagel Synthesis of Coumarin-3-Carboxylic Acids. *J. Org. Chem*. **1999**, *64*(3), 1033–1035.

34.   Bahulayan, D.; Das, S.K.; Iqbal, J. Montmorillonite K10 Clay: An Efficient Catalyst for the One-Pot Stereoselective Synthesis of β-Acetamido Ketones. *J. Org. Chem*. **2003**, *68*(14), 5735–5738.

35.   Simini, M.; Checkai, R. Soil Mixtures and Battelle Irradiated Soils: Methods, Calculations and Descriptions. Letter Report, U.S. Army Research Development and Engineering Command: Aberdeen Proving Ground, MD, April 2010; UNCLASSIFIED Report.

36.   Klupinski, T. Soil Characterization Data, Methods, and Soil Textural Graphic. Letter Report, Battelle Memorial Institute, Columbus, OH, April 2010; UNCLASSIFIED Report.

37.   Certificate of Analysis: VX. Lot Number VX-U-7330-CTF-N. Document no. 000016, U.S. Army Research, Development and Engineering Command: Aberdeen Proving Ground, MD, January 2009.

38.   Standard Operating Procedure, Neat Agent Purity Determination by Gas Chromatography Using Thermal Conductivity Detection, Analytical Chemistry Team Method 007, November 1997.

39.   Clark, D. *Review of Reactions of Chemical Agents in Water: Final Report*. Contract number 88PP8847; U.S. Army Medical Research and Development Command and Battelle Memorial Institute: Columbus, OH, January 1989; UNCLASSIFIED Report (ADA213287).

40.   Munro, N.B.; Talmage, S.S.; Griffin, G.D.; Waters, L.C.; Watson, A.P.; King, J.F.; Hauschild, V. The Sources, Fate, and Toxicity of Chemical Warfare Agent Degradation Products. *Environ. Health Perspect*. **1999**, *107*(12) 933–974.

41.   Hendrickson, D.M.; Nunes, R.B.; Morrissey, K.M.; Durst, H.D. *Isomeric Fractionation When GD Interacts with Concrete*. Presented at the 2007 ECBC Scientific Conference on Chemical and Biological Research, Timonium, MD, 13–15 November 2007.

42.   Hesleitner, P.; Kallay, N.; Matijevic, E. Adsorption at Solid/Liquid Interfaces. 6. The Effect of Methanol and Ethanol on the Ionic Equilibria at the Hematite/Water Interface. *Langmuir* **1991**, *7*(1), 178–184.

43.   Zhang, Z.Z.; Sparks, D.L.; Pease, R.A. Sorption and Desorption of Acetonitrile on Montmorillonite from Aqueous Solutions. *Soil Sci. Am. J*. **1990**, *54*, 351–356.

44.   Sorensen-Stowell, K.; Hengge, A.C. Thermodynamic Origin of the Increased Rate of Hydrolysis of Phosphate and Phosphorothioate Esters in DMSO/Water Mixtures. *J. Org. Chem.* **2006**, *71*(19), 7180–7184.

45.   Morrissey, K.M.; Connell, T.R.; Nunes, R.; Durst, H.D. *Isomeric Selectivity in the Interaction of GD with Environmental Sample Matrices*. Presented at the Fifth Singapore International Symposium on Protection Against Toxic Substances, Singapore City, Singapore, 27 November–01 December 2006.

46.   McGuire, J.M.; Jakubowski, E.M.; Thomson, S.A. *A Novel Method for Measuring Physicochemical Parameters of Highly Toxic Compounds.* Presented at the Chemical and Biological Defense Science and Technology Conference, Orlando, FL, 15–19 November 2010.

47.   Bizzigotti, G.O.; Castelly, H.; Hafez, A.M.; Smith, W.H.B.; Whitmire, M.T. Parameters for Evaluation of the Fate, Transport, and Environmental Impacts of Chemical Agents in Marine Environments. *Chem. Rev.* **2009**, *109*(1), 236–256.

48.   Morrissey, K.M.; Connell, T.R.; Creasy, W.R.; Stuff, J.R.; Durst, H.D.; O'Connor, R.J. *Quantitative Analysis of VX in Caustic Neutralization Solutions by Solid Phase Extraction and GC/MSD: Analysis of Hydrolysates as Separated Organic and Aqueous Phases*; ECBC-TR-009; U.S. Army Soldier Biological Chemical Command: Aberdeen Proving Ground, MD, 1999; UNCLASSIFIED Report (ADA360497).

49.   Morrissey, K.M.; Connell, T.R.; Stuff, J.R.; Durst, H.D.; O'Connor, R.J. *Quantitative Analysis of VX in Caustic Neutralization Solutions by Solid Phase Extraction and GC/MSD: Analysis of Hydrolysate as Unseparated Phases;* ECBC-TR-010; U.S. Army Soldier Biological Chemical Command: Aberdeen Proving Ground, MD, 1999; UNCLASSIFIED Report (ADA362643).

50.   Arroyo, L.J.; Hui, L.; Teppen, B.J.; Johnston, C.T.; Boyd, S.A. Hydrolysis of Carbaryl by Carbonate Impurities in Reference Clay SWy-2. *J. Agric. Food Chem.* **2004**, *52*, 8066–8073.

51.   Arroyo, L.J.; Hui, L.; Teppen, B.J.; Johnston, C.T. A Simple Method for Partial Purification of Reference Clays. *Clays and Clay Minerals* **2005**, *53*(5), 511–519.

52.   Keren, R.; Sparks, D.L. The Role of Edge Surfaces in Flocculation of 2:1 Clay Minerals. *Soil Sci. Soc. Am. J.* **1995**, *59*(2), 430–435.

53.   Jelesarov, I.; Bosshard, H.R. Isothermal Titration Calorimetry and Differential Scanning Calorimetry as Complementary Tools to Investigate the Energetics of Biomolecular Recognition. *J. Mol. Recognit.* **1999**, *12*, 3–18.

54.   *Biocalorimetry 2*; Ladbury, J.E.; Doyle, M.L., Eds.; John Wiley and Sons: Hoboken, NJ, 2004. Chapter titled "Isothermal Titration Calorimetry: A Tutorial."

55.   Mukherjee, S.; Huang, C.; Guerra, F.; Wang, K.; Oldfield, E. Thermodynamics of Biphosphonates Binding to Human Bone: A Two-Site Model. *J. Am. Chem. Soc.* **2009**, *131*, 8374–8375.

56.   Kearney, A.; Avramovic, A.; Castro, M.A.A.; Carmo, A.M.; Davis, S.J.; Van der Merwe, P.A. The Contribution of Conformational Adjustments and Long-range Electrostatic Forces to the CD2/CD58 Interaction. *J. Biol. Chem.* **2007**, *282*(18), 13160–13166.

57.   Reeves, T.E. *Stoichiometry in Assessing Bioscavenger Proteins*. Presented at the Current Trends in Microcalorimetry and Biacore Symposium, Baltimore, MD, 18–21 October 2009.

58.   Penn, C.J.; Warren, J.C. Investigating Phosphorus Sorption onto Kaolinite Using Isothermal Titration Calorimetry. *Soil Sci. Soc. Am. J.* **2009**, *73*(2), 560–568.

59.   Penn, C.J.; Zhang, H. Isothermal Titration Calorimetry as an Indicator of Phosphorus Sorption Behavior. *Soil Sci. Soc. Am. J.* **2010**, *74*(2), 502–511.

60.   Buchholz, F.; Wick, L.Y.; Harms, H.; Maskow, T. The Kinetics of Polycyclic Aromatic Hydrocarbon (PAH) Biodegradation Assessed by Isothermal Titration Calorimetry (ITC). *Thermochimica Acta* **2007**, *458*, 47–53.

61.   Perry, T.D.; Klepac-Ceraj, V.; Zhang, X.V.; McNamara, C.J.; Polz, M.F.; Martin, S.T.; Berke, N.; Mitchell, R. Binding of Harvested Bacterial Exopolymers to the Surface of Calcite. *Environ. Sci. Technol.* **2005**, *39*(22), 8770–8775.

62.   Bi, R.; Schmidt, T.C.; Haderlein, S.B. Environmental Factors Influencing Sorption of Heterocyclic Aromatic Compounds to Soil. *Environ. Sci. Technol.* **2007**, *41*(9), 3172–3178.

63.   Kim, Y.H.; Heinze, T.M.; Kim, S.J.; Cerniglia, C.E. Adsorption and Clay-Catalyzed Degradation of Erythromycin A on Homoionic Clays. *J. Envir. Qual.* **2004**, *33*(1), 257–264.

64.   Liu, Y.; Sturtevant, J.M. Significant Differences Between van't Hoff and Calorimetric Enthalpies. II. *Protein Sci.* **1995**, *4*(12), 2559–2561.

65.   Liu, Y.; Sturtevant, J.M. Significant Differences Between van't Hoff and Calorimetric Enthalpies. III. *Biophys. Chem.* **1997**, *64*(1–3), 121–126.

66.   Chaires, J.B. Possible Origin of Difference Between van't Hoff and Calorimetric Enthalpy Estimates. *Biophys. Chem.* **1997**, *64*(1–3), 15–23.

67.   Frasca, V. *Introductory Isothermal Titration Calorimetry Tutorial*. Presented at the 2009 Current Trends in Microcalorimetry and Biacore Symposium, Baltimore, MD, 18–21 October 2009.

68.   Morrissey, K.M.; Ruth, J.L.; Cheicante, R.L.; Schenning, AM.; Fouse, J.C.; Hulet, M.S.; Creasy, W.R.; Durst, H.D.; O'Connor, R.J.; Berg, F.J.; McMahon, L.R.; Forrest, L.P.; Weiss, M.P. *Characterization and Neutralization of Recovered Lewisite Munitions*; ECBC-TR-531; U.S. Army Edgewood Chemical Biological Center: Aberdeen Proving Ground, MD, 2006; UNCLASSIFIED Report (ADA460761).

69.   Morrissey, K.M.; Cheicante, R.L.; Connell, T.R.; Creasy, W.R.; Fouse, J.C.; Hulet, M.S.; Ruth, J.L.; Schenning, A.M.; Williams, B.W.; Durst, H.D.; O'Connor, R.J.; Winemiller, M.D.; McMahon, L.R.; McGuire, K.; Forrest, L.P.; Weiss, M.P.; Smith, P.B. *Characterization and Neutralization of Arsenical-Based WWII Era Chemical Munition Fills*. ECBC-TR-479, U.S. Army Edgewood Chemical Biological Center: Aberdeen Proving Ground, MD, 2006; UNCLASSIFIED Report (ADA455660).

70.   Erney, D.R.; Gillespie, A.M.; Gilvydis, D.M.; Poole, C.F. Explanation of the Matrix-Induced Chromatographic Response Enhancement of Organophosphorus Pesticides During Open Tubular Column Gas Chromatography with Splitless or Hot On-Column Injection and Flame Photometric Detection. *J. Chrom. A* **1993**, *638*(1), 57–63.

71.   Erney, D.R.; Pawlowski, T.M.; Poole, C.F. Matrix-Induced Peak Enhancement of Pesticides in Gas Chromatography: Is There a Solution?. *J. High Res. Chrom.* **1997**, *20*(7), 375–378.

72.   Hook, G.L.; Kimm, G.; Koch, D.; Savage, P.B.; Ding, B.; Smith, P.A. Detection of VX Contamination in Soil Through Solid-Phase Microextraction Sampling and Gas Chromatography/Mass Spectrometry of the VX Degradation Product Bis(diisopropylaminoethyl)disulfide. *J. Chrom. A* **2003**, *992*, 1–9.

73.   Reiter, G.; Mikler, J.; Hill, I.; Weatherby, K.; Thiermann, H.; Worek, F. Simultaneous Quantification of VX and Its Toxic Metabolite in Blood and Plasma Samples and Its Application for In Vivo and In Vitro Toxicological Studies. *J. Chromatogr. B Analyst. Technol. Biomed. Life Sci.* **2011**, *879*(26), 2704–2713.

74.   Morrissey, K.M.; Schenning, A.M.; Smith, P.B.; Sumpter, K.B. *Fate of VX in Potable Waters*. Presented at the Chemical and Biological Defense Science and Technology Conference, Orlando, FL, 15–19 November 2010.

75.   Morrissey, K.M.; Schenning, A.M.; Fouse, J.C.; Ruth, J.L.; Sumpter, K.B. *Degradation of VX in Formulated Source and Potable Waters*; ECBC-TR-1004; U.S. Army Edgewood Chemical Biological Center: Aberdeen Proving Ground, MD, 2012; UNCLASSIFIED Report.

76.   Cheicante, R.L.; Stuff, J.R.; Durst, H.D. Analysis of Chemical Weapons Degradation Products by Capillary Electrophoresis with UV Detection. *J. Cap. Elec*. **1995**, *4*, 157–163.

77.   Cheicante, R.L.; Stuff, J.R.; Durst, H.D. Separation of Sulfur Containing Chemical Warfare Related Compounds in Aqueous Samples by Micellar Electrokinetic Chromatography. *J. Chrom.* **1995**, *711*, 347–352.

78.   *Encyclopedia of Analytical Chemistry: Applications, Theory, and Instrumentation*; Meyers, R.A., Ed.; John Wiley and Sons: Chichester, UK, 2000. Chapter titled "Capillary Electrophoresis in Detection of Chemicals Related to the Chemical Weapons Convention", pp 909–923. ISBN: 978-0-471-97670-7.

79.   Haderlein, S.B.; Weissmahr, K.W.; Schwarzenbach, R.P. Specific Adsorption of Nitroaromatic Explosives and Pesticides to Clay Minerals. *Environ. Sci. Technol.* **1996**, *30*(2), 612–622.

80.   Zhang, Z.Z.; Sparks, D.L.; Scrivner, N.C. Sorption and Desorption of Quaternary Amine Cations on Clays. *Environ. Sci. Technol*. **1993**, *27*(8), 1625–1631.

81.   Rebhun, M.; Kalabo, R.; Grossman, L.; Manka, J.; Rav-Acha, C. Sorption of Organics on Clay and Synthetic Humic-Clay Complexes Simulating Aquifer Processes. *Wat Res* **1992**, *26*(1), 79–84.

82.   Kingery, A.F.; Saxe, J.K.; Allen, H.E. *Environmental Fate of Alkyl Methyl Phosphonates Arising from Chemical Surety Material*. Presented at the 219[th]American Chemical Society National Meeting, San Francisco, CA, 26–30 March 2000.

83.   *Batch-Type Procedures for Estimating Soil Adsorption of Chemicals*; EPA/530/SW-87/006-F; Office of Solid Waste and Emergency Response, U.S. Environmental Protection Agency: Washington, DC, April 1992.

84.   *Fate, Transport and Transformation Test Guidelines*, *OPPTS 835.1220: Sediment and Soil Adsorption/Desorption Isotherm;* EPA 712-C-98-048; Office of Prevention, Pesticides, and Toxic Substances; U.S. Environmental Protection Agency: Washington, DC, January 1998.

85.   U.S. Department of Agriculture, Agricultural Research Service. Microsoft Excel Spreadsheets for Fitting Sorption Data. http://www.ars.usda.gov/pandp/docs.htm?docid=14971, accessed July, 2010.

86.   Bolster, C.H.; Hornberger, G.M. On the Use of Linearized Langmuir Equations. *Soil Sci. Soc. America. J.* **2007**, *71*(6), 1796–1806.

87.   Bolster, C.H.; Hornberger, G.M. On the Use of Linearized Langmuir Equations-CORRECTION. *Soil Sci. Soc. America. J.* **2008**, *72*(6), 1848.

88.   Balch, R.T. Measurement of Turbidity with a Spectrophotometer with Especial Reference to Sugarhouse Products. *Ind. Eng. Chem. Anal. Ed*. **1931**, *3*(2), 124–127.

89.   *Turbidity: Absorptometric Method 8237,* Edition 9. Application note; HACH Chemical Company: Loveland, CO, 2009.

90.   *VP-ITC Microcalorimeter: Users Manual*, Version MAU130030 REV E-2. MicroCal: Northampton, MA.

91.   EDTA-CACL$_2$ Test Kit Instructions for VP-ITC. MicroCal: Northampton, MA, 2008.

92. Ewin, G.J.; Erno, B.P.; Hepler, L.G. Clay Chemistry: Investigation of Thermodynamics of Ion Exchange Reactions by Titration Calorimetry. *Can. J. Chem.* **1981**, *59*, 2927–2933.

93. Morel, J.P.; Marry, V.; Turq, P.; and Morel-Desrosiers, N. Effect of Temperature on the Retention of Cs^+ by Na-Montmorillonite: Microcalorimetric Investigation. *J. Materials Chem.* **2007**, *17*, 2812–2817.

94. Imae, T.; Konishi, H.; Ikeda, S. Lower and Upper Consolute Boundaries of Dilute Aqueous Solutions of Dimethyloleylamine Oxide in the Presence of NaCl and HCl. A "Closed Loop" Phase Diagram. *J. Phys. Chem*. **1986**, *90*(7), 1417–1423.

95. Martin, M.J.S.; Villa, M.V.; Sanchez-Camazano, M. Glyphosphate-Hydrotalcite Interaction as Influenced by pH. *Clays and Clay Minerals* **1999**, *47*(6), 777–783.

96. Chorover, J.; Kretzschmar, R.; Garcia-Pichel, F.; Sparks, D.L. Soil Biogeochemical Processes Within the Critical Zone. *Elements* **2007**, *3*(5), 321–326.

97. Stodeman, M.; Dhar, N. Microcalorimetric Titration of a Tetra-p-Sulfonated Calix[4]Arene with Alkylammonium Ions in Aqueous Solution. *J. Chem. Soc., Faraday Trans*. **1998**, *94*(7), 899–903.

98. Perozzo, R.; Folkers, G.; Scapozza, L. Thermodynamics of Protein-Ligand Interactions: History, Present, and Future Aspects. *J. Receptors Signal Transduction* **2004**, *24*(1–2), 1–52.

99. Boncina, M.; Lah, J.; Rescic, J.; Vlachy, V. Thermodynamics of the Lysozyme-Salt Interaction from Calorimetric Titrations. *J. Phys. Chem. B* **2010**, *114*(12), 4313–4319.

100. Garidel, P. Blume, A. Interaction of Alkaline Earth Cations with the Negatively Charged Phospholipid 1,2-Dimyristoyl-sn-glycero-3-phosphoglycerol: A Differential Scanning and Isothermal Titration Calorimetric Study. *Langmuir* **1999**, *15*(17), 5526–5539.

101. Guinto, E.R. Cera, E.D. Large Heat Capacity Change in a Protein-Monovalent Cation Interaction. *Biochemistry* **1996**, *35*(27), 8800–8804.

102. Avery, H.E. *Basic Reaction Kinetics and Reaction Mechanisms*, Macmillan Press: London, U.K., 1974 (ISBN 0-333-12696-3).

103. Li, X.R.; Koseki, H. Thermal Decomposition Kinetic of Liquid Organic Peroxides. *J. Loss Prev. Process Industries* **2005**, *18*(4–6), 460–464.

104. Andujar-Sanchez, M.; Heras-Vazquez, F.J.L.; Clemente-Jimenez, J.M.; Martinez-Rodriguez, S.M.; Camara-Artigas, A.; Rodriguez-Vico, F.; Jara-Perez, V. Enzymatic Activity Assay of D-Hydantoinase by Isothermal Titration Calorimetry. Determination of the Thermodynamic Activation Parameters for the Hydrolysis of Several Substrates. *J. Biochem. Biophys. Methods* **2006**, *67*, 57–66.

105. Wright, M.R. *An Introduction to Chemical Kinetics*, John Wiley and Sons: West Sussex, U.K., 2004 (ISBN 0-470-09058-8).

106. Haque, R.; Lindstrom, F.T.; Freed, V.H.; Sexton, R. Kinetic Study of the Sorption of 2,4-D on Some Clays. *Environ. Sci. Technol*., **1968**, *2*(3), 207–211.

107. Morrissey, K.M.; Nunes, R.B.; Schenning, A.M.; Durst, H.D. *Degradation of the Chemical Warfare Agent Soman in Potable Waters*. Presented at the 238th American Chemical Society National Meeting, Washington, DC, 16–20 August 2009.

108. Jiang, W.; Gan, J.; Haver, D. Sorption and Desorption of Pyrethroid Insecticide Permethrin on Concrete. *Environ. Sci. Technol*. **2011**, *45*(2), 602–607.

109. Connaughton, D.F.; Stedinger, J.R.; Lion, L.W.; Shuler. M.L. Description of Time-Varying Desorption Kinetics: Release of Naphthalene from Contaminated Soils. *Environ. Sci. Technol*., **1993**, *27*(12), 2397–2403.

110. Sharer, M.; Park, J.H.; Voice, T.C.; Boyd, S.A. Aging Effects on the Sorption-Desorption Characteristics of Anthropogenic Organic Compounds in Soil. *J. Environ. Qual*. **2002**, *32*(4), 1385–1392.

111. Frenkel, M.; Solomon, D.H. The Decomposition of Organic Amines on Montmorillonites Under Ambient Conditions. *Clays and Clay Minerals* **1977**, *25*, 463–464.

112. Rosenblatt, D.H.; Small, M.J.; Kimmell, T.A.; Anderson, A.W. *Background Chemistry for Chemical Warfare Agents and Decontamination Processes in Support of Delisting Waste Streams at the U.S. Army Dugway Proving Ground, UT*; ANL/EAD/TM-56; Argonne National Laboratory, Environmental Assessment Division: Argonne, IL, April 1996; UNCLASSIFIED Report.

113. Czerwinski, S.E.; Skvorak, J.P.; Maxwell, D.M.; Lenz, D.E.; Baskin, S.I. Effect of Octanol:Water Partition Coefficients of Organophosphorus Compounds on Biodistribution and Percutaneous Toxicity. *J. Biochem. Molecular Toxicology* **2006**, *20*(5), 241–246.

ACRONYMS AND ABBREVIATIONS

ACS	American Chemical Society
CAS	Chemical Abstracts Service
CASARM	Chemical Agent Standard Analytical Reference Material
CE	capillary electrophoresis
CEC	cation-exchange capacity
CEC_{A+B}	acidic and basic cation-exchange capacity
CTAB	hexadecyltrimethylammonium bromide
CWA	chemical warfare agent
ΔC_p	constant pressure heat capacity change
ΔG	Gibbs free energy change
ΔH_{obs}	observed enthalpy
ΔS	entropy change
DIW	deionized water
DoD	U.S. Department of Defense
E_a	activation energy
ECBC	U.S. Army Edgewood Chemical Biological Center
EDTA	ethylenediaminetetraacetic acid
EMPA	ethyl methylphosphonic acid
f_{OC}	organic carbon fraction
FSW	formulated source water
GC	gas chromatography
GD	soman, pinacolyl methylphosphonofluoridate
ITC	isothermal titration calorimetry
K	partition coefficient
K_b	equilibrium binding constant
K_d	equilibrium dissociation constant
K_{OC}	organic carbon partitioning coefficient
K_{OW}	octanol-water partitioning coefficient
LC	liquid chromatography
LCT	lower consolute temperature
MES	2-(*N*-morpholino)ethanesulfonic acid
MPA	methyl phosphonic acid
MS	mass spectrometer or spectrometery
MSD	mass-selective detector
m/z	mass-to-charge ratio
ND	non-detect
NIST	National Institute of Standards and Technology
NMR	nuclear magnetic resonance
pK_a	acid dissociation constant
QC	quality control
R	universal gas constant
RSH	2-(diisopropyl)aminoethanethiol
RSR	bis(2-diisopropylaminoethyl) sulfide

RSSR	bis(2-diisopropylaminoethyl) disulfide
SEM	scanning electron micrograph
SIM	selective ion monitoring
S_{max}	saturation capacity
SRM	standard reference material
SSD	sample standard deviation
STS	substrate-to-solution (ratio)
t	critical value
$t_{1/2}$	half-life
T	absolute temperature
VX	O-ethyl-S-[2-N,N-(diisopropylamino)ethyl]methylphosphonothioate
VX-bis	S,S-bis-(2-diisopropylaminoethyl)methylphosphonodithioate
VX_F	VX recovered in dissolved (filtered) fraction
VX_{INT}	average initial VX
VX_{REC}	VX recovered
VX_{TOT}	total amount of VX bound to substrate
VX_{UF}	whole (unfiltered) recovered VX